Supplementary Information (SI) for Faraday Discussions.
This journal is © The Royal Society of Chemistry 2025

Electronic Supplementary Information

Efficient and Controlled Ring-Opening Copolymerization of Cyclohexene Oxide with Cyclic Anhydrides Catalyzed by Proline-based Chiral Alkyl Al(III) Compounds

Ranay Kumar Ray[a], P. K. Sudhadevi Antharjanam[b] and Debashis Chakraborty*[a]

dchakraborty@iitm.ac.in

[a] *Organometallics and Polymer Chemistry Laboratory, Department of Chemistry, Indian Institute of Technology Madras, Chennai 600036, Tamil Nadu, India*

[b] *Sophisticated Analytical Instrument Facility, Indian Institute of Technology Madras, Chennai 600036, Tamil Nadu, India*

Contents

Experimental Section

1 General Methods

All NMR experiments were conducted on a Bruker Avance-500 instrument, with chemical shifts (δ) referenced to the residual solvent (δ^{H}, δ^{C} = 0 for $Si(CH_3)_4$. Data processing was carried out using Topspin software. High-resolution mass spectrometry (HRMS) data were obtained using an Agilent Micromass Q-TOF mass spectrometer. Gel permeation chromatography (GPC) analysis of the polymers was performed on a WATERS LC-20AD instrument, equipped with a refractive index (RI) detector, operating at 40 °C and a flow rate of 0.8 mL/min. Prior to analysis, samples were dissolved in HPLC-grade THF and filtered through 0.2 µm PTFE filters. The instrument calibration was done using narrow-M_n polystyrene standards. MALDI-TOF measurements were performed using a Bruker Daltonics instrument using dihydroxybenzoic acid (DHBA) matrix. Single crystals suitable for X-ray diffraction were grown in a glove box from a concentrated toluene and THF solution of the Al(III) complexs **2a**, **2c** and **2d**. Single crystal X-ray diffraction (SC-XRD) data were collected on a Bruker D8 VENTURE diffractometer equipped with Mo (Kα) radiation source of $\lambda = 0.71073$ Å. The selected crystals were mounted in a HAMPTON cryoloops with the help of paratone-N oil. Data collection was performed at liquid nitrogen temperatures of 120-100 K. An optimized strategy was adopted for the full data collection by keeping an average 4-fold redundancy for the reflections. The program APEX4-SAINT[1] was used for integrating the frames, followed by a multi-scan absorption correction using the program SADABS[2]. The structure was solved by SHELXT-2018[3] and refined by full-matrix least squares techniques using SHELXL-2019[4] software package incorporated in WingX suite[5]. Hydrogens on all carbon atoms were fixed at calculated positions and refined as a riding model with respect to its parent atom. ORTEP-3 was used to prepare the ORTEPs. The crystallographic data are summarized in **Table S1** and **Table S2** and have been deposited with the CCDC under the following reference number: [CCDC number: 2446004-2446007]. Differential scanning calorimetry (DSC) measurements were performed on a NETZSCH DSC 204 F1 PHOENIX at a heating rate of 10 °C/min. Thermogravimetric analysis (TGA) was done with a TA Instruments Q500. 5 mg of each sample was loaded onto a platinum pan and subjected to a dynamic high-resolution scan with a heating rate of 20 °C min^{-1} in a nitrogen atmosphere. Each sample was heated up to 900 °C from room temperature. Powder X-ray diffraction (XRD) data were collected on a Bruker D8 Advance diffractometer equipped with Cu Kα radiation (λ = 1.54056 Å) at 40 kV, 30 mA power over the 2θ range of 5-80° with a scan speed of 0.128548/s and a step size of 0.0288969° at room temperature. HPLC analysis were performed on an Agilent 1100 HPLC with Agilent HP-Chiral 19091G-B213, 30 m×0.25 mm id×0.25µm film.

2 Materials

All moisture and air-sensitive reactions were conducted under an inert argon atmosphere using a MBraun glovebox. The reagents *L*-proline, *D*-proline, thionyl chloride, triethylamine, di-tert-butyl dicarbonate, bromobenzene, 1-bromo-4-fluorobenzene, methylmagnesium bromide solution (3 M in diethyl ether), trimethylaluminum solution (2 M in toluene), Mg turnings, cyclohexene oxide (CHO), phthalic anhydride (PA), maleic anhydride (MA), succinic anhydride (SA), tetraphenylphosphonium chloride (TPPCl), tetrabutylammonium bromide (TBAB), bis(triphenylphosphine)iminium chloride (PPNCl) were purchased from Sigma-Aldrich and used as received unless otherwise specified. Tetrahydrofuran (THF) and toluene were dried over sodium/benzophenone and freshly distilled prior to use. Cyclohexene oxide (CHO) was dried over calcium hydride (CaH_2) and freshly distilled before use. Phthalic anhydride (PA) was crystallized twice from hot chloroform ($CHCl_3$) and sublimed under vacuum before use. Monomer Maleic anhydride and succinic anhydride also sublimed in vacuum prior to use. NMR solvent $CDCl_3$ purchased from Cambridge Isotope Laboratories, Inc. and dried over CaH_2 and distilled prior to use. Tetra-n-butylammonium bromide (TBAB) was purified by crystallization from toluene and then dried under vacuum before use. Tetraphenylphosphonium chloride (TPPCl) and bis(triphenylphosphine)iminium chloride (PPNCl) were purified by crystallizing from chloroform and hexane, followed by drying under vacuum. Argon and nitrogen gas was purchased from Indogas, Bangalore, India.

3 Synthesis

3.1 Synthesis of Al(III) compounds

3.1.1 Compound **2a**

In an argon-filled glove box, $AlMe_3$ (2 M in toluene, 0.14 mL, 0.28 mmol) was added dropwise to a stirred solution of **1a** (0.100g, 0.28 mmol) in 8 mL toluene at -24 °C. The solution was allowed to attain room temperature and stirred for an additional period of 12 h. The solvent was removed under vacuo giving a white solid product which was then recrystallised from concentrated dry toluene at –24 °C to give white crystals of **2a** (Yield = 78 %). ^{1}H NMR ($\mathrm{CDCl_3}$, 500 MHz, 298 K) : δ (ppm) : 7.14-7.31 (m, 10H, Ph**H**), 4.97-4.99 (dd, J = 7.6, 1.3 Hz, 1H, N**H)**, 3.17-3.23 (m, 1H, $\mathrm{NC}\mathbf{H}_2$), 2.67-2.72 (m, 1H, $\mathrm{NC}\mathbf{H}_2$), 2.11-2.15 (m, 1H, $\mathrm{NCHC}\mathbf{H}_2$), 1.98-2.01 (m, 1H, $\mathrm{NCH_2C}\mathbf{H}_2$), 1.51 (s, 9H, $\mathrm{C(C}\mathbf{H}_\mathbf{3})_9$), 1.28-1.34 (m, 1H, $\mathrm{(NCH_2C}\mathbf{H}_2$), 0.23-0.30 (m, 1H, NCHC**H**2), -0.94 (s, 3H, $\mathrm{Al\text{-}C}\mathbf{H}_\mathbf{3}$), -1.28 (s, 3H, $\mathrm{Al\text{-}C}\mathbf{H}_\mathbf{3}$). ^{13}C {^{1}H} NMR ($\mathrm{CDCl_3}$, 500 MHz, 298 K) : δ (ppm) : 159.57, 148.70, 146.48, 129.05, 128.42, 128.24, 127.86, 127.54, 126.28, 86.11, 80.67, 68.68, 48.82, 29.42, 28.63, 21.73, -8.97, -9.85. HRMS m/z calculated for $[\mathrm{M+NH_4}]^+$ $\mathrm{C_{24}H_{32}NO_3AlNH_4}$: 427.25 found 427.2529.

3.1.2 Compound **2b**

In an argon-filled glove box, $\mathrm{AlMe_3}$ (2 M in toluene, 0.14 mL, 0.28 mmol) was added dropwise to a stirred solution of **1b** (0.100g, 0.28 mmol) in 8 mL toluene at -24 °C. The solution was allowed to attain room temperature and stirred for an additional period of 12 h. The solvent was removed under vacuo giving a white solid product which was then recrystallised from concentrated dry toluene at –24 °C to give white crystals of **2b** (Yield = 71 %). ^{1}H NMR ($\mathrm{CDCl_3}$, 500 MHz, 298 K) : δ (ppm) : 4.15-4.16 (dd, J = 8.9, 3.7 Hz, 1H, N**H)**, 3.60-3.65 (m, 1H, $\mathrm{NC}\mathbf{H}_2$), 3.34 (s, 1H, $\mathrm{NC}\mathbf{H}_2$), 1.96-2.04 (m, 2H, $\mathrm{NCHC}\mathbf{H}_2$), 1.77-1.83 (m, 1H, $\mathrm{NCH_2C}\mathbf{H}_2$), 1.74 (s, 9H, $\mathrm{C(CH_\mathbf{3})_9}$, 1.13-1.21 (s, 1H, $\mathrm{(\text{-}C\text{-}C}\mathbf{H}_3$), 1.04 (s, 3H, $\mathrm{\text{-}C\text{-}C}\mathbf{H}_3$), -0.83 (s, 3H, $\mathrm{Al\text{-}C}\mathbf{H}_\mathbf{3}$), -0.92 (s, 3H, $\mathrm{Al\text{-}C}\mathbf{H}_\mathbf{3}$). HRMS m/z calculated for $[\mathrm{M+H}]^+$ $\mathrm{C_{15}H_{32}NO_3AlH}$: 302.23 found 302.2293.

3.1.3 Compound **2c**

In an argon-filled glove box, $\mathrm{AlMe_3}$ (2 M in toluene, 0.14 mL, 0.28 mmol) was added dropwise to a stirred solution of **1c** (0.100g, 0.28 mmol) in 8 mL toluene at -24 °C. The solution was allowed to attain room temperature and stirred for an additional period of 12 h. The solvent was removed under vacuo giving a white solid product which was then recrystallised from concentrated dry toluene at –24 °C to give white crystals of **2c** (Yield = 83 %). ^{1}H NMR ($\mathrm{CDCl_3}$, 500 MHz, 298 K) : δ (ppm) : 7.26-7.34 (m, 4H, Ph**H**), 6.91-7.00 (m, 4H, Ph**H**), 4.98-5.00 (dd, J = 9, 2 Hz, 1H, N**H)**, 3.26-3.34 (m, 1H, $\mathrm{NC}\mathbf{H}_2$), 2.78-2.84 (m, 1H, $\mathrm{NC}\mathbf{H}_2$), 2.16-2.27 (m, 1H, $\mathrm{NCHC}\mathbf{H}_2$), 1.95-2.02 (m, 1H, $\mathrm{NCH_2C}\mathbf{H}_2$), 1.58 (s, 9H, $\mathrm{C(CH_\mathbf{3})_9}$, 1.40-1.48 (m, 1H, $\mathrm{(NCH_2C}\mathbf{H}_2$), 0.32-0.44 (m, 1H, (NCHC**H**2), -0.88 (s, 3H, Al-C**H₃**), -1.22 (s, 3H, Al-C**H₃**). ^{13}C {^{1}H} NMR ($CDCl_3$, 500 MHz, 298 K) : *δ* (ppm) : 163.20, 162.57, 161.25, 160.62, 159.84, 144.58, 142.36, 129.97, 129.50, 114.58, 114.41, 114.33, 114.17, 86.63, 50.05, 68.74, 48.91, 29.48, 28.73, 21.94, -8.91, -9.82. HRMS m/z calculated for $[M+K]^+$ $C_{24}H_{30}NO_3F_2AlK$: 484.16 found 484.1711.

3.1.4 Compound **2d**

In an argon-filled glove box, $AlMe_3$ (2 M in toluene, 0.14 mL, 0.28 mmol) was added dropwise to a stirred solution of **1d** (0.100g, 0.28 mmol) in 8 mL toluene at -24 °C. The solution was allowed to attain room temperature and stirred for an additional period of 12 h. The solvent was removed under vacuo giving a white solid product which was then recrystallised from concentrated dry toluene at –24 °C to give white crystals of **2d** (Yield = 75 %). ^{1}H NMR ($CDCl_3$, 500 MHz, 298 K) : *δ* (ppm) : 7.14-7.31 (m, 10H, Ph**H**), 4.97-4.99 (dd J = 7.5, 1.5 hz, 1H, N**H)**, 3.17-3.23 (m, 1H, NCH_2), 2.68-2.72 (m, 1H, NCH_2), 2.11-2.15 (m, 1H, $NCHCH_2$), 1.97-2.01 (m, 1H, NCH_2CH_2), 1.51 (s, 9H, $C(CH_3)_9$), 1.29-1.34 (m, 1H, (NCH_2CH_2), 0.25-0.27 (m, 1H, (NCHC**H**2), -0.94 (s, 3H, Al-C**H₃**), -1.28 (s, 3H, Al-C**H₃**). ^{13}C {^{1}H} NMR ($CDCl_3$, 500 MHz, 298 K) : *δ* (ppm) : ^{13}C {^{1}H} NMR ($CDCl_3$, 125 MHz, 298 K) : *δ* (ppm) : 159.89, 149.06, 146.81, 128.75, 128.18, 127.85, 127.58, 127.03, 126.77, 86.43, 81.02, 69.04, 49.14, 29.75, 28.95, 22.06, -8.67, -9.51. HRMS m/z calculated for $[M+NH_4]^+$ $C_{24}H_{32}NO_3AlNH_4$: 427.25 found 427.2529.

3.2 General polymerization procedure for ROCOP of epoxide and anhydride

The reaction for the ROCOP of epoxide and anhydride was performed in a oven dried glass reaction tube equipped with a magnetic stirring bar. The constituents of the reaction were weighed inside the glove box and mixed such that CHO : PA : Cat : Cocat. = 400:100:1:1 followed by the addition of 1mL of dry toluene. The reaction tube was sealed properly by applying grease and taken out of the glove box. The tube was dipped in an oil bath maintained at 100 °C. The progress of the reaction was monitored by the analysis of the ^{1}H NMR spectra of the aliquots taken at different time interval. After the desired time interval, the solvent was evaporated under vacuum. Upon removal of the solvent, the crude product was dissolved in dichloromethane and precipitated by the addition of cold methanol. The polymer was filtered and dried under vacuum until the pure product gave constant weight.

3.2.1 Kinetics for the ROCOP of CHO with PA respect to PA

In order to determine the order of the reaction with respect to phthalic anhydride the reactions were performed with CHO : PA : Cat : Cocat. = 400:100:1:1. The aliquots were taken at different time interval and it was observed that PA decreases linearly over time indicating reaction is zero order with respect to PA.[6]

3.2.2 Kinetics for the ROCOP of CHO with PA respect to CHO

In order to determine the order of the reaction with respect to CHO, the reactions were performed with CHO : PA : Cat : Cocat. = 400:100:1:1. The aliquots were taken at different time interval and amount of CHO reacted was determined at each time interval. The amount of CHO reacted was calculated by taking the integral for polyester linkage (δ = 4.80-5.26 ppm) and polyether linkage (δ = 3.22-3.64 ppm) relative to unreacted CHO (3.08 ppm). It was observed that the plot of $\ln([CHO]_0/[CHO]_t)$ versus time was linear indicating that the reaction is first order in concentration of monomer CHO.

3.2.3 Kinetics for the ROCOP of CHO with PA respect to catalyst

To determine the order of the reaction with respect to catalyst the reactions were performed such that CHO:PA:cocatalyst was kept constant to 400:100:1 and set of experiments were performed by varying the equivalents of catalyst from 0.5 to 2. In each case the percentage conversion of phthalic anhydride was determined by integrating the signals for unreacted PA (δ = 7.97 ppm) and phenylene signal in the polymer chain (7.30-7.83 ppm) at different time interval and initial rate (k_{obs}) was determined for each set of experiments, from the plot of $[PA]_t$ versus time. The plot of k_{obs} versus [cat] was linear.

3.2.4 Kinetics for the ROCOP of CHO with PA respect to cocatalyst

To determine the order of the reaction with respect to catalyst and the reactions were performed such that CHO:PA:catalyst was kept constant to 400:100:1 and set of experiments were performed by varying the equivalents of cocatalyst from 0.5 to 2. In each case the percentage conversion of phthalic anhydride was determined by integrating the signals for unreacted PA (δ = 7.97 ppm) and phenylene signal in the polymer chain (7.30-7.83 ppm) at different time interval and initial rate (k_{obs}) was determined for each set of experiments, from the plot of $[PA]_t$ versus time. The plot of k_{obs} versus [cat] was linear.

3.3 **Hydrolysis of poly(PA-*alt*-CHO) to *trans*-1,2-cyclohexanediol**

The hydrolysis of poly(PA-alt-CHO) was performed following the procedure reported previously in the literature.[7] The ^{1}H NMR spectra of the diol and sodium phthalate matched with the literature. The diol was subjected to HPLC analysis to determine the enantiomeric ratio.

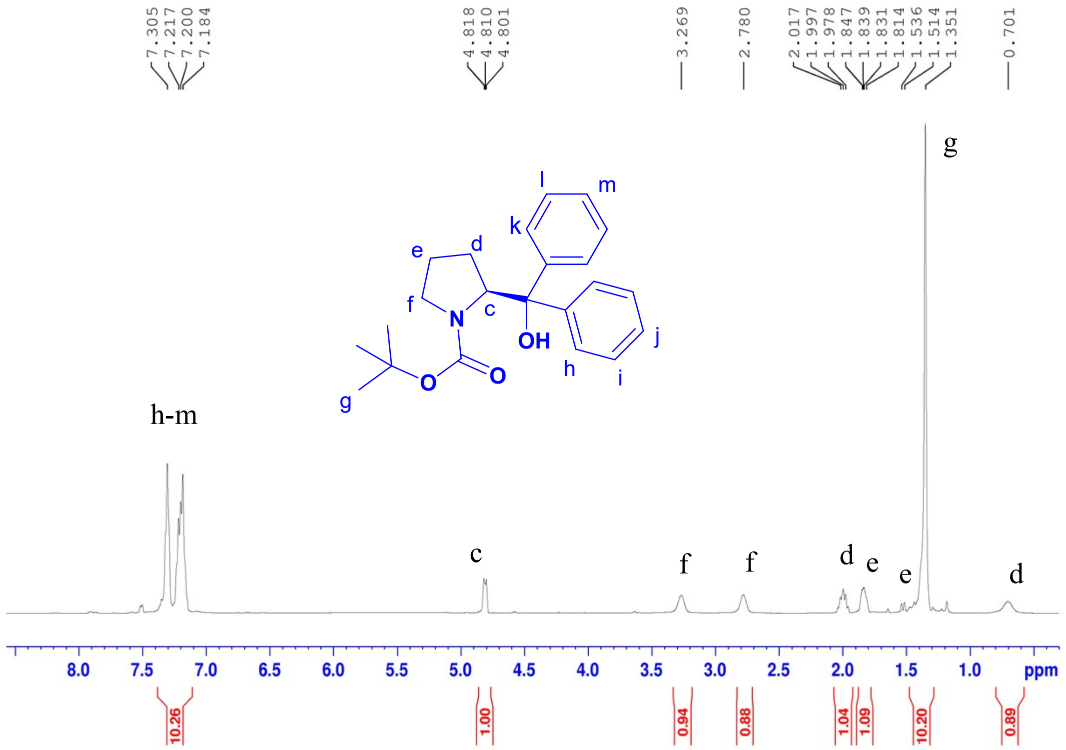

Fig. S1. ^{1}H NMR spectrum of **1a** in $CDCl_3$ (300 K).

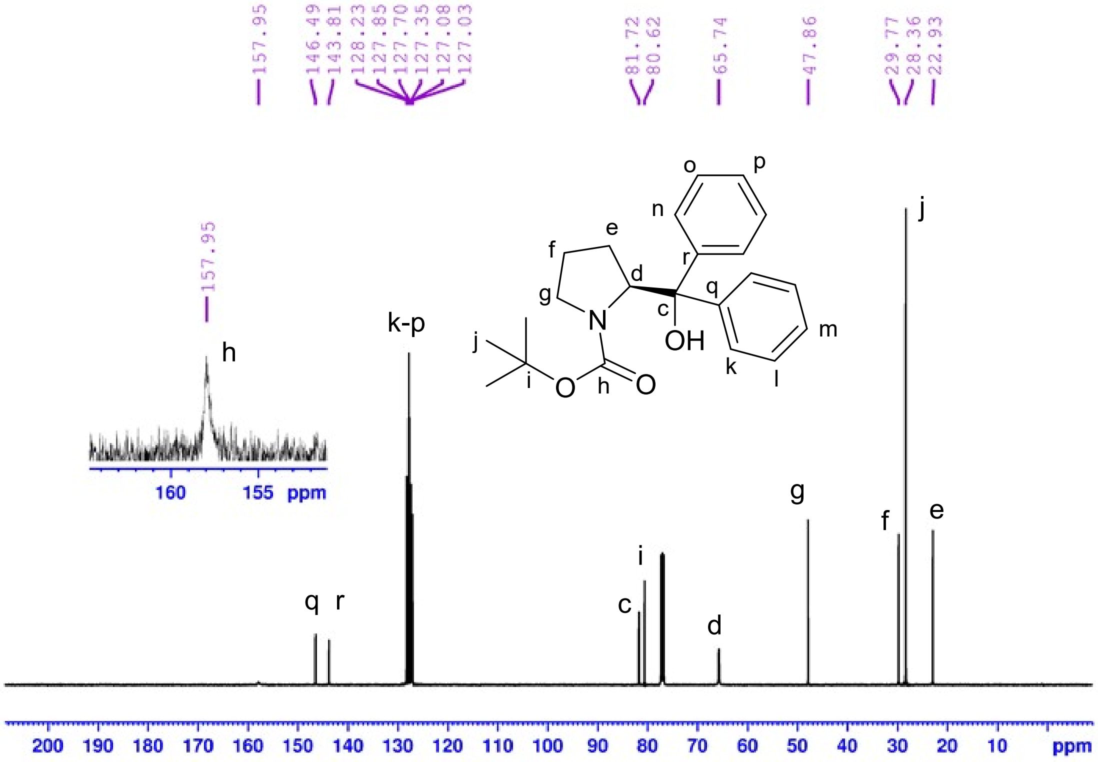

Fig. S2. ^{13}C NMR spectrum of **1a** in $CDCl_3$ (300 K).

Compound Details

Cpd. 1: C22 H27 N O3

Name	Formula	Mass m/z
	C22 H27 N O3	353.1988

Species	m/z
(M+H)+	354.2054
(M+Na)+	376.1883

Compound Spectra (overlaid)

Spectrum Peaks

m/z	Z	Diff (ppm)	Ion Species	Formula
354.2054	1	-2.82	(M+H)+	C22H27NO3
355.2085	1	-3.43	(M+H)+	C22H27NO3
376.1883	1	-0.11	(M+Na)+	C22H27NO3
377.1910	1	-1.52	(M+Na)+	C22H27NO3
378.1928	1	-4.56	(M+Na)+	C22H27NO3
379.1917	1	-14.74	(M+Na)+	C22H27NO3

Compound ID Table

Cpd Key	Formula	Mass	Cal. Mass	Species	Diff (mDa)
3084	C22 H27 N O3	353.1988	353.1991	(M+H)+ (M+Na)+	-0.3

Compound Spectra

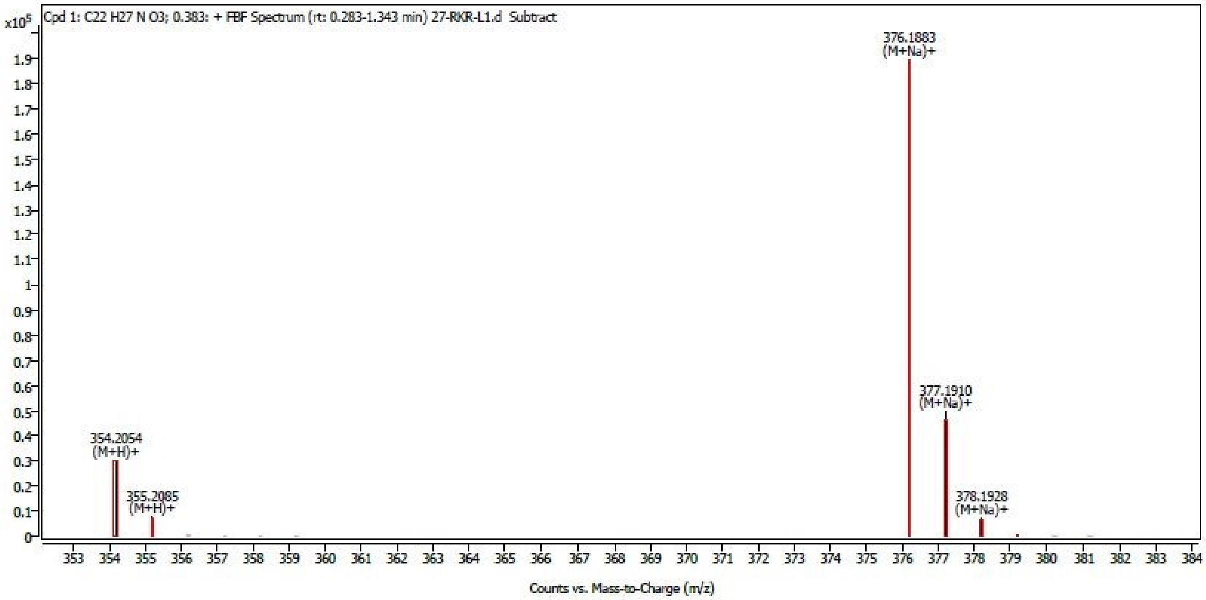

Fig. S3. HRMS spectrum of **1a.**

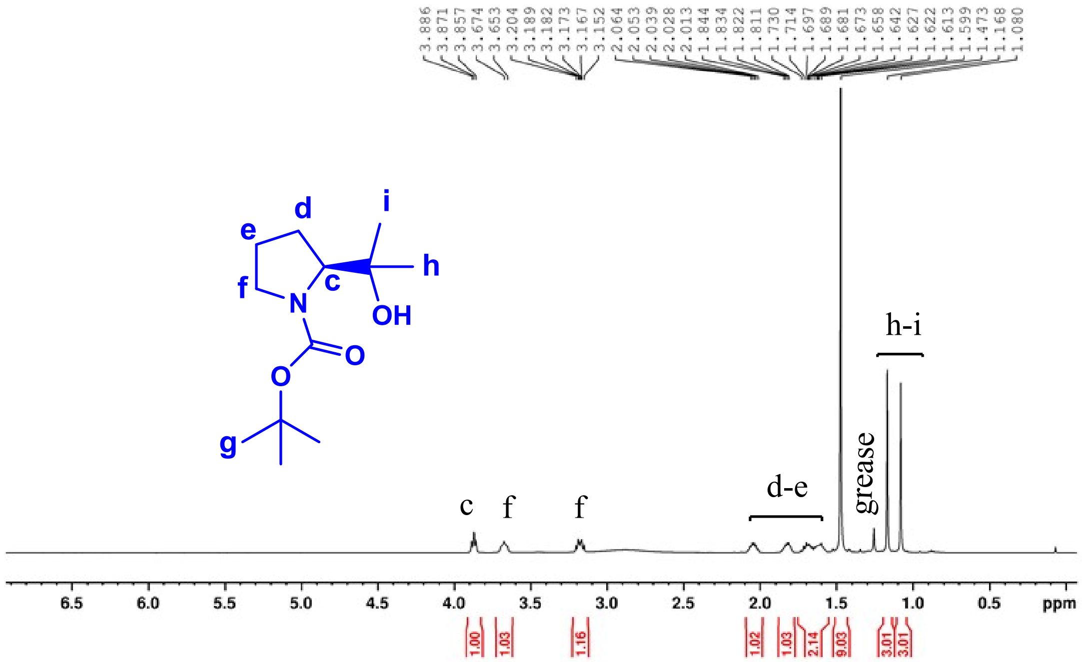

Fig. S4. ^{1}H NMR spectrum of **1b** in $CDCl_3$ (300K).

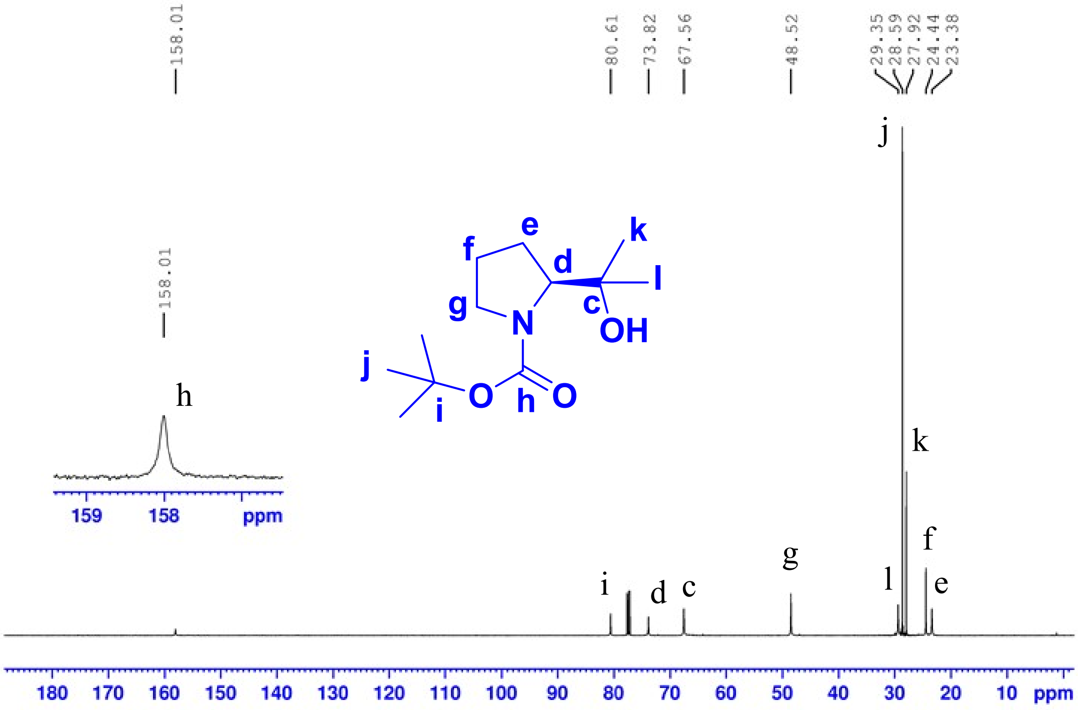

Fig. S5. ^{13}C NMR spectrum of **1b** in $CDCl_3$ (300K).

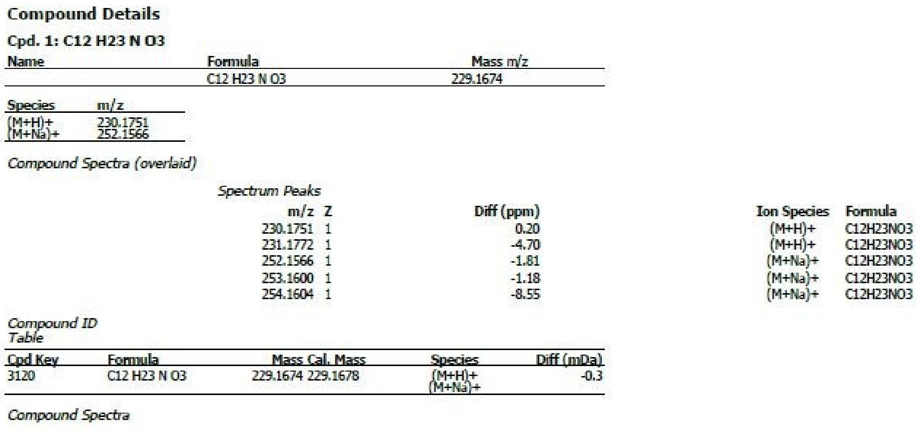

Compound Details

Cpd. 1: C12 H23 N O3

Name	Formula	Mass m/z
	C12 H23 N O3	229.1674

Species	m/z
(M+H)+	230.1751
(M+Na)+	252.1566

Compound Spectra (overlaid)

Spectrum Peaks

m/z	Z	Diff (ppm)	Ion Species	Formula
230.1751	1	0.20	(M+H)+	C12H23NO3
231.1772	1	-4.70	(M+H)+	C12H23NO3
252.1566	1	-1.81	(M+Na)+	C12H23NO3
253.1600	1	-1.18	(M+Na)+	C12H23NO3
254.1604	1	-8.55	(M+Na)+	C12H23NO3

Compound ID Table

Cpd Key	Formula	Mass	Cal. Mass	Species	Diff (mDa)
3120	C12 H23 N O3	229.1674	229.1678	(M+H)+ (M+Na)+	-0.3

Compound Spectra

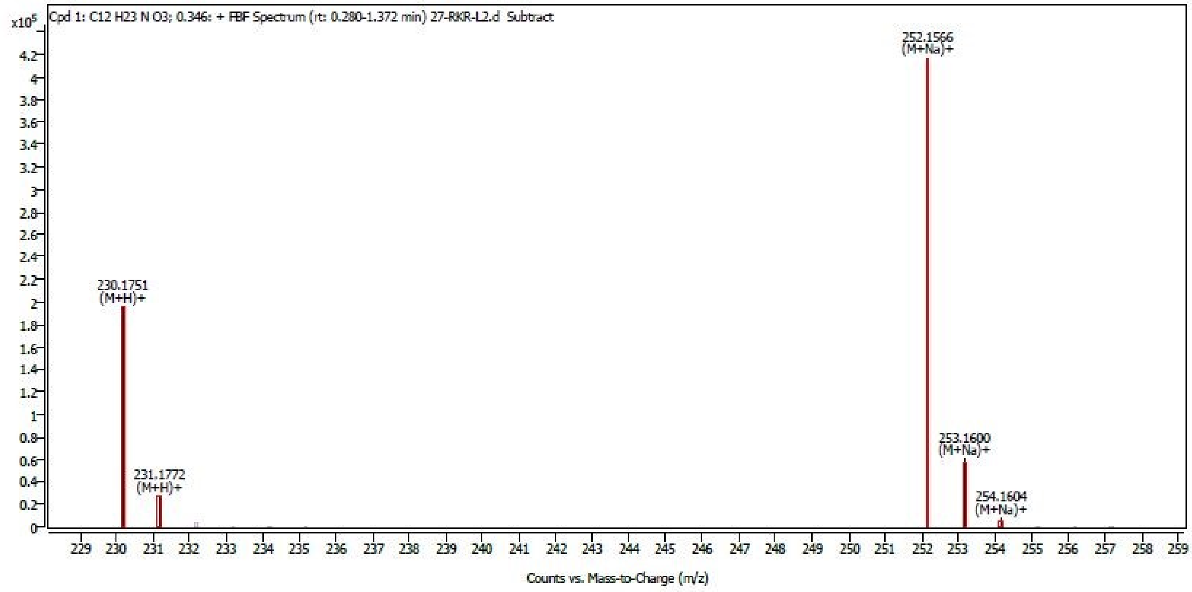

Fig. S6. HRMS spectrum of **1b**.

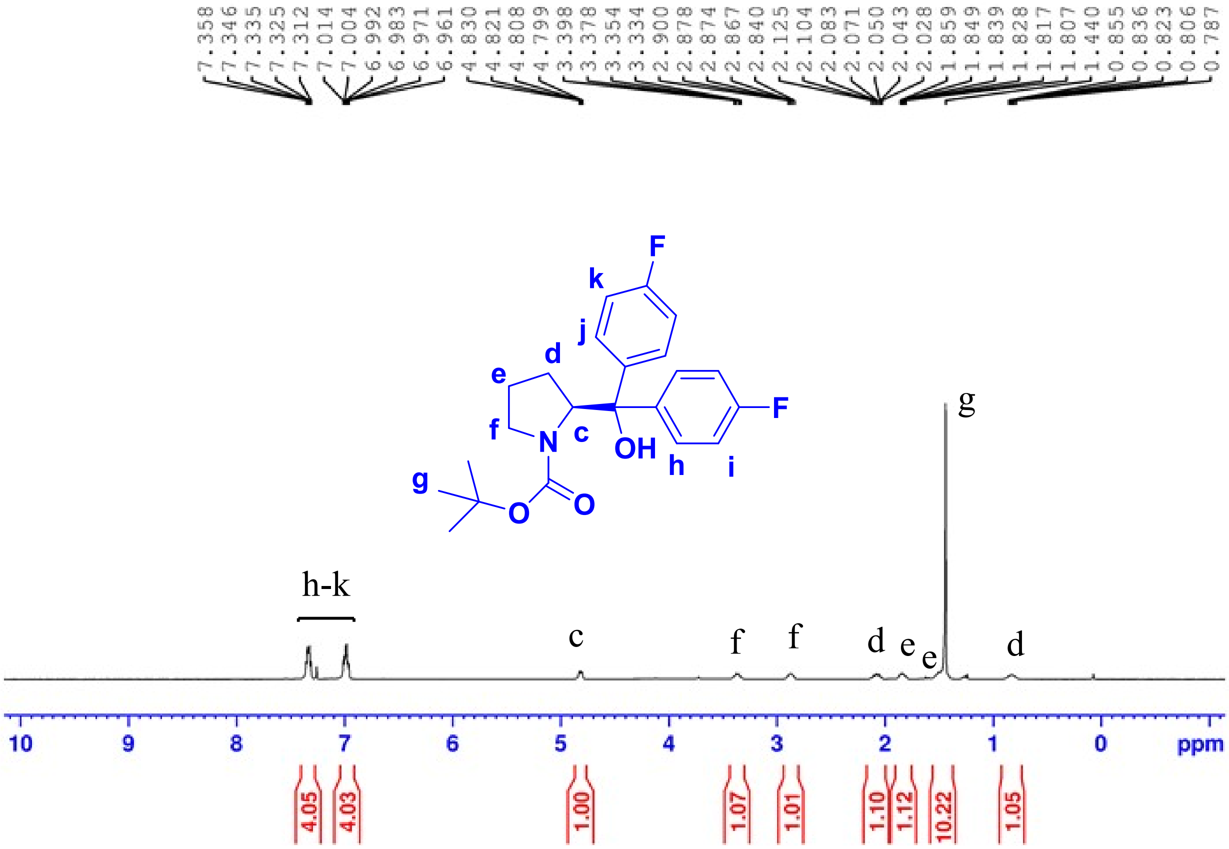

Fig. S7. ^{1}H NMR spectrum of **1c** in CDCl$_3$ (300K).

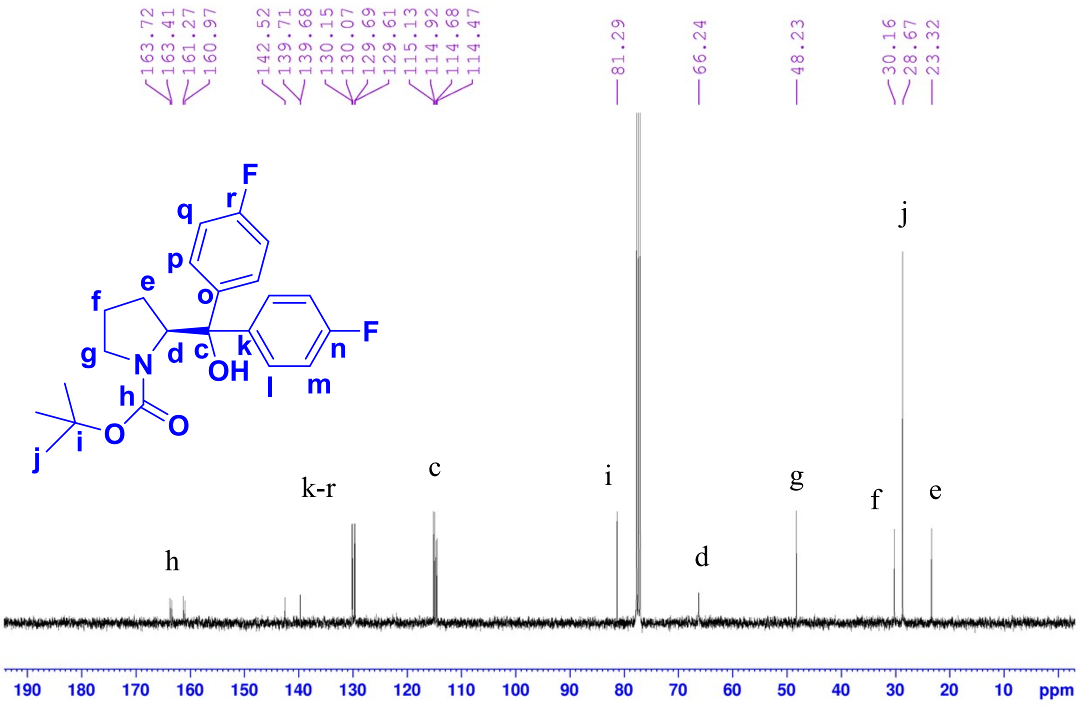

Fig. S8. ^{13}C NMR spectrum of **1c** in $CDCl_3$ (300K).

Compound Details

Cpd. 1: C22 H25 F2 N O3

Name	Formula	Mass m/z
	C22 H25 F2 N O3	389.1787

Species	m/z
(M+H)+	390.1831
(M+NH4)+	407.2129
(M+Na)+	412.1685

Compound Spectra (overlaid)

Spectrum Peaks

m/z	Z	Diff (ppm)	Ion Species	Formula
390.1831	1	-11.44	(M+H)+	C22H25F2NO3
391.1855	1	-13.58	(M+H)+	C22H25F2NO3
392.2011	1	18.95	(M+H)+	C22H25F2NO3
407.2129	1	-2.96	(M+NH4)+	C22H25F2NO3
412.1685	1	-2.46	(M+Na)+	C22H25F2NO3
413.1708	1	-4.78	(M+Na)+	C22H25F2NO3
414.1684	1	-17.55	(M+Na)+	C22H25F2NO3

Compound ID Table

Cpd Key	Formula	Mass	Cal. Mass	Species	Diff (mDa)
3152	C22 H25 F2 N O3	389.1787	389.1803	(M+H)+ (M+NH4)+ (M+Na)+	-1.6

Compound Spectra

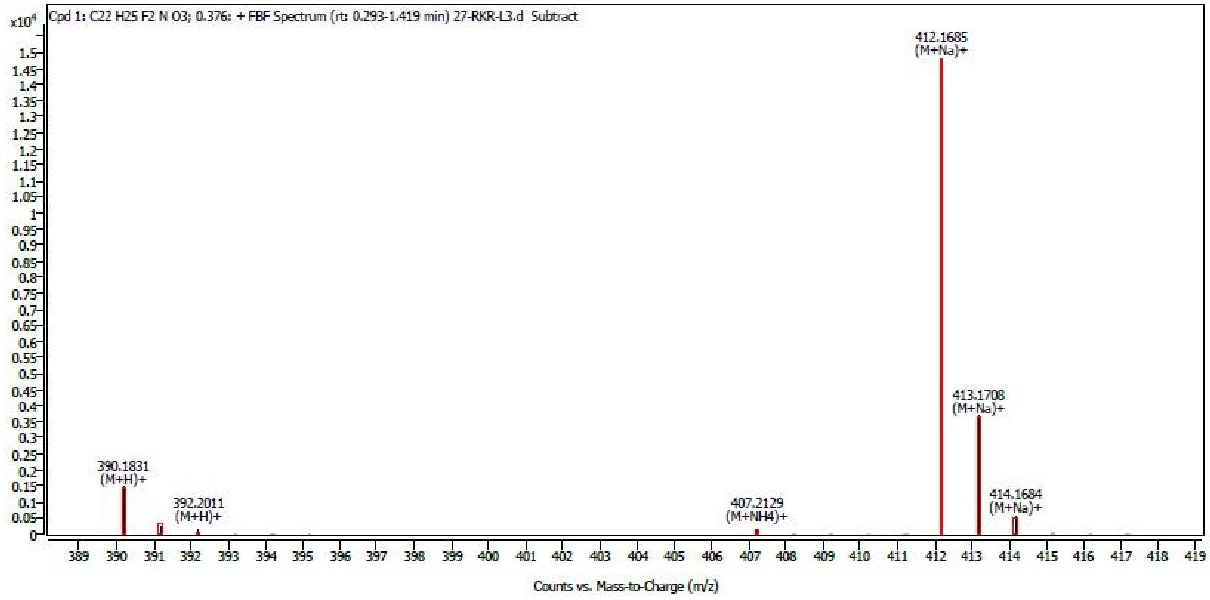

Fig. S9. HRMS spectrum of **1c**.

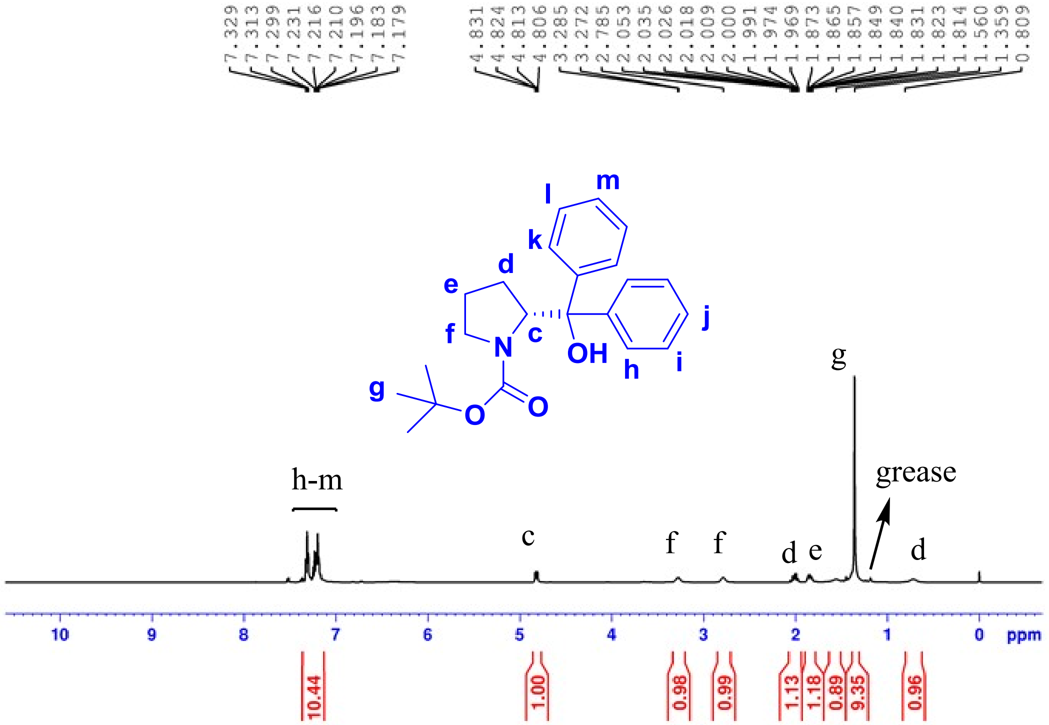

Fig. S10. ^{1}H NMR spectrum of **1d** in $CDCl_3$ (300K).

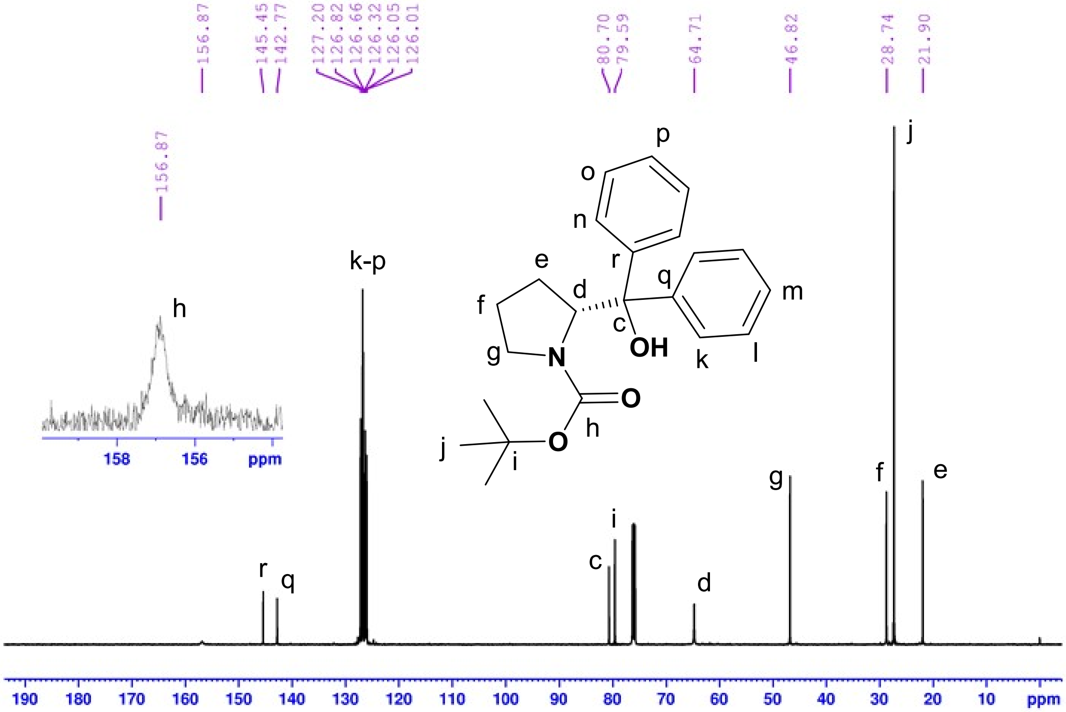

Fig. S11. ^{13}C NMR spectrum of **1d** in $CDCl_3$ (300K).

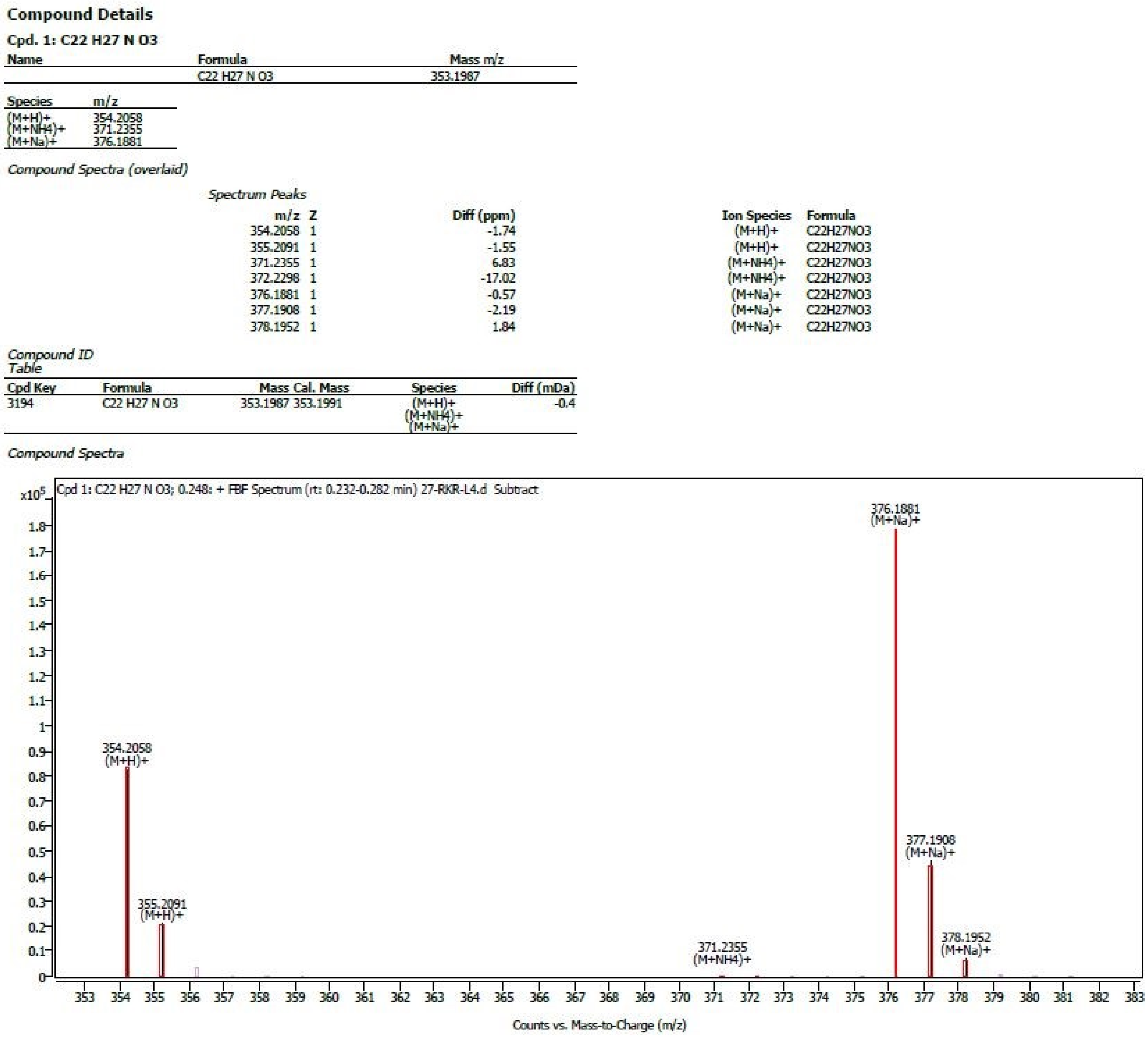

Compound Details

Cpd. 1: C22 H27 N O3

Name	Formula	Mass m/z
	C22 H27 N O3	353.1987

Species	m/z
(M+H)+	354.2058
(M+NH4)+	371.2355
(M+Na)+	376.1881

Compound Spectra (overlaid)

Spectrum Peaks

m/z	Z	Diff (ppm)	Ion Species	Formula
354.2058	1	-1.74	(M+H)+	C22H27NO3
355.2091	1	-1.55	(M+H)+	C22H27NO3
371.2355	1	6.83	(M+NH4)+	C22H27NO3
372.2298	1	-17.02	(M+NH4)+	C22H27NO3
376.1881	1	-0.57	(M+Na)+	C22H27NO3
377.1908	1	-2.19	(M+Na)+	C22H27NO3
378.1952	1	1.84	(M+Na)+	C22H27NO3

Compound ID Table

Cpd Key	Formula	Mass	Cal. Mass	Species	Diff (mDa)
3194	C22 H27 N O3	353.1987	353.1991	(M+H)+ (M+NH4)+ (M+Na)+	-0.4

Compound Spectra

Fig. S12. HRMS spectrum of **1d**.

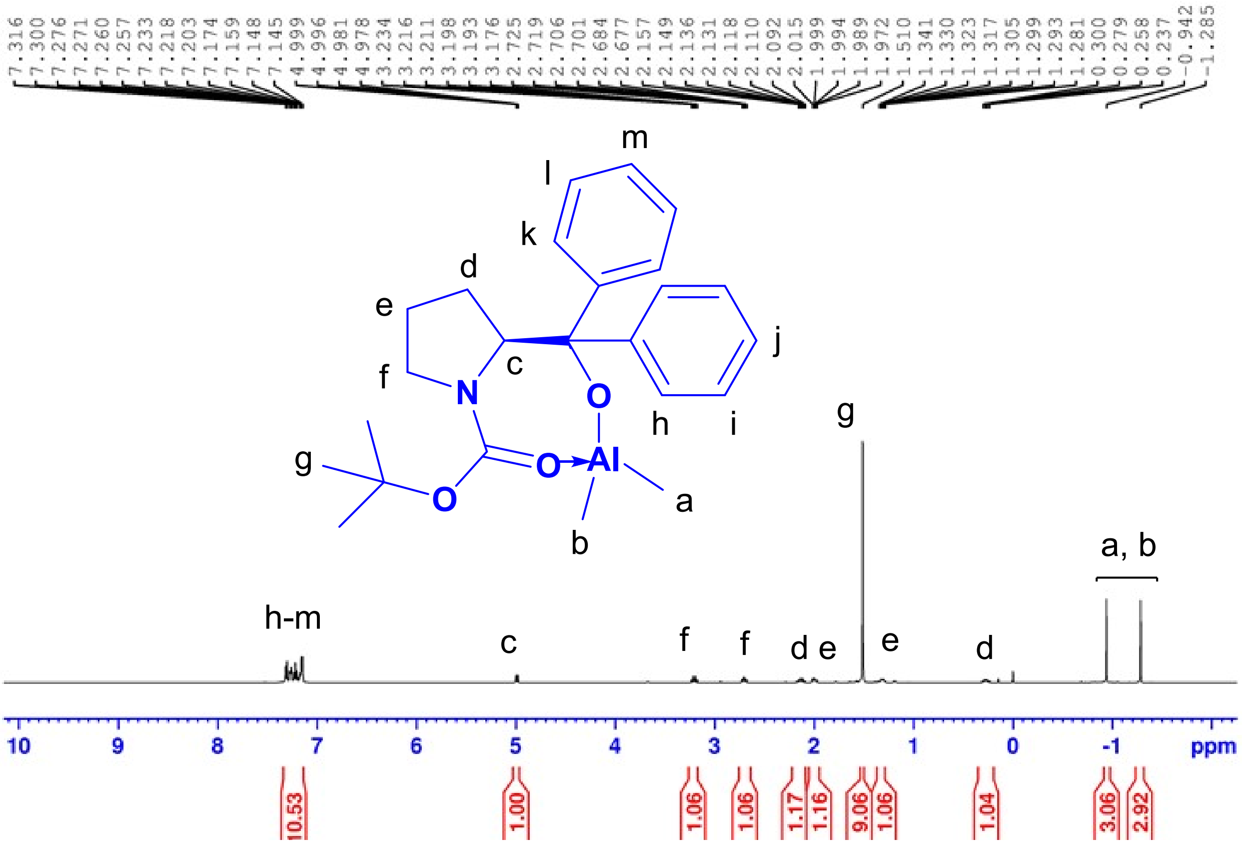

Fig. S13. ^{1}H NMR spectrum of **2a** in $CDCl_3$ (300K).

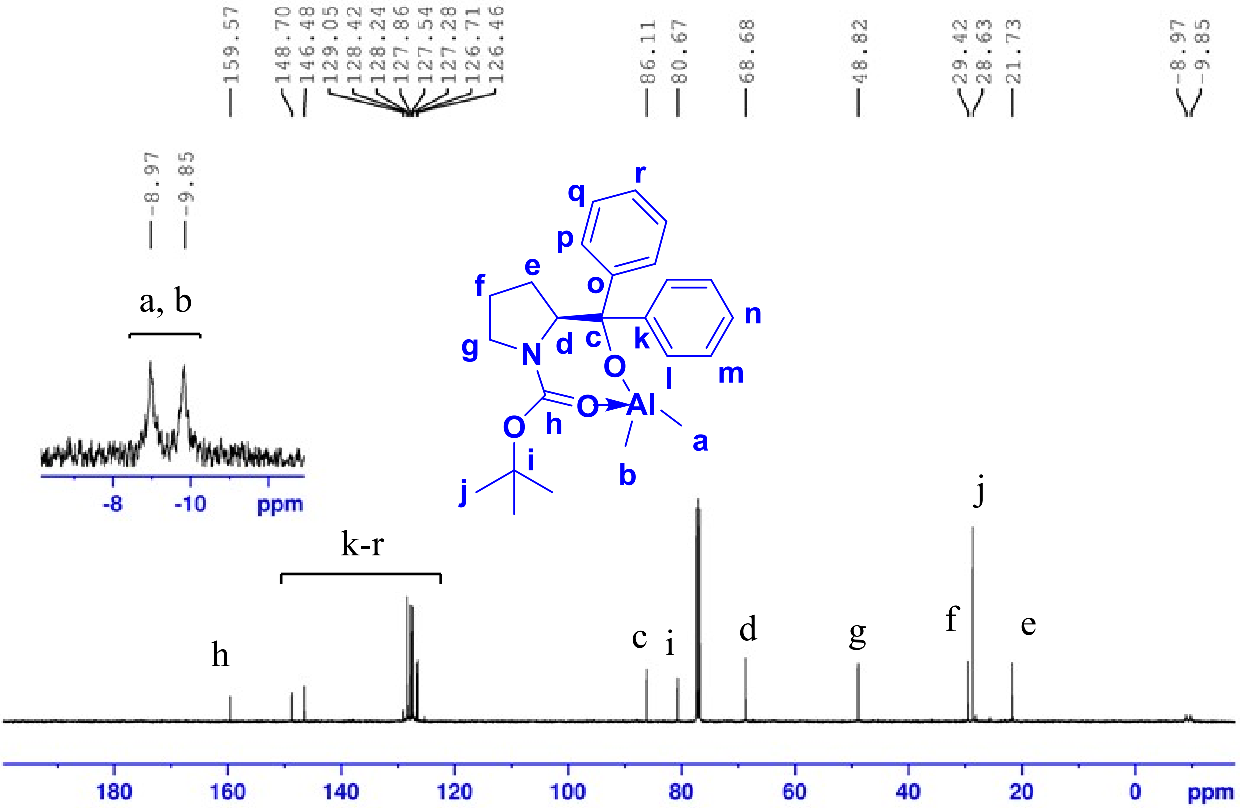

Fig. S14. ^{13}C NMR spectrum of **2a** in $CDCl_3$ (300K).

HRMS DST-FIST Funded, Department of Chemistry, IIT Madras

ESI Mass Report

Name	09022024-DC	**Data File Path**	D:\MassHunter\Data\2024\FEB\DC\RKR-AL-1.d
Sample ID		**Acq. Time (Local)**	09-02-2024 11:23:14 (UTC+05:30)
Instrument	Instrument 1	**Method Path (Acq)**	D:\MassHunter\Methods\TRIALS\FIA_POS_organic_02.m
MS Type	QTOF	**Version (Acq SW)**	6200 series TOF/6500 series Q-TOF 10.1 (48.0)
Inj. Vol. (ul)	0.5	**IRM Status**	Success
Position	P2-F11	**Method Path (DA)**	D:\MassHunter\Methods\10.0\PROCESSING_01.m
Plate Pos.		**Target Source Path**	
Operator		**Result Summary**	1 qualified (1 targets)

Compound Details

Cpd. 1: C24 H32 Al N O3

Compound Spectra (overlaid)

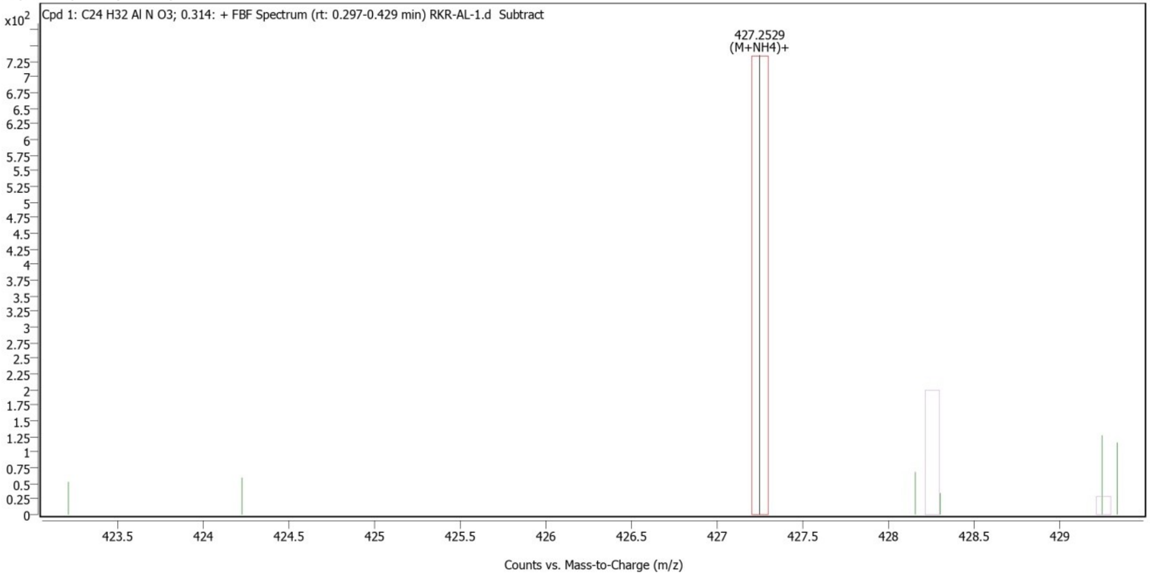

Compound ID Table

Cpd	Formula	Mass (Tgt)	Calc. Mass	Mass	Species	Diff(Tgt.ppm)	mDa
1	C24 H32 Al N O3	409.2198	409.2191	427.2529	(M+NH4)+	-1.65	-0.67

Fig. S15. HRMS spectrum of **2a**.

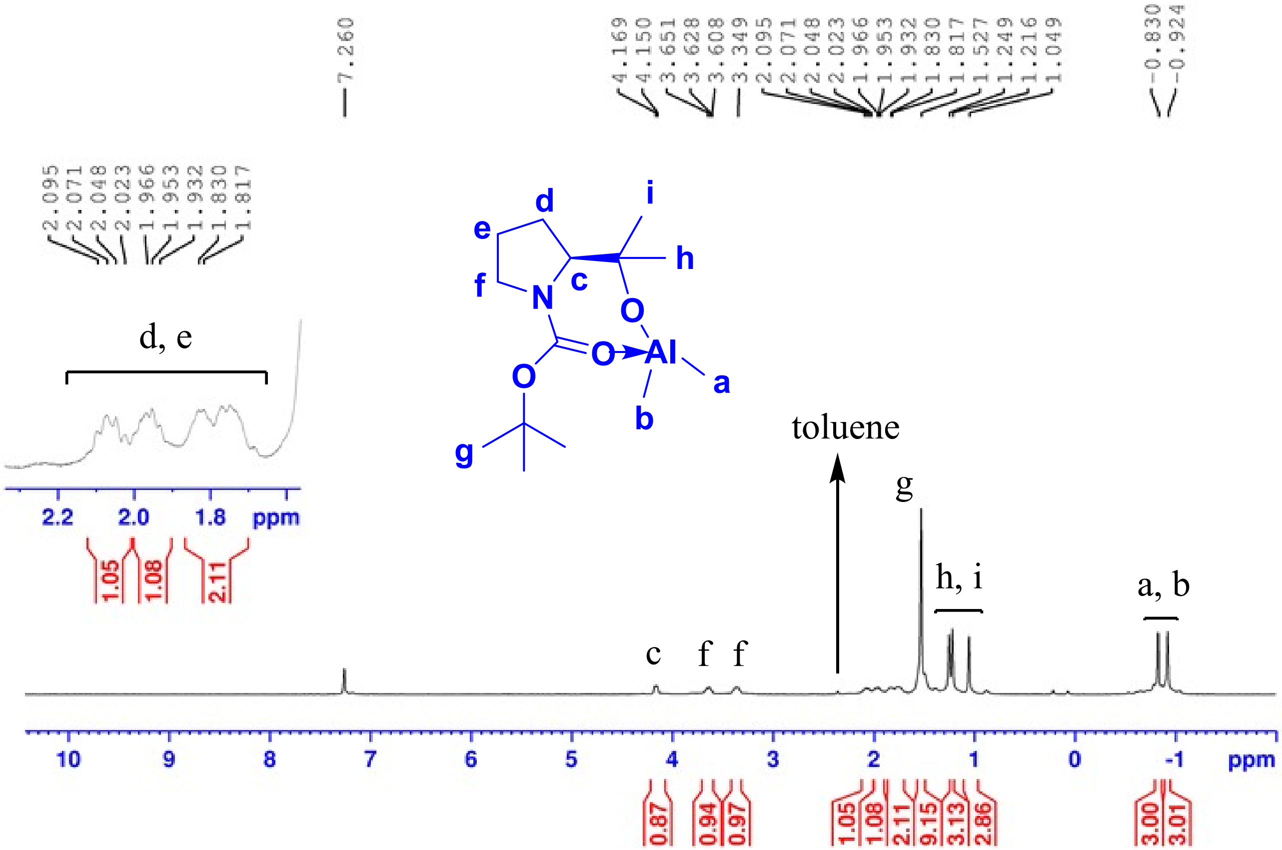

Fig. S16. ^{1}H NMR spectrum of **2b** in $CDCl_3$ (300K).

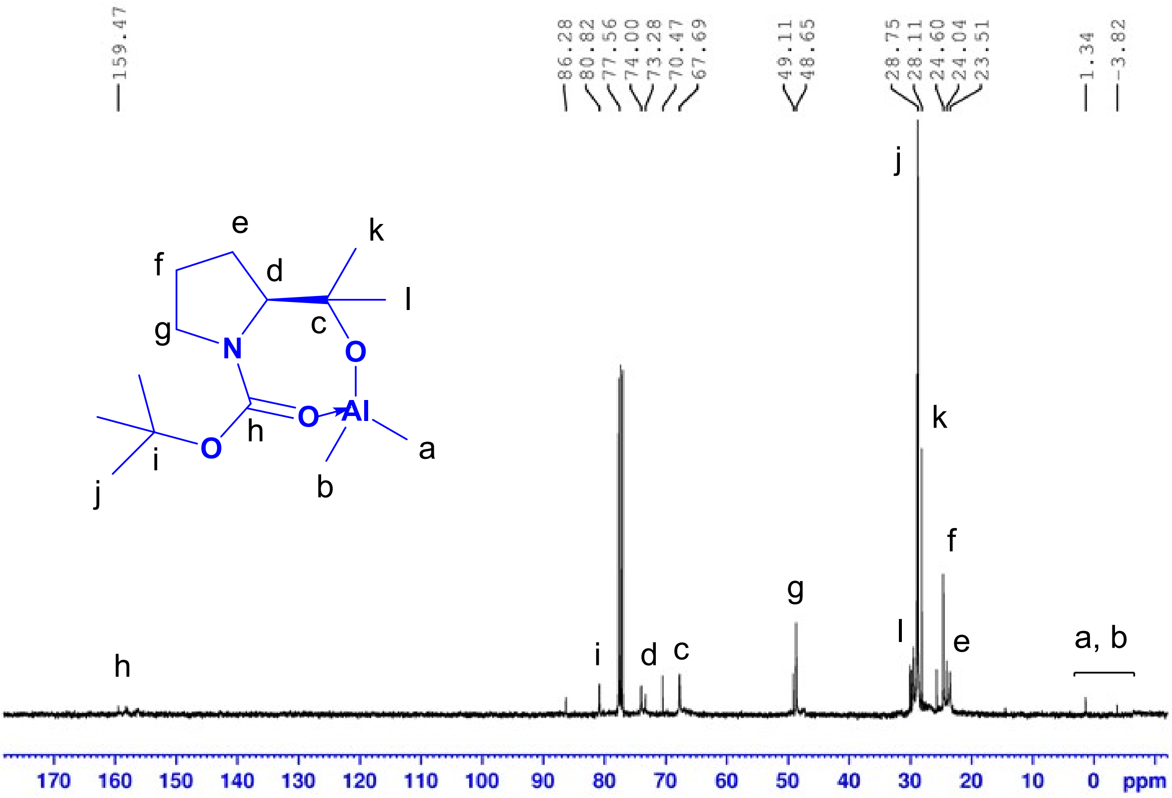

Fig. S17. ^{13}C NMR spectrum of **2b** in $CDCl_3$ (300K).

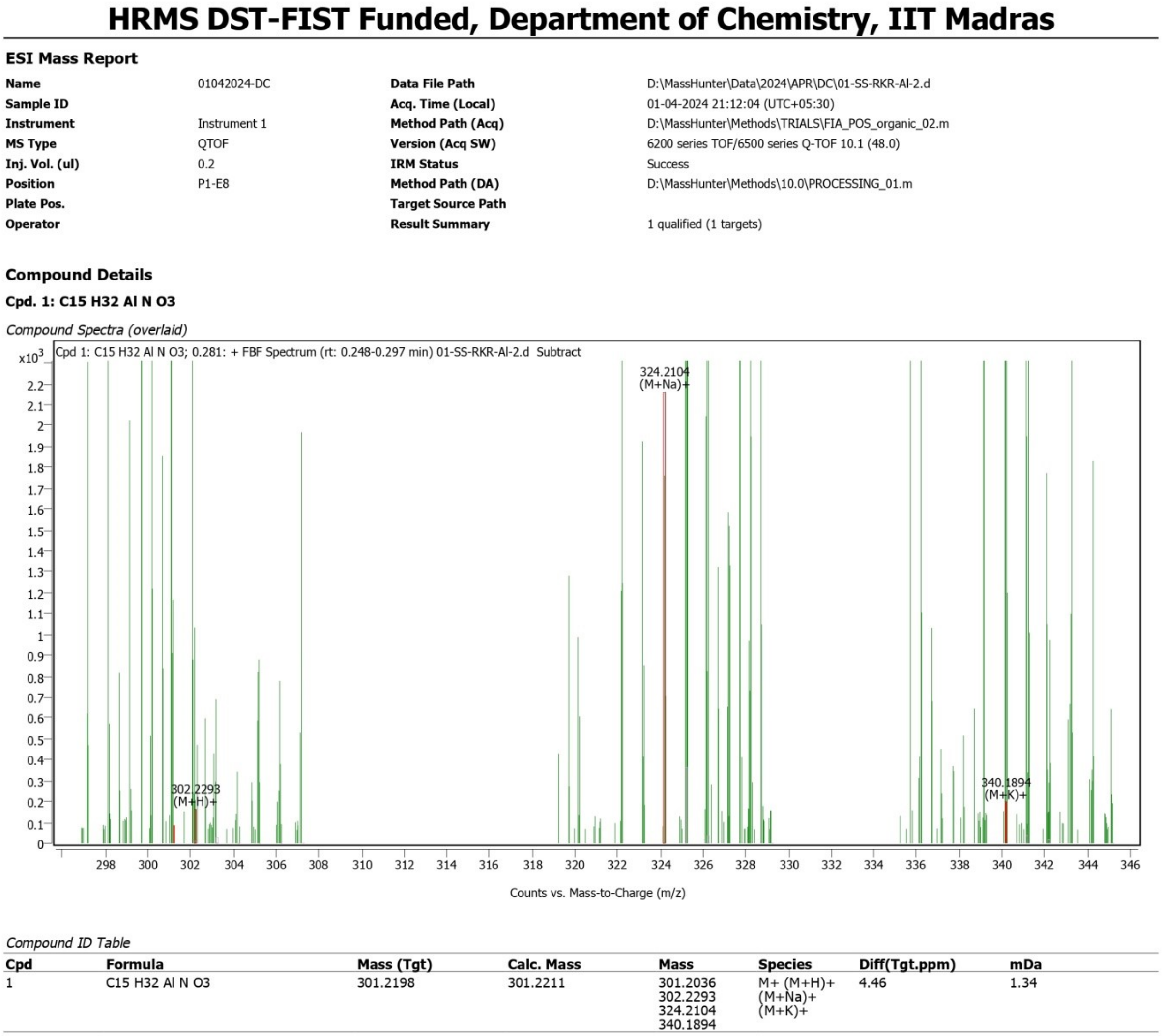

HRMS DST-FIST Funded, Department of Chemistry, IIT Madras

ESI Mass Report

Name	01042024-DC	**Data File Path**	D:\MassHunter\Data\2024\APR\DC\01-SS-RKR-Al-2.d
Sample ID		**Acq. Time (Local)**	01-04-2024 21:12:04 (UTC+05:30)
Instrument	Instrument 1	**Method Path (Acq)**	D:\MassHunter\Methods\TRIALS\FIA_POS_organic_02.m
MS Type	QTOF	**Version (Acq SW)**	6200 series TOF/6500 series Q-TOF 10.1 (48.0)
Inj. Vol. (ul)	0.2	**IRM Status**	Success
Position	P1-E8	**Method Path (DA)**	D:\MassHunter\Methods\10.0\PROCESSING_01.m
Plate Pos.		**Target Source Path**	
Operator		**Result Summary**	1 qualified (1 targets)

Compound Details

Cpd. 1: C15 H32 Al N O3

Compound Spectra (overlaid)

Compound ID Table

Cpd	Formula	Mass (Tgt)	Calc. Mass	Mass	Species	Diff(Tgt.ppm)	mDa
1	C15 H32 Al N O3	301.2198	301.2211	301.2036 302.2293 324.2104 340.1894	M+ (M+H)+ (M+Na)+ (M+K)+	4.46	1.34

Fig. S18. HRMS spectrum of **2b**.

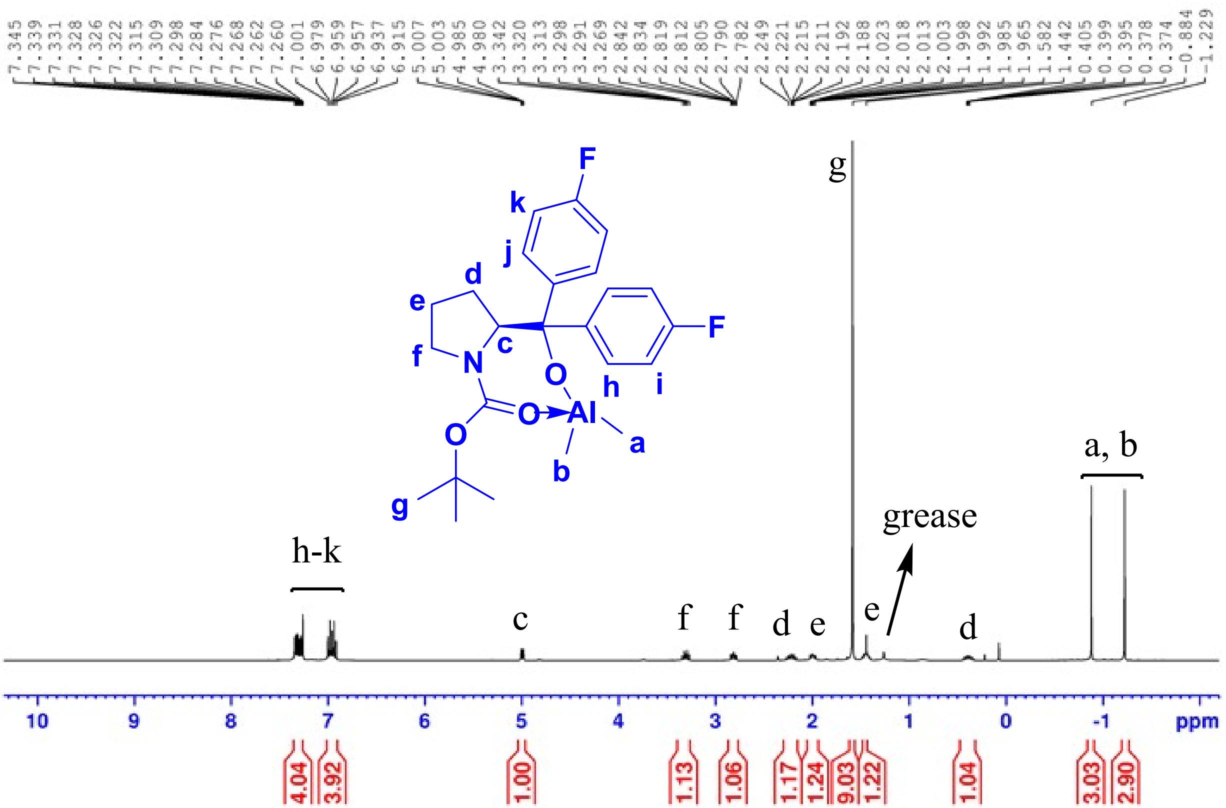

Fig. S19. ^{1}H NMR spectrum of **2c** in $CDCl_3$ (300K).

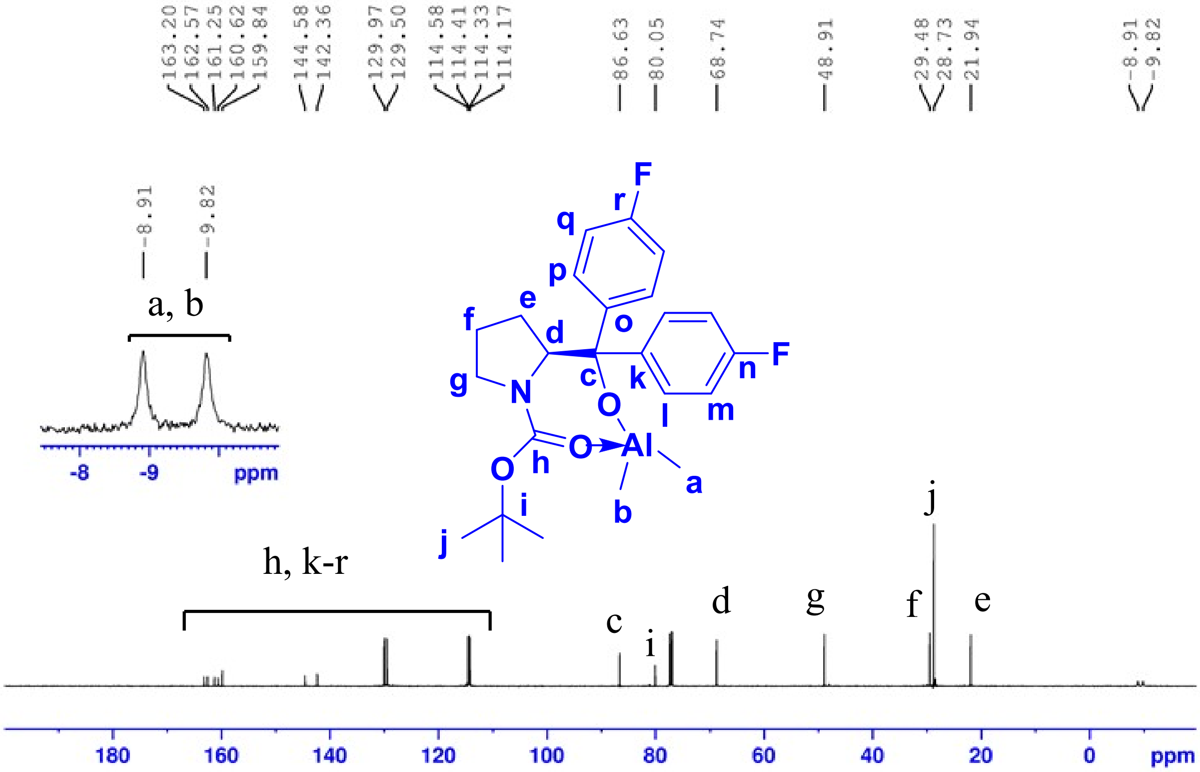

Fig. S20. ^{13}C NMR spectrum of **2c** in CDCl$_3$ (300K).

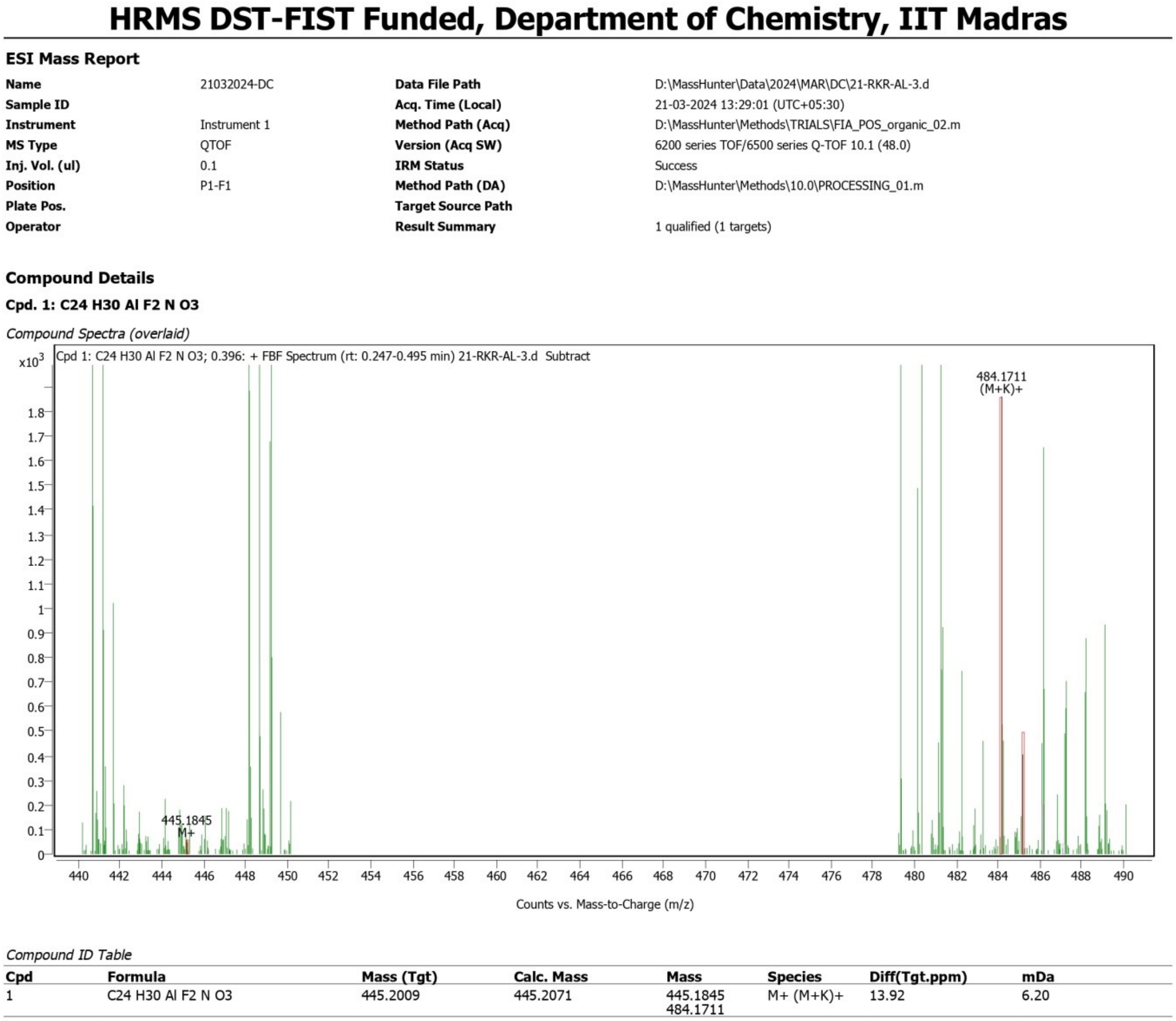

HRMS DST-FIST Funded, Department of Chemistry, IIT Madras

ESI Mass Report

Name	21032024-DC	**Data File Path**	D:\MassHunter\Data\2024\MAR\DC\21-RKR-AL-3.d
Sample ID		**Acq. Time (Local)**	21-03-2024 13:29:01 (UTC+05:30)
Instrument	Instrument 1	**Method Path (Acq)**	D:\MassHunter\Methods\TRIALS\FIA_POS_organic_02.m
MS Type	QTOF	**Version (Acq SW)**	6200 series TOF/6500 series Q-TOF 10.1 (48.0)
Inj. Vol. (ul)	0.1	**IRM Status**	Success
Position	P1-F1	**Method Path (DA)**	D:\MassHunter\Methods\10.0\PROCESSING_01.m
Plate Pos.		**Target Source Path**	
Operator		**Result Summary**	1 qualified (1 targets)

Compound Details

Cpd. 1: C24 H30 Al F2 N O3

Compound Spectra (overlaid)

Compound ID Table

Cpd	Formula	Mass (Tgt)	Calc. Mass	Mass	Species	Diff(Tgt.ppm)	mDa
1	C24 H30 Al F2 N O3	445.2009	445.2071	445.1845 484.1711	M+ (M+K)+	13.92	6.20

Fig. S21. HRMS spectrum of **2c**.

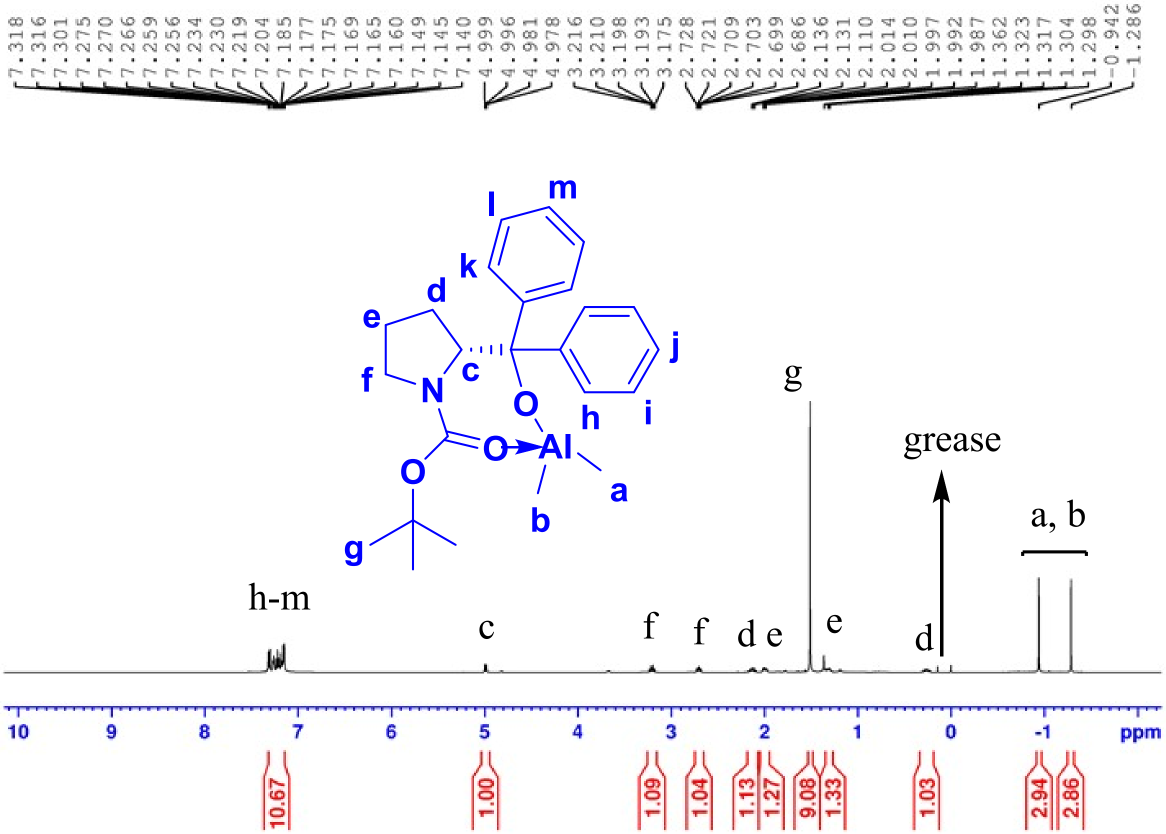

Fig. S22. ^{1}H NMR spectrum of **2d** in $CDCl_3$ (300K).

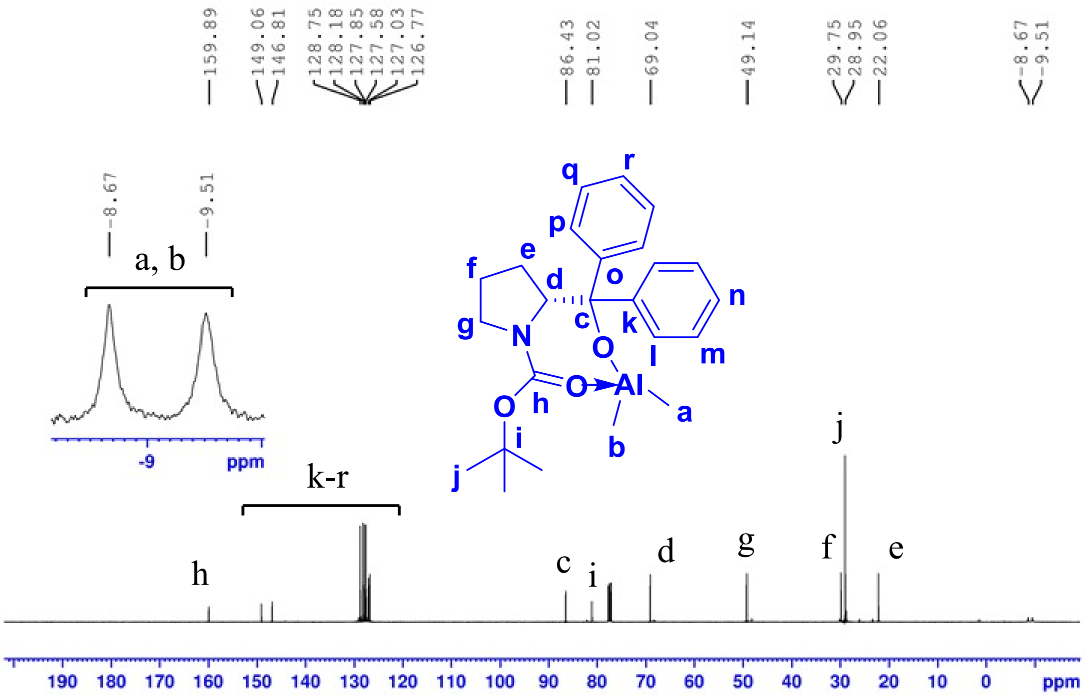

Fig. S23. ^{13}C NMR spectrum of **2d** in $CDCl_3$ (300K).

Fig. S24. HRMS spectrum of **2d**.

Table S1. Crystal data for ligand **1a**.

Compound	**1a**
Molecular formula	$C_{22}H_{27}NO_3$
Formula weight	353.44 g/mol
T/K	100(2)
Wavelength (Å)	0.71073
Crystal system,	Orthorhombic
Space group	$P2_12_12_1$
a/ Å	8.9084(5)
b/ Å	9.6525(7)
c/ Å	22.6244(15)
α (°)	90.00
β (°)	90.00
γ (°)	90.00
V/ $Å^3$	1945.4(2)
Z, Calculated density (Mg/m^3)	4, 1.207
Absorption coefficient(mm^{-1})	0.080
θ range/°	3.240 to 30.518
Reflections collected	50541
Unique Independent reflections	5941 [R(int) = 0.0317]
Data/restraints/parameters	5941 / 0 / 238
Goodness-of-fit on F^2	1.051
Final R indices [$I > 2\sigma(I)$]	R1 = 0.0359, wR2 = 0.0944
R indices (all data)	R1 = 0.0380, wR2 = 0.0958
Max. and min. transmission	0.7461 and 0.6871

$R_1 = \sum|F_0| - |F_c|/\sum|F_0|$, $wR_2 = [\sum (F_0^2 - F_c^2)^2/\sum w(F_0^2)^2]^{1/2}$

Table S2. Crystallographic data and details of refinement for compounds **2a**, **2c** and **2d**.

Compounds	**2a**	**2c**	**2d**
Molecular formula	$C_{52}H_{72}Al_2N_2O_7$	$C_{31}H_{38}AlNO_3F_2$	$C_{31}H_{40}AlNO_3$
Formula weight	891.07 g/mol	537.60 g/mol	501.62 g/mol
T/K	120(2)	110(2)	100(2)
Wavelength (Å)	0.71073	0.71073	0.71073
Crystal system,	Trigonal	Monoclinic	Orthorhombic
Space group	$P3_221$	$P2_1$	$P2_12_12_1$
a/ Å	9.466(2)	13.2631(7)	9.4226(4)
b/ Å	9.466(2)	7.2788(5)	14.8275(5)
c/ Å	49.901(10)	15.3502(9)	20.4148(8)
α (°)	90.00(3)	90	90
β (°)	90.00(3)	100.335(2)	90
γ (°)	120.00(3)	90	90
V/ $Å^3$	3872.6(18)	1457.86(15)	2852.23(19)
Z, Calculated density (Mg/m^3)	3, 1.146	2, 1.225	4, 1.168
Absorption coefficient(mm^{-1})	0.106	0.114	0.102
θ range/°	2.518 to 25.418	3.172 to 28.706	2.747 to 25.499
Reflections collected	90594	49752	65234
Unique Independent reflections	4816 [R(int) = 0.0813]	7501 [R(int) = 0.0439]	5306 [R(int) = 0.0625]
Data/restraints/parameters	4816 / 65 / 308	7501 / 1 / 343	5306 / 230 / 359
Goodness-of-fit on F2	1.180	1.030	1.074
Final R indices [$I>2\sigma(I)$]	R1 = 0.0591, wR2 = 0.1369	R1 = 0.0356, wR2 = 0.0946	R1 = 0.0360, wR2 = 0.0872
R indices (all data)	R1 = 0.0641, wR2 = 0.1400	R1 = 0.0373, wR2 = 0.0962	R1 = 0.0391, wR2 = 0.0891
Max. and min. transmission	0.7455 and 0.6776	0.7458 and 0.5680	0.963 and 0.946

$R_1 = \sum|F_0| - |F_c|/\sum|F_0|$, $wR_2 = [\sum (F_0^2 - F_c^2)^2/\sum w(F_0^2)^2]^{1/2}$

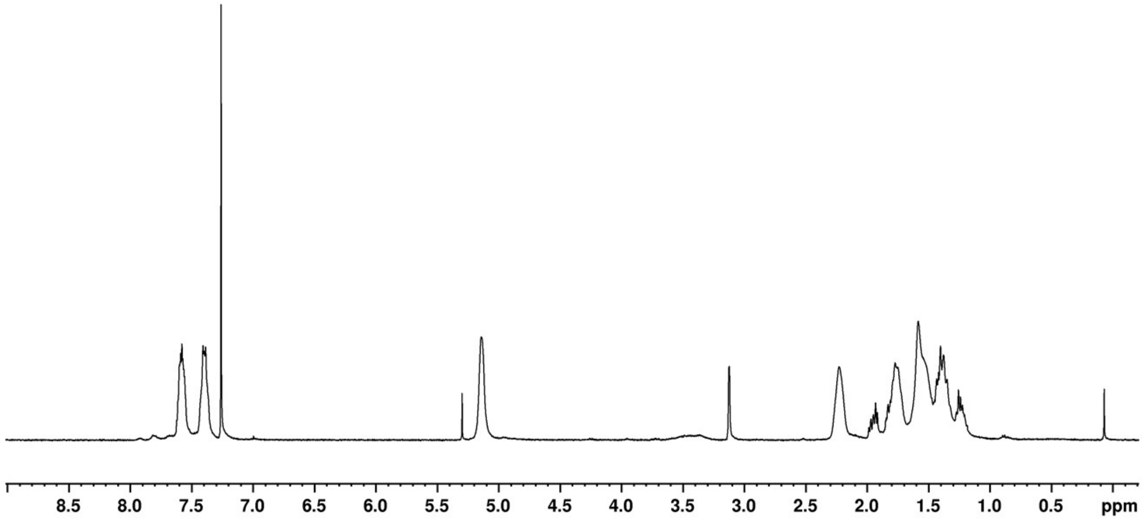

Fig. S25. ^{1}H NMR ($CDCl_3$) spectrum of the crude polyester of CHO/PA with **2a**/TPPCl in neat condition (Table 1, Entry 4).

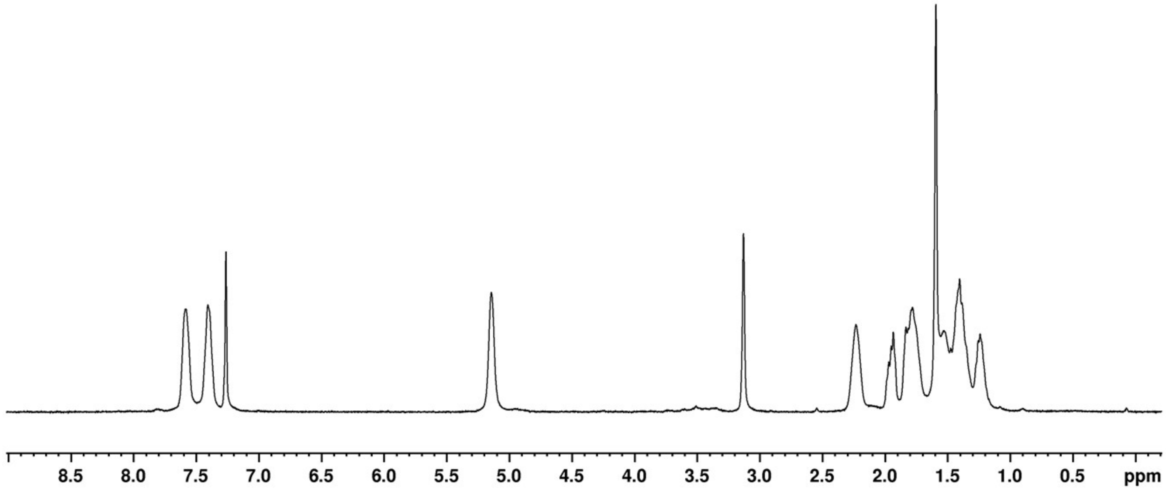

Fig. S26. ^{1}H NMR ($CDCl_3$) spectrum of the crude polyester of CHO/PA with **2b**/TPPCl in neat condition (Table 1, Entry 5).

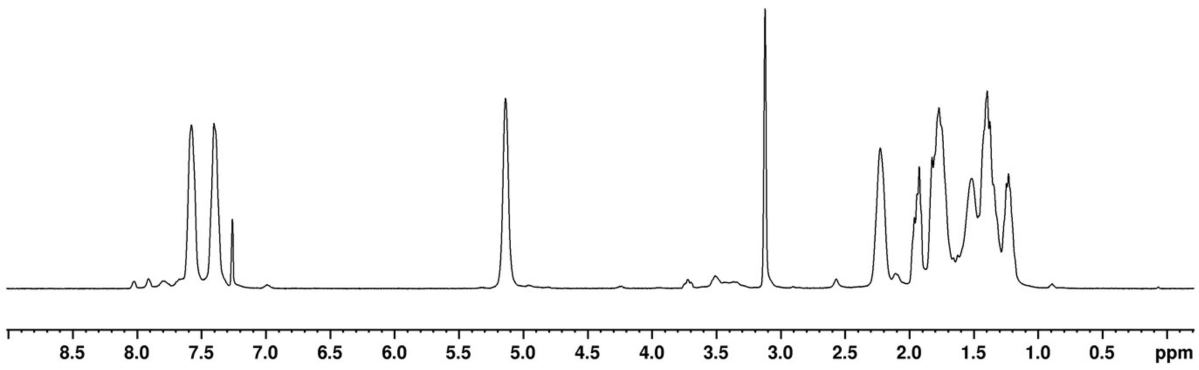

Fig. S27. ^{1}H NMR ($CDCl_3$) spectrum of the crude polyester of CHO/PA with **2c**/TPPCl in neat condition (Table 1, Entry 6).

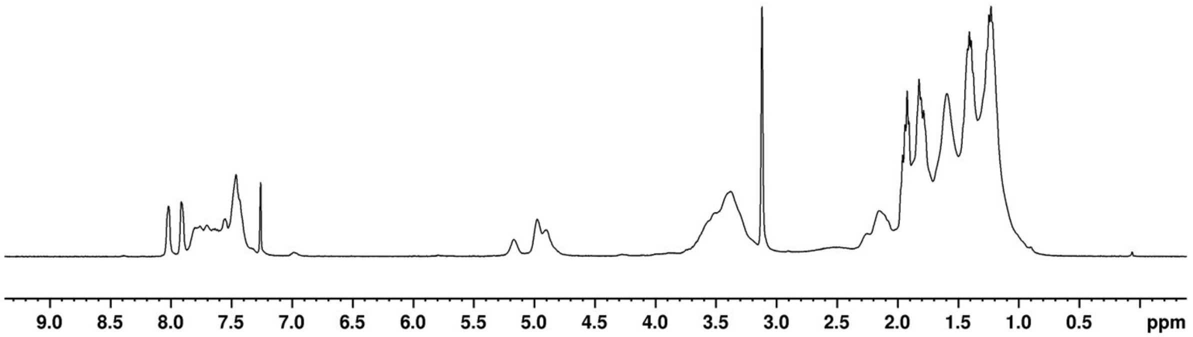

Fig. S28. ^{1}H NMR ($CDCl_3$) spectrum of the crude polyester of CHO/PA with **2d**/TPPCl in neat condition (Table 1, Entry 7).

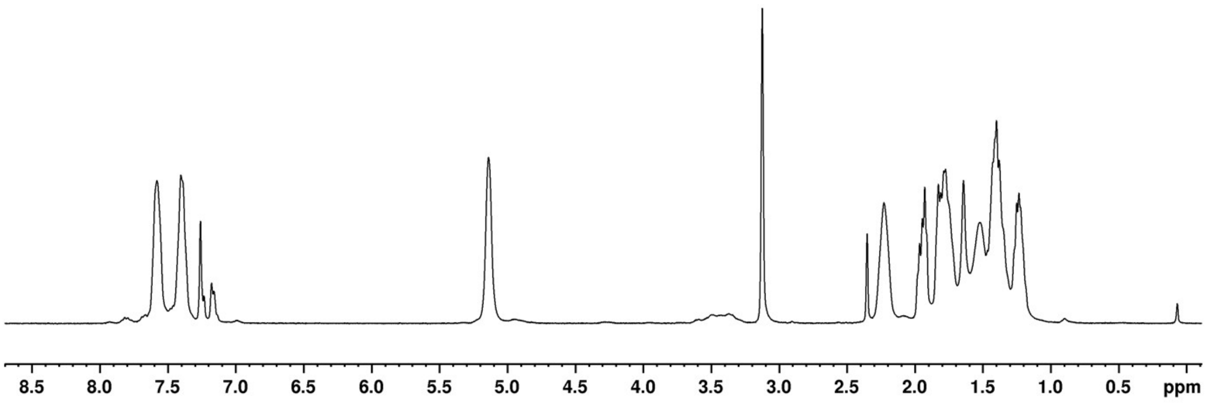

Fig. S29. ^{1}H NMR ($CDCl_3$) spectrum of the crude polyester of CHO/PA with **2a**/TPPCl in toluene (Table 1, Entry 8).

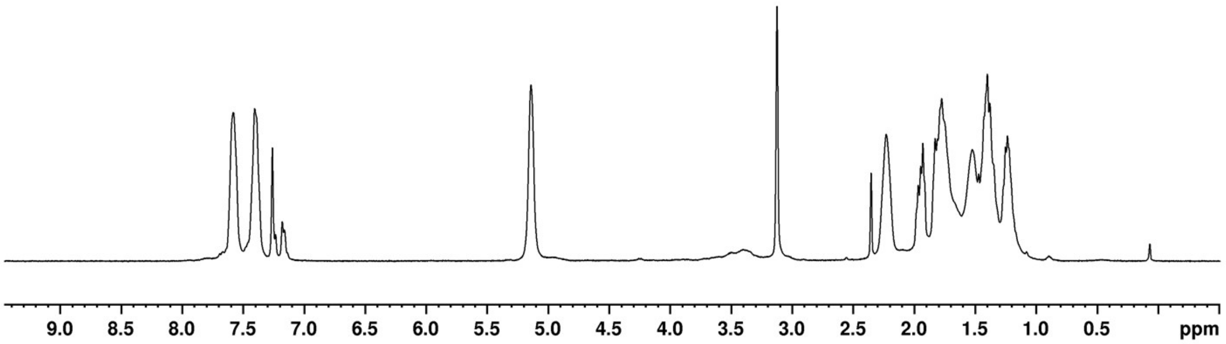

Fig. S30. ^{1}H NMR ($CDCl_3$) spectrum of the crude polyester of CHO/PA with **2b**/TPPCl in toluene (Table 1, Entry 9).

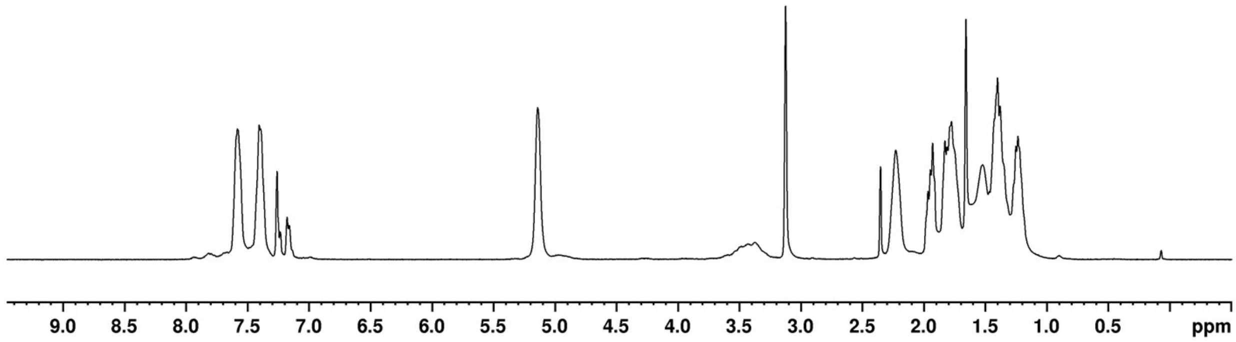

Fig. S31. ^{1}H NMR ($CDCl_3$) spectrum of the crude polyester of CHO/PA with **2c**/TPPCl in toluene (Table 1, Entry 10).

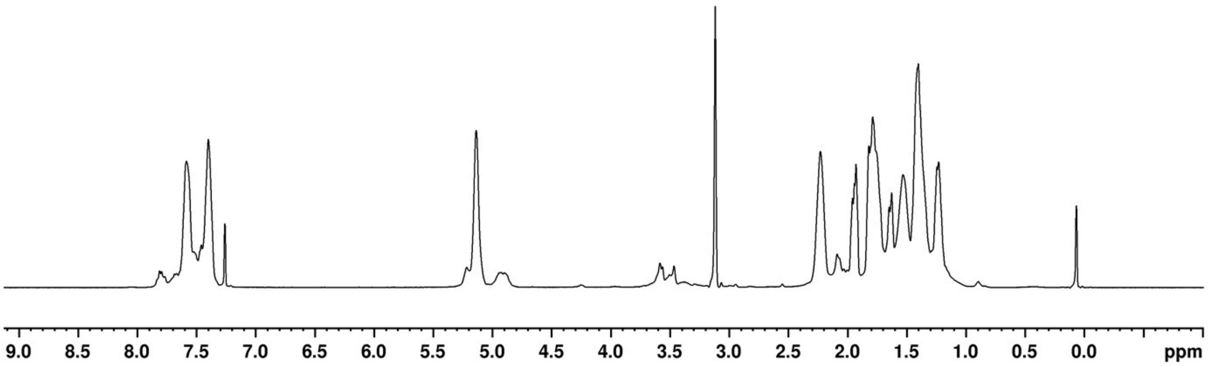

Fig. S32. ^{1}H NMR ($CDCl_3$) spectrum of the crude polyester of CHO/PA with TPPCl in neat condition (Table 1, Entry 13).

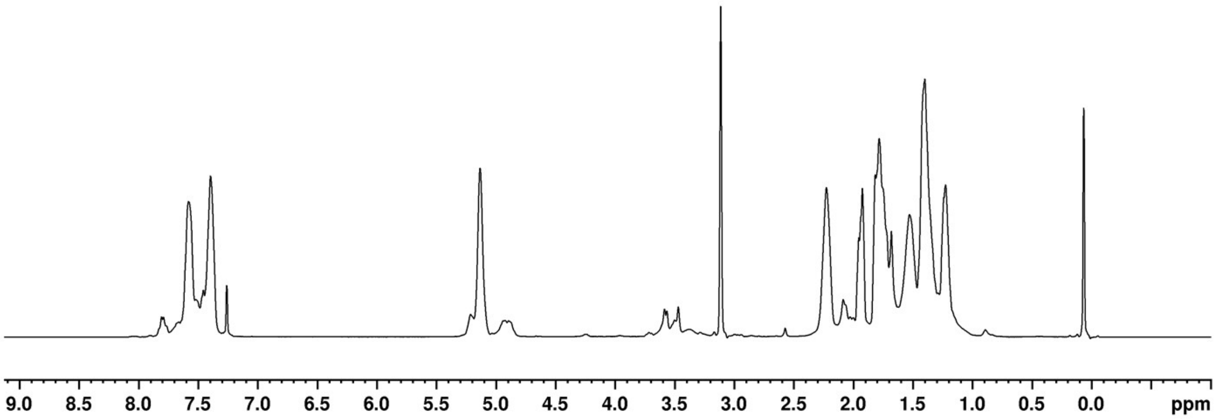

Fig. S33. ^{1}H NMR ($CDCl_3$) spectrum of the crude polyester of CHO/PA with **2a**/TPPCl at 80 °C neat condition (Table 1, Entry 12).

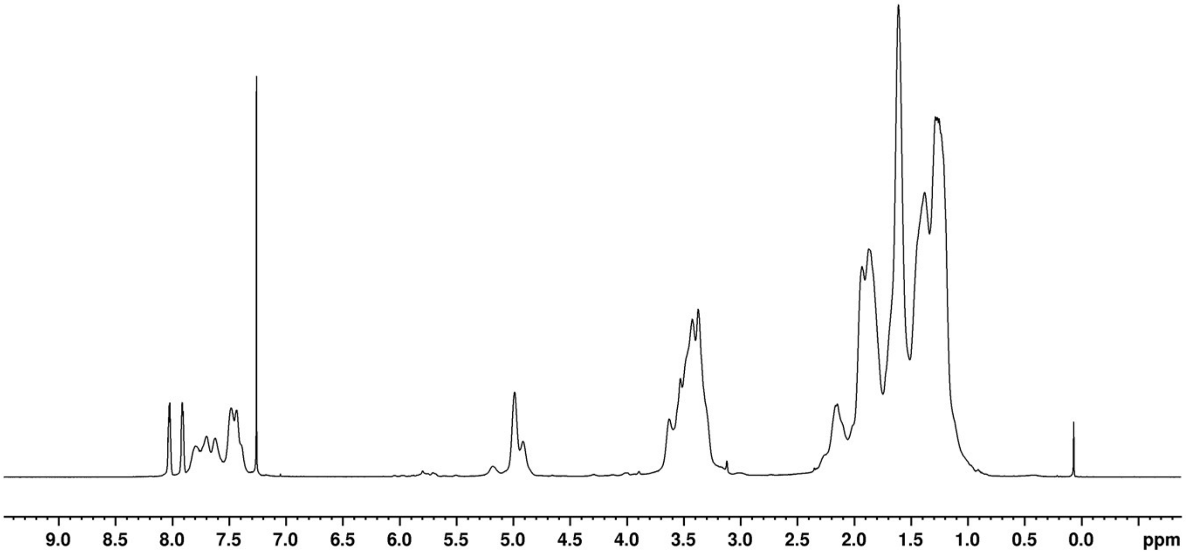

Fig. S34. ^{1}H NMR ($CDCl_3$) spectrum of the crude polyester of CHO/PA with **2d** in neat condition (Table 1, Entry 7).

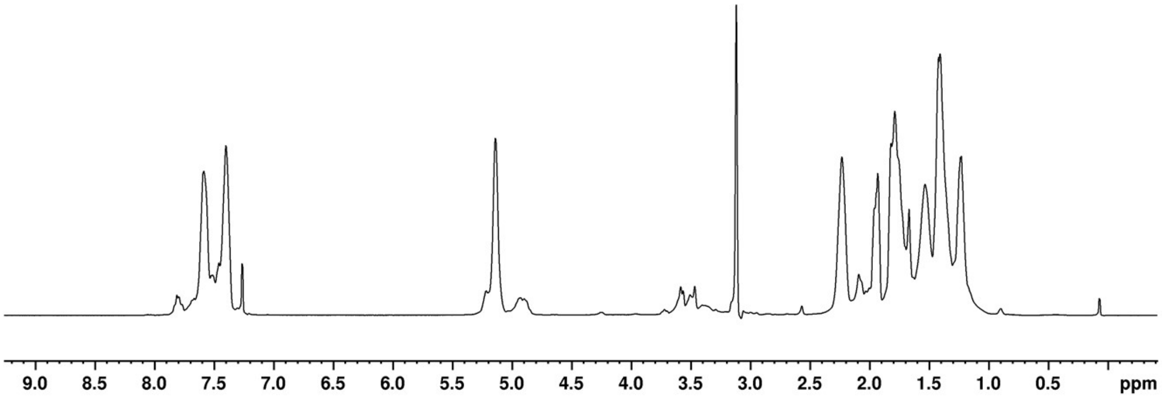

Fig. S35. ^{1}H NMR ($CDCl_3$) spectrum of the crude polyester of CHO/PA with **2d**/TPPCl in toluene (Table 1, Entry 11).

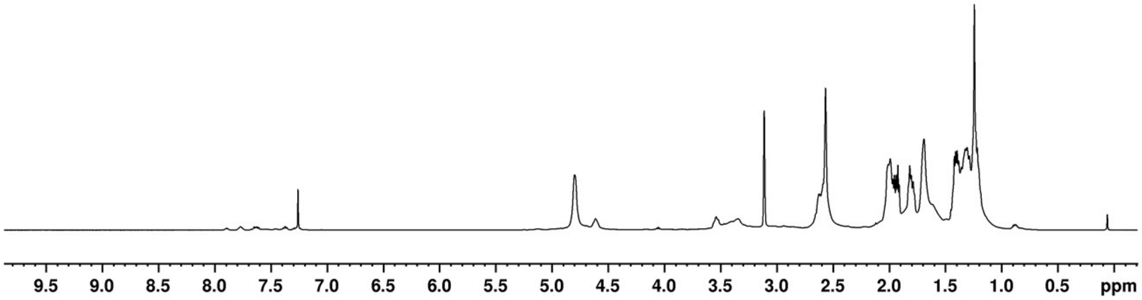

Fig. S36. ^{1}H NMR ($CDCl_3$) spectrum of the crude polyester of CHO/SA with **2a**/TPPCl (Table 2, Entry 1).

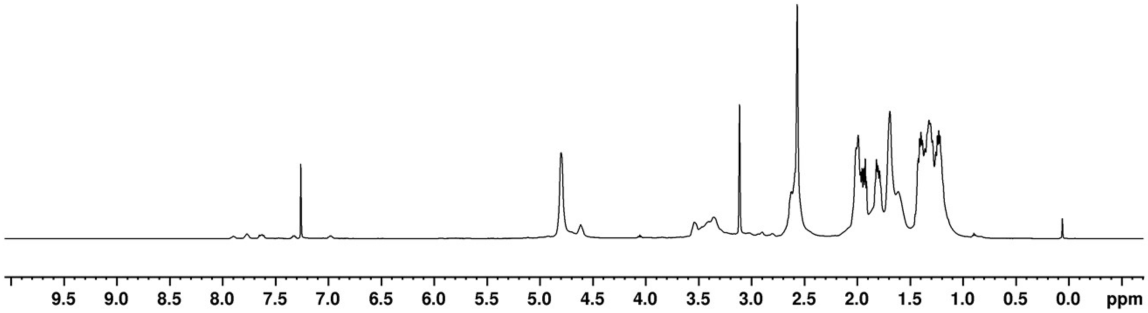

Fig. S37. ^{1}H NMR ($CDCl_3$) spectrum of the crude polyester of CHO/SA with **2c**/TPPCl (Table 2, Entry 3).

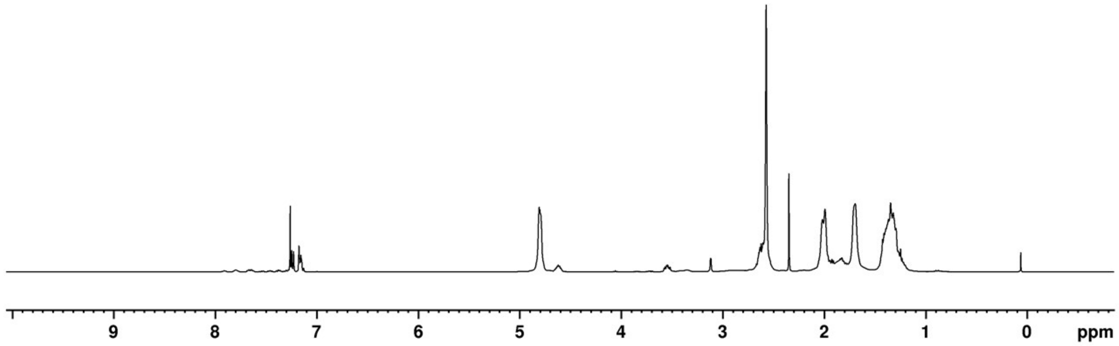

Fig. S38. ^{1}H NMR ($CDCl_3$) spectrum of the crude polyester of CHO/SA with **2d**/TPPCl (Table 2, Entry 4).

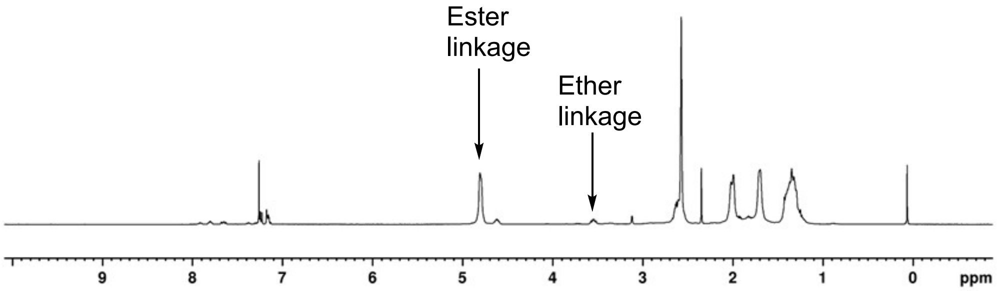

Fig. S39. ^{1}H NMR ($CDCl_3$) spectrum of the crude polyester of CHO/SA with **2b**/TPPCl (Table 2, Entry 2).

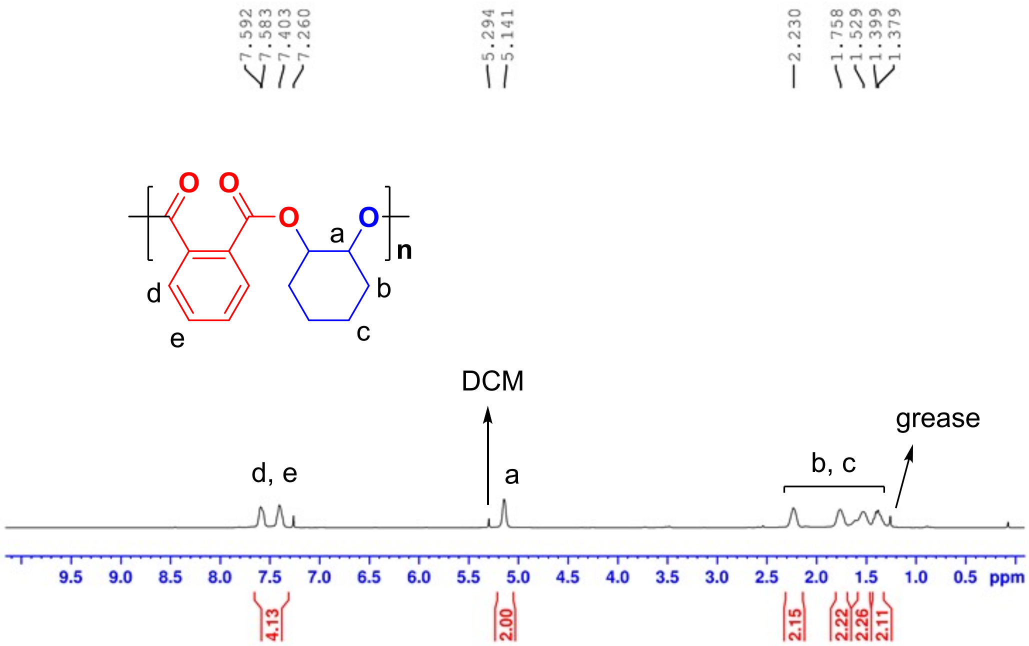

Fig. S40. ^{1}H NMR ($CDCl_3$) spectrum of isolated poly(PA-*alt*-CHO) synthesized from CHO/PA/**2b**/TPPCl (Table 1, Entry 4).

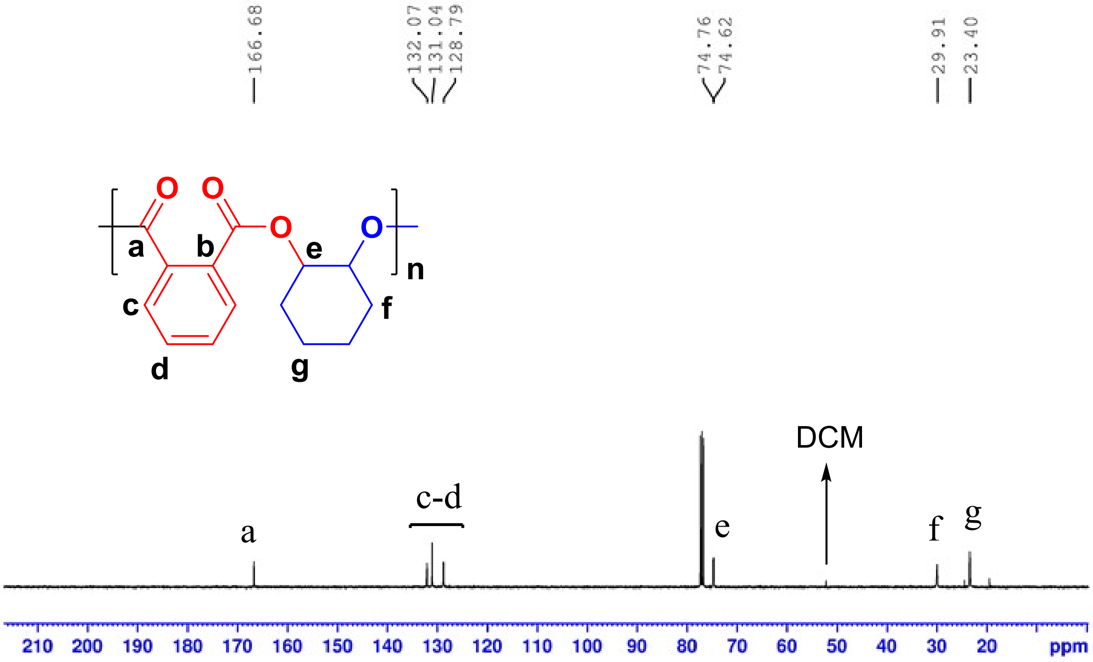

Fig. S41. ^{13}C NMR ($CDCl_3$) spectrum of isolated poly(PA-*alt*-CHO) synthesized from CHO/PA/**2b**/TPPCl (Table 1, Entry 4).

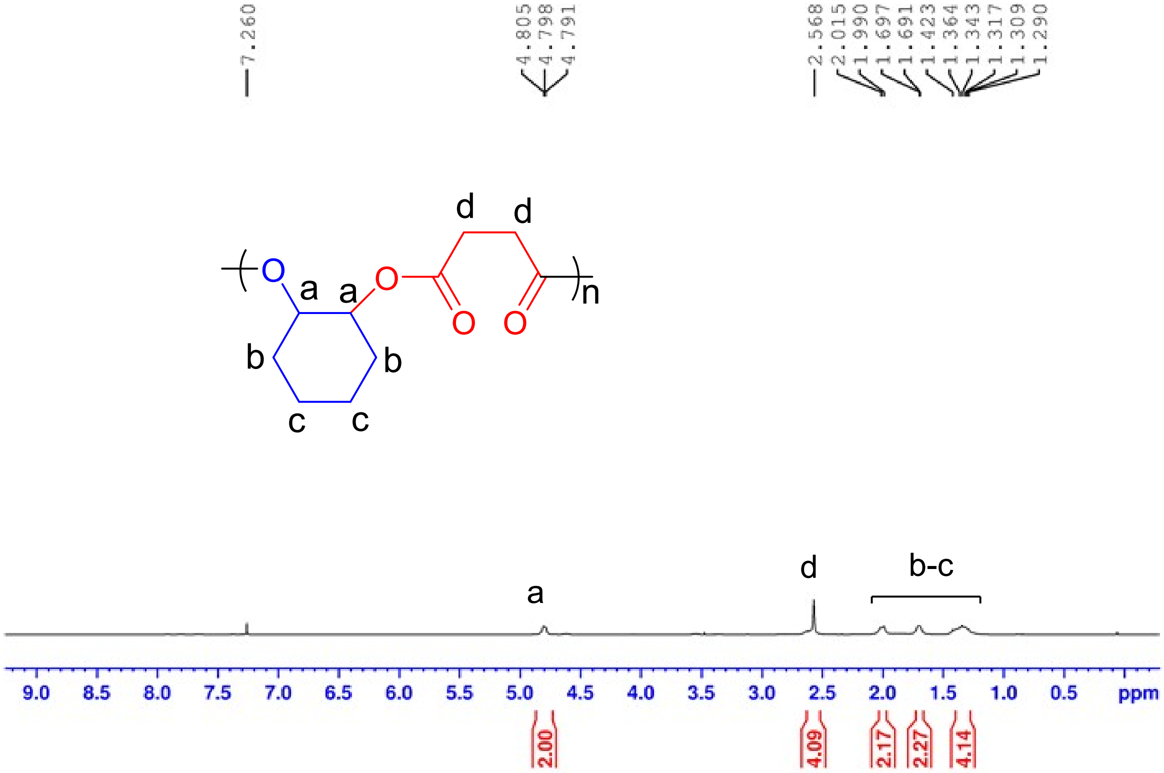

Fig. S42. 1H NMR ($CDCl_3$) spectrum of isolated poly(SA-*alt*-CHO) synthesized from CHO/SA/**2b**/TPPCl (Table 2, Entry 2).

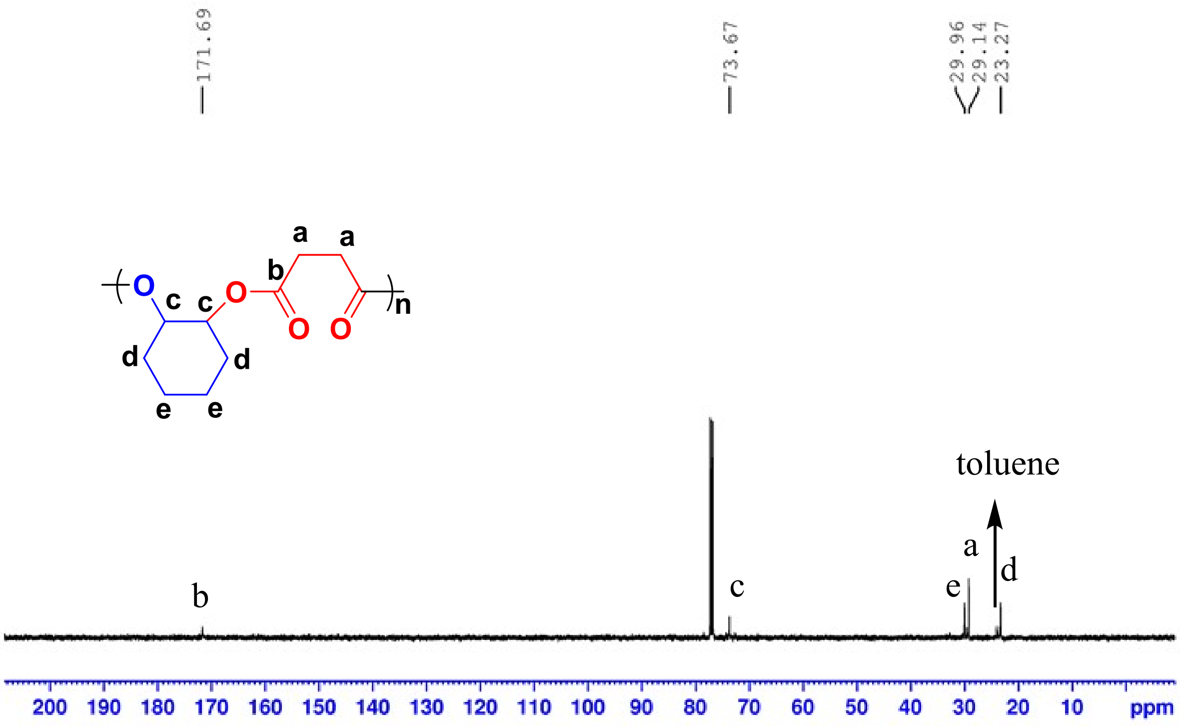

Fig. S43. ^{13}C NMR ($CDCl_3$) spectrum of isolated poly(SA-*alt*-CHO) synthesized from CHO/SA/**2b**/TPPCl (Table 2, Entry 2).

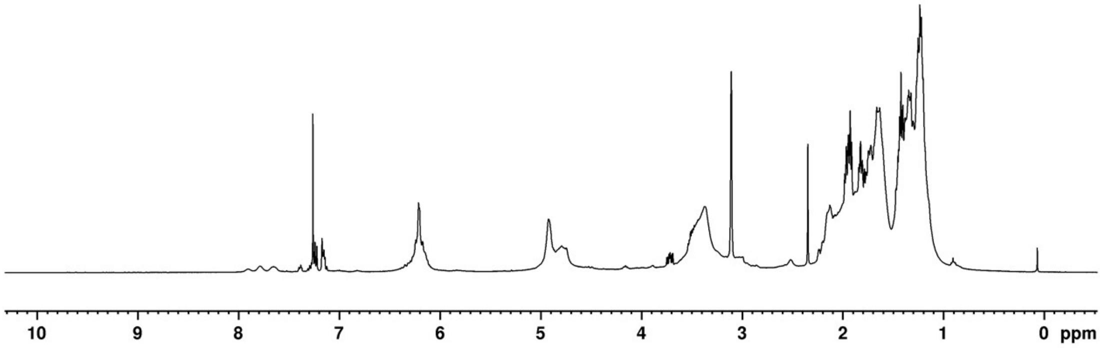

Fig. S44. ^{1}H NMR ($CDCl_3$) spectrum of crude polyester synthesized from CHO/MA/**2a**/TPPCl in toluene (Table 3, Entry 5).

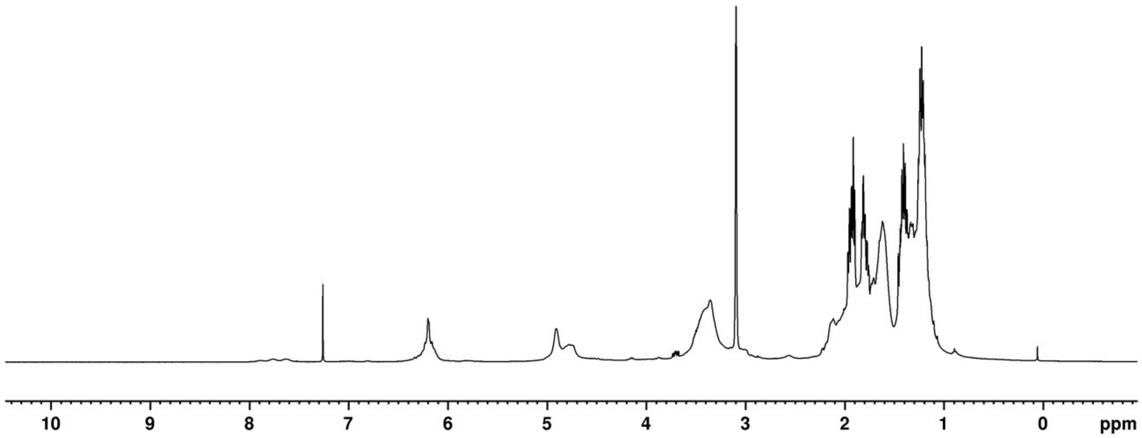

Fig. S45. ^{1}H NMR ($CDCl_3$) spectrum of crude polyester synthesized from CHO/MA/**2b**/TPPCl (Table 3, Entry 2).

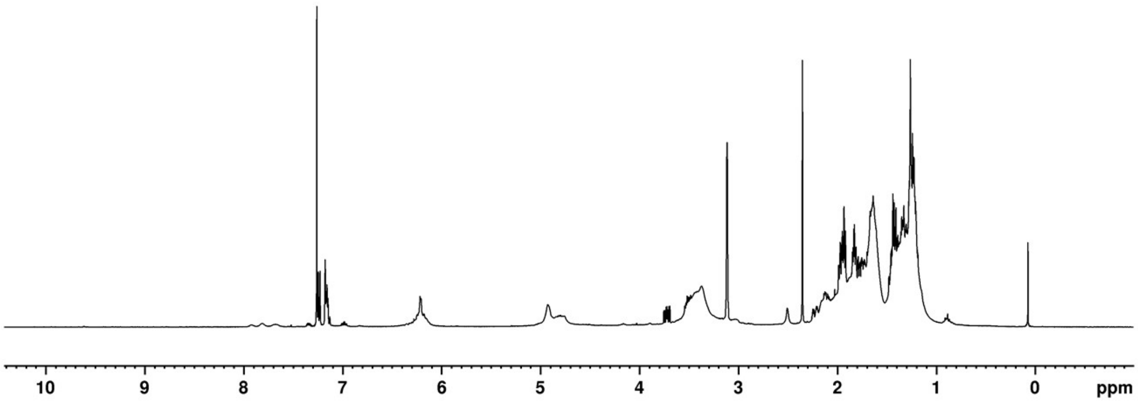

Fig. S46. ^{1}H NMR ($CDCl_3$) spectrum of crude polyester synthesized from CHO/MA/**2c**/TPPCl in toluene (Table 3, Entry 6).

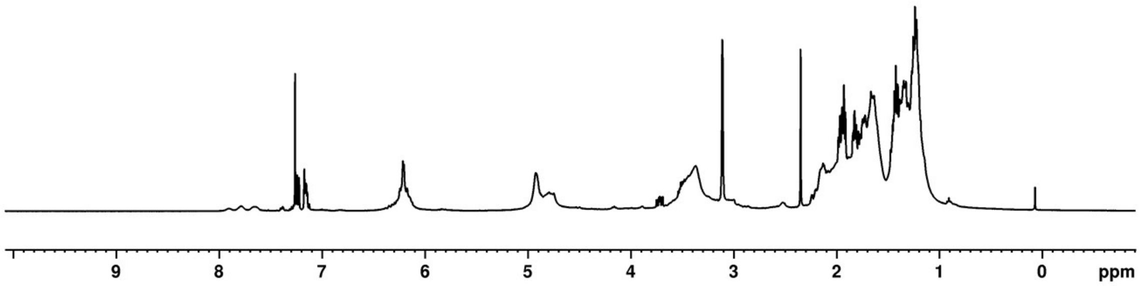

Fig. S47. ^{1}H NMR ($CDCl_3$) spectrum of crude polyester synthesized from CHO/MA/**2d**/TPPCl in toluene (Table 3, Entry 7).

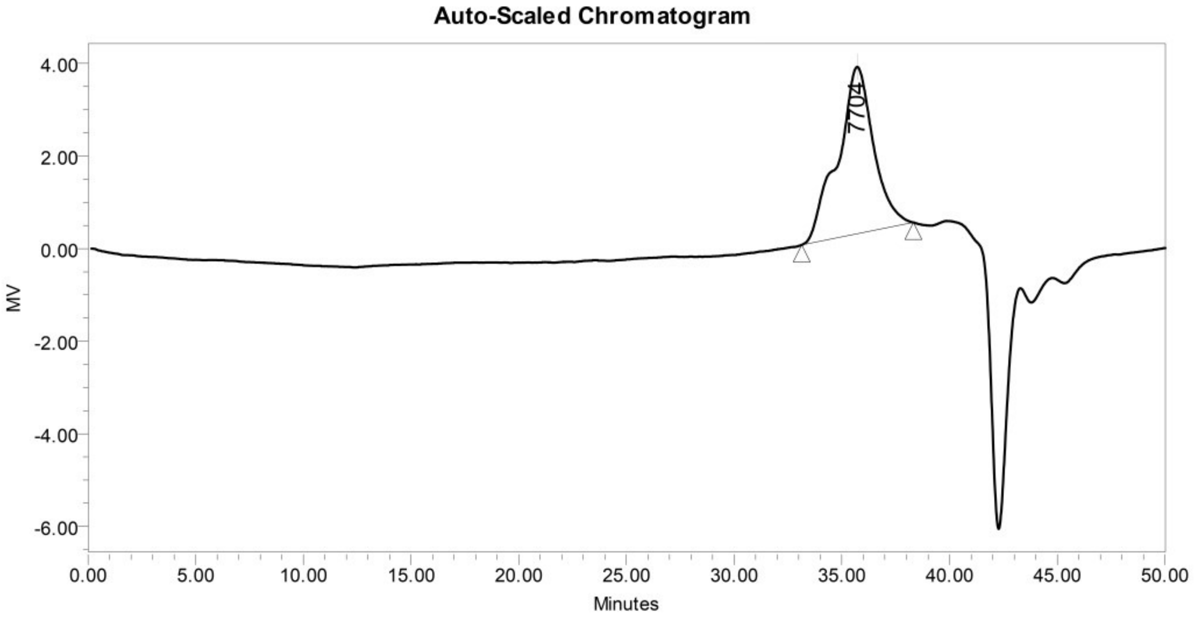

GPC Results

	Dist Name	Mn	Mw	MP	Mz	Mz+1	Mv	Poly dispersity	MW Marker 1	MW Marker 2
1		7490	8848	7704	10423	12106		1.181226		

Fig. S48. GPC trace of polyester from PA/CHO using **2a** and TPPCl in neat condition (Table 1, Entry 4).

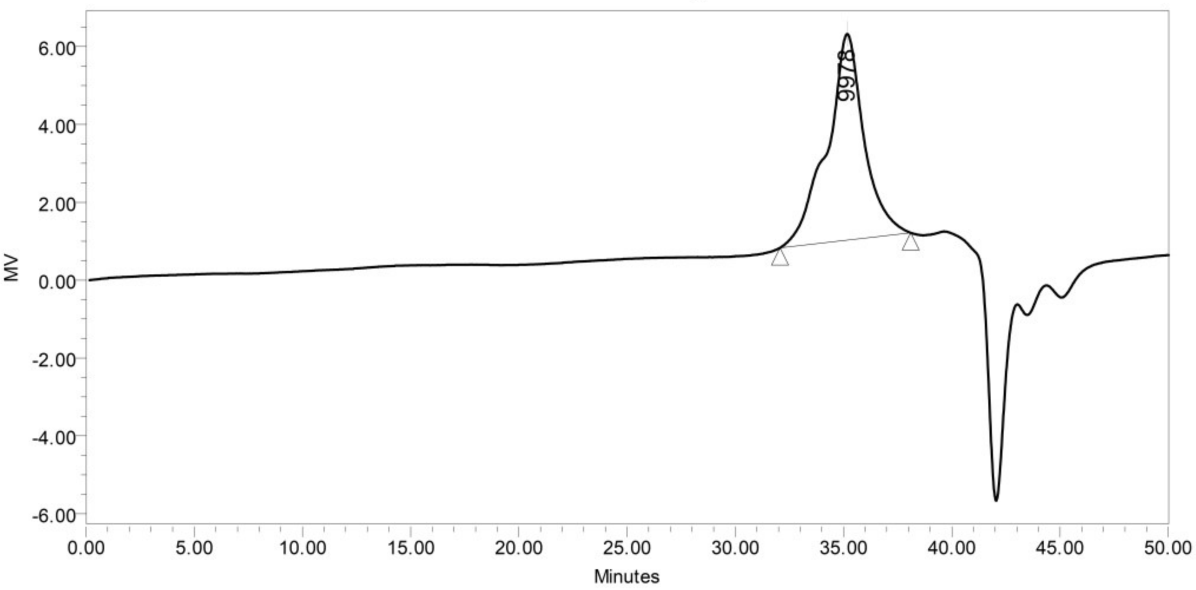
Auto-Scaled Chromatogram

GPC Results

	Dist Name	Mn	Mw	MP	Mz	Mz+1	Mv	Polydispersity	MW Marker 1	MW Marker 2
1		9589	11771	9978	14499	17701		1.227485		

Fig. S49. GPC trace of polyester from PA/CHO using **2b** and TPPCl in neat condition (Table 1, Entry 5).

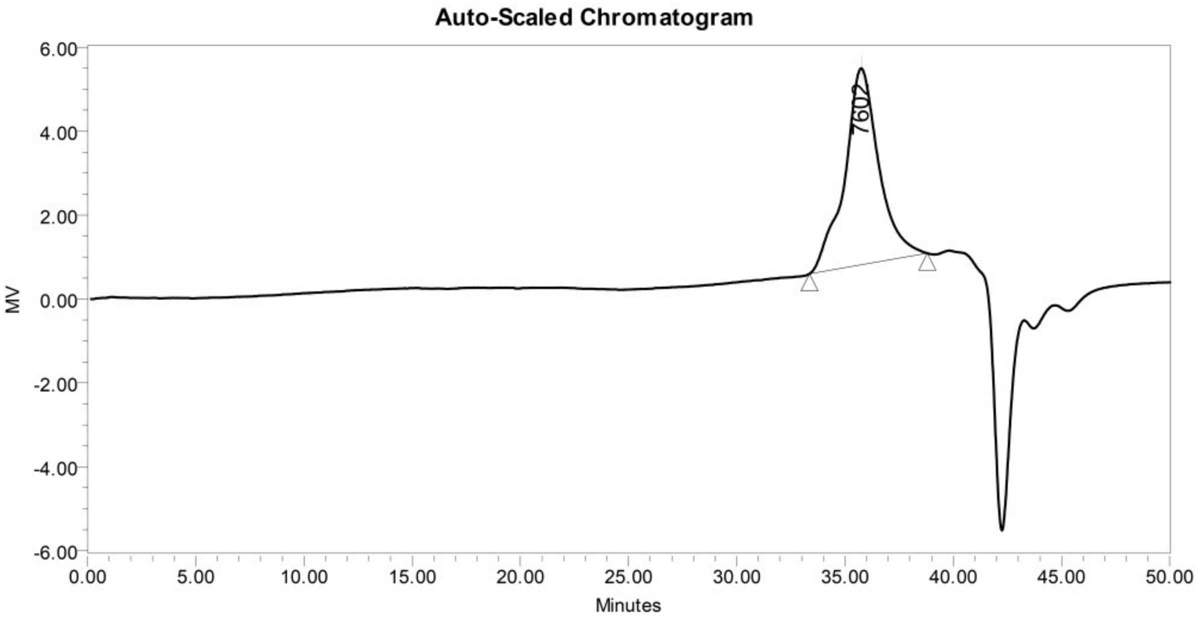

GPC Results

	Dist Name	Mn	Mw	MP	Mz	Mz+1	Mv	Polydispersity	MW Marker 1	MW Marker 2
1		6803	8028	7602	9384	10866		1.180125		

Fig. S50. GPC trace of polyester from PA/CHO using **2c** and TPPCl in neat condition (Table 1, Entry 6).

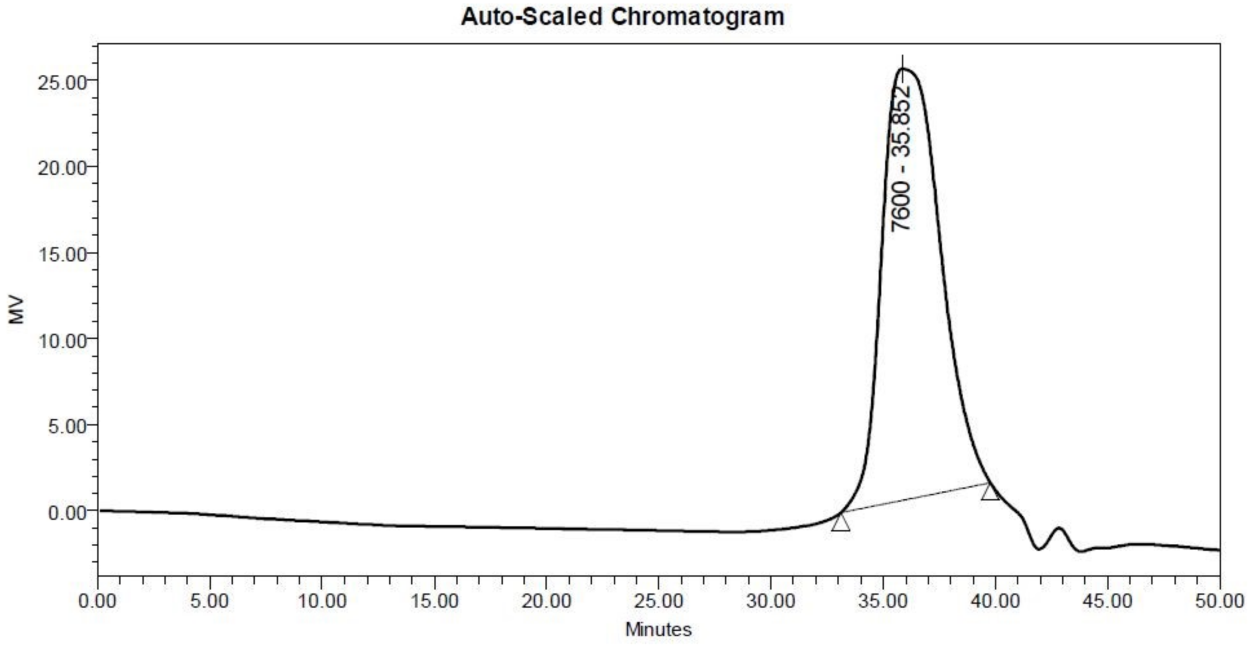

GPC Results

	Dist Name	Mn	Mw	MP	Mz	Mz+1	Mv	Polydispersity	MW Marker 1	MW Marker 2
1		5049	6732	7600	8503	10246		1.333534		

Fig. S51. GPC trace of polyester from PA/CHO using **2d** and TPPCl in toluene (Table 1, Entry 11).

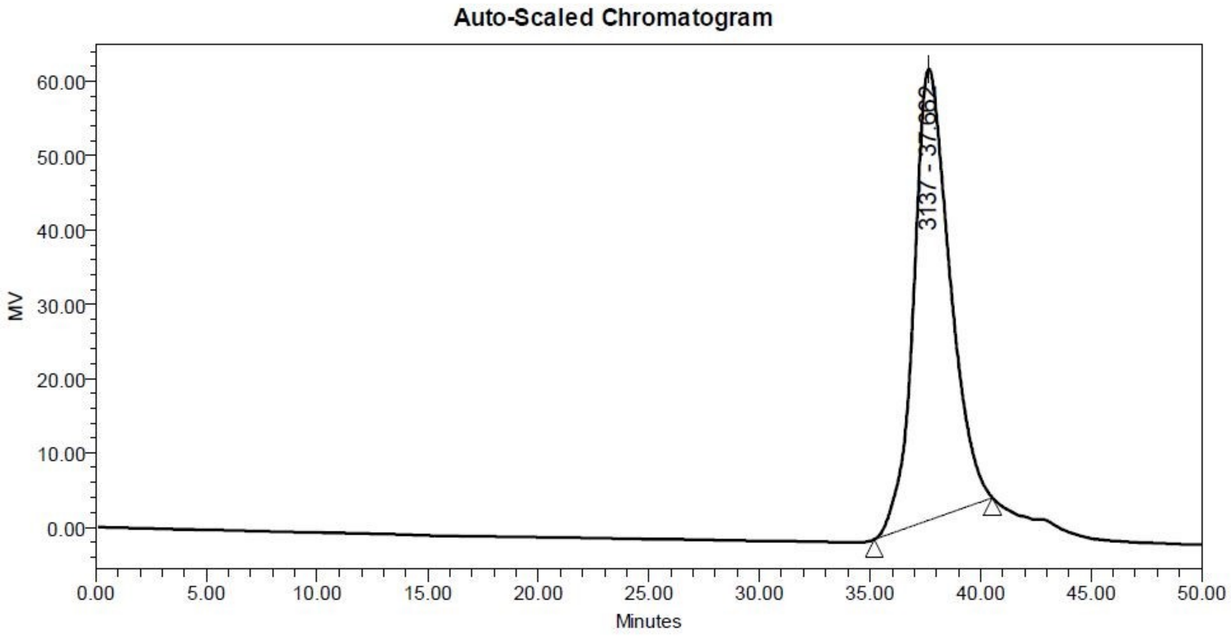

GPC Results

	Dist Name	Mn	Mw	MP	Mz	Mz+1	Mv	Polydispersity	MW Marker 1	MW Marker 2
1		2553	3025	3137	3522	4051		1.185073		

Fig. S52. GPC trace of polyester from PA/CHO using **2a** and TPPCl at 80 °C in neat condition (Table 1, Entry 12).

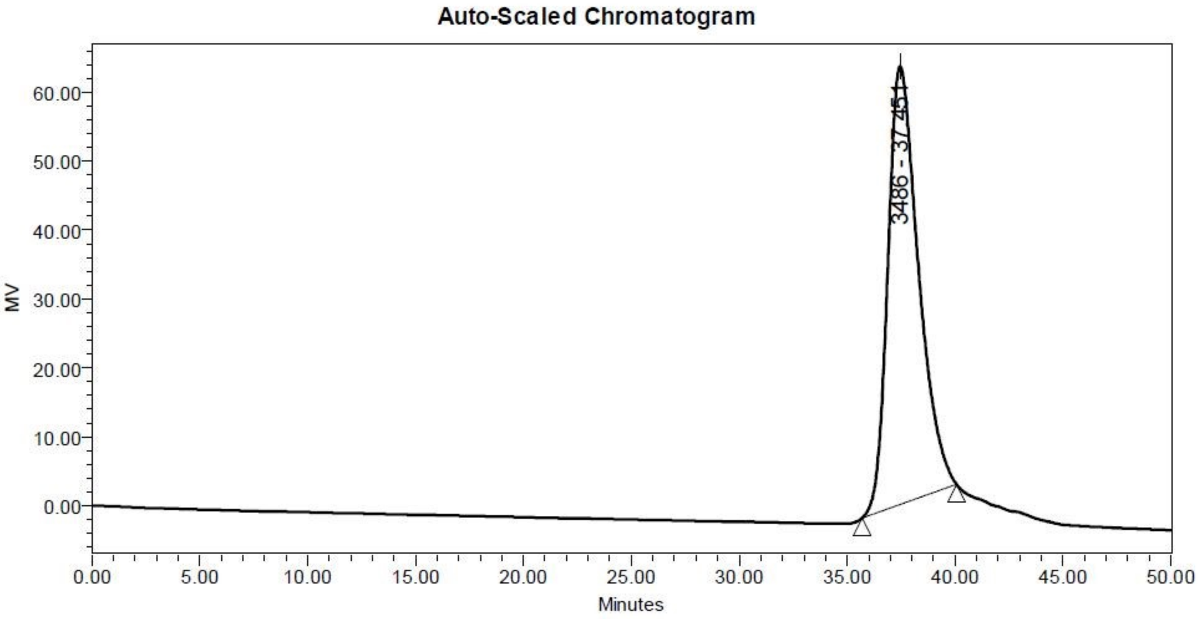

GPC Results

	Dist Name	Mn	Mw	MP	Mz	Mz+1	Mv	Polydispersity	MW Marker 1	MW Marker 2
1		2861	3235	3486	3584	3906		1.130875		

Fig. S53. GPC trace of polyester from PA/CHO using TPPCl in neat condition (Table 1, Entry 13).

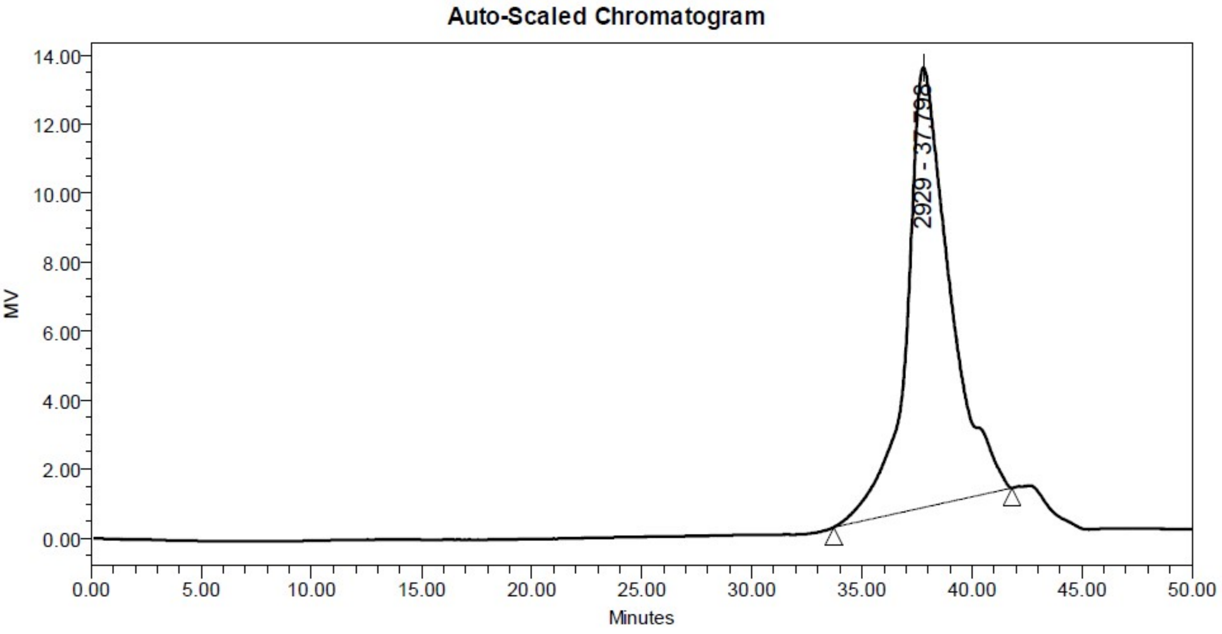

GPC Results

	Dist Name	Mn	Mw	MP	Mz	Mz+1	Mv	Polydispersity	MW Marker 1	MW Marker 2
1		2026	2948	2929	4306	6430		1.455566		

Fig. S54. GPC trace of polyester from CHO/SA using **2a** and TPPCl (Table 2, Entry 1).

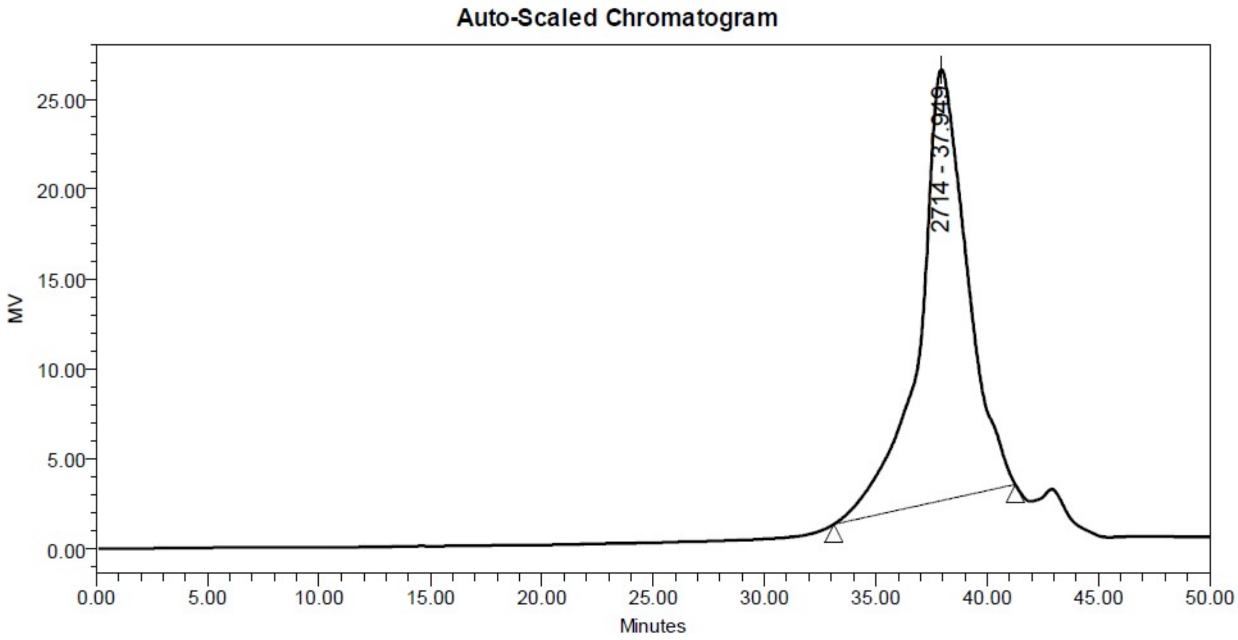

GPC Results

	Dist Name	Mn	Mw	MP	Mz	Mz+1	Mv	Polydispersity	MW Marker 1	MW Marker 2
1		2196	3343	2714	5639	9325		1.522693		

Fig. S55. GPC trace of polyester from CHO/SA using **2c** and TPPCl (Table 2, Entry 3).

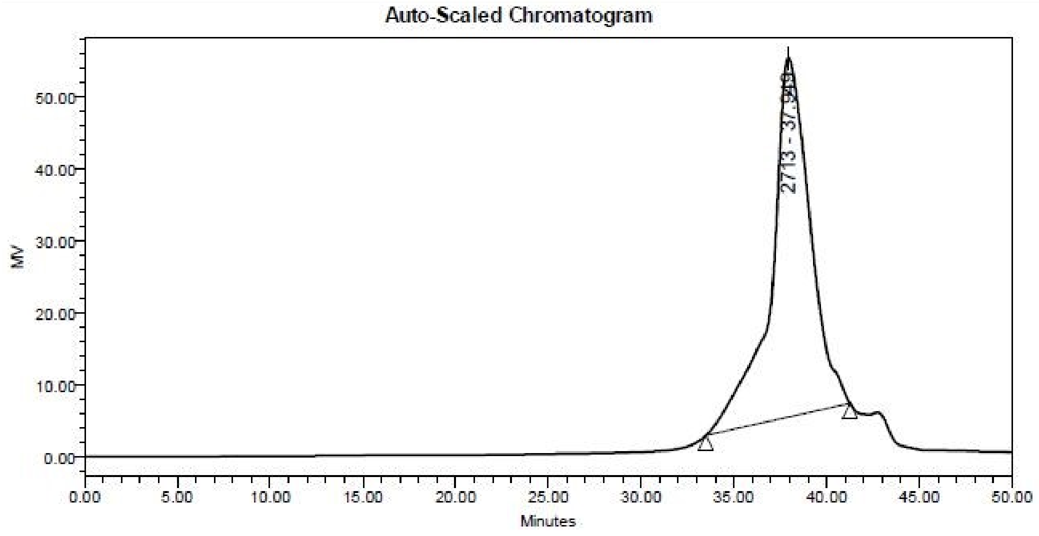

GPC Results

	Dist Name	Mn	Mw	MP	Mz	Mz+1	Mv	Polydispersity	MW Marker 1	MW Marker 2
1		2210	3316	2713	5466	8672		1.500648		

Fig. S56. GPC trace of polyester from CHO/SA using **2b** and TPPCl (Table 2, Entry 2).

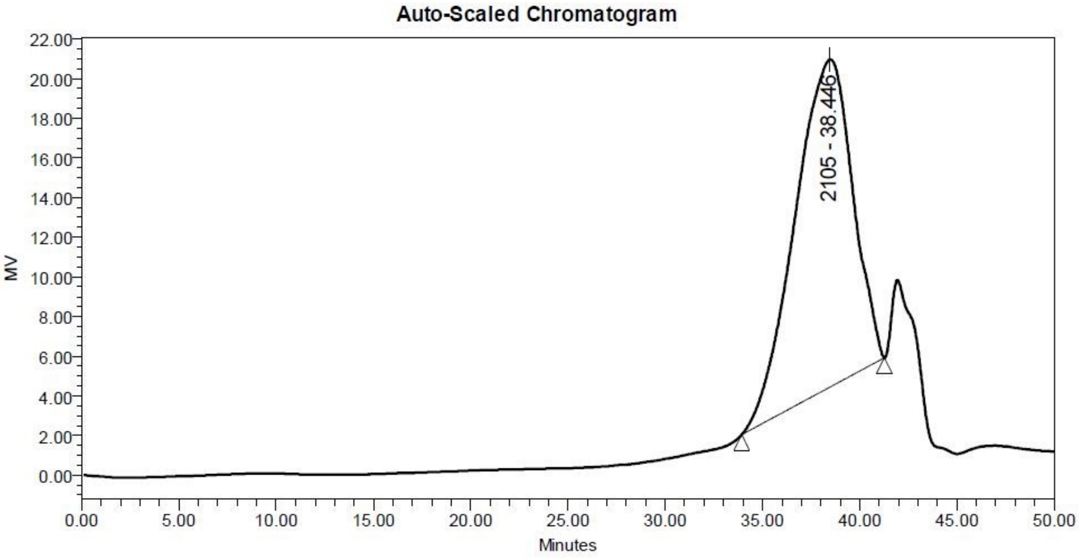

GPC Results

	Dist Name	Mn	Mw	MP	Mz	Mz+1	Mv	Polydispersity	MW Marker 1	MW Marker 2
1		2047	3181	2105	4881	6886		1.554123		

Fig. S57. GPC trace of polyester from CHO/SA 400:100 using **2a** and TPPCl (Table 2, Entry 5).

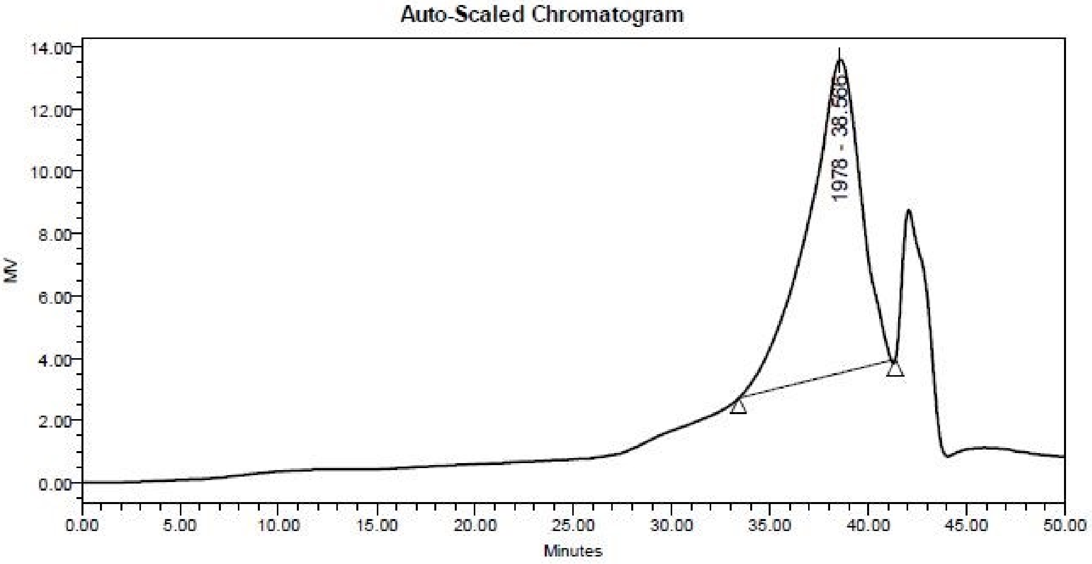

GPC Results

	Dist Name	Mn	Mw	MP	Mz	Mz+1	Mv	Polydispersity	MW Marker 1	MW Marker 2
1		2036	3328	1978	5781	9002		1.634655		

Fig. S58. GPC trace of polyester from CHO/SA 400:100 using **2d** and TPPCl (Table 2, Entry 6).

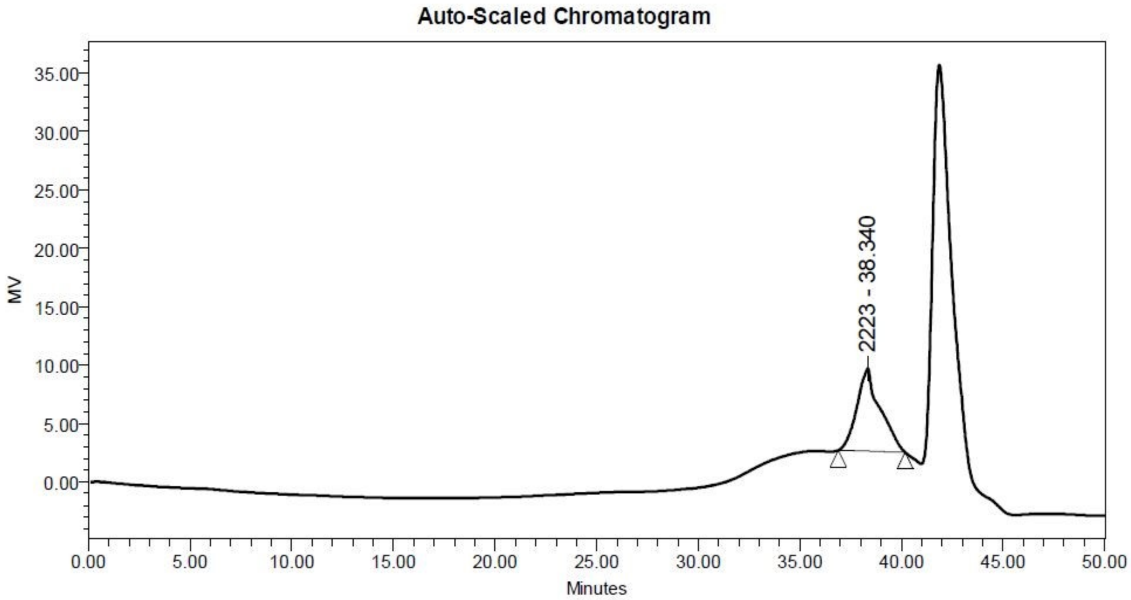

GPC Results

	Dist Name	Mn	Mw	MP	Mz	Mz+1	Mv	Polydispersity	MW Marker 1	MW Marker 2
1		1970	2170	2223	2364	2548		1.101398		

Fig. S59. GPC trace of polyester from CHO/MA using **2a** and TPPCl in toluene (Table 3, Entry 5).

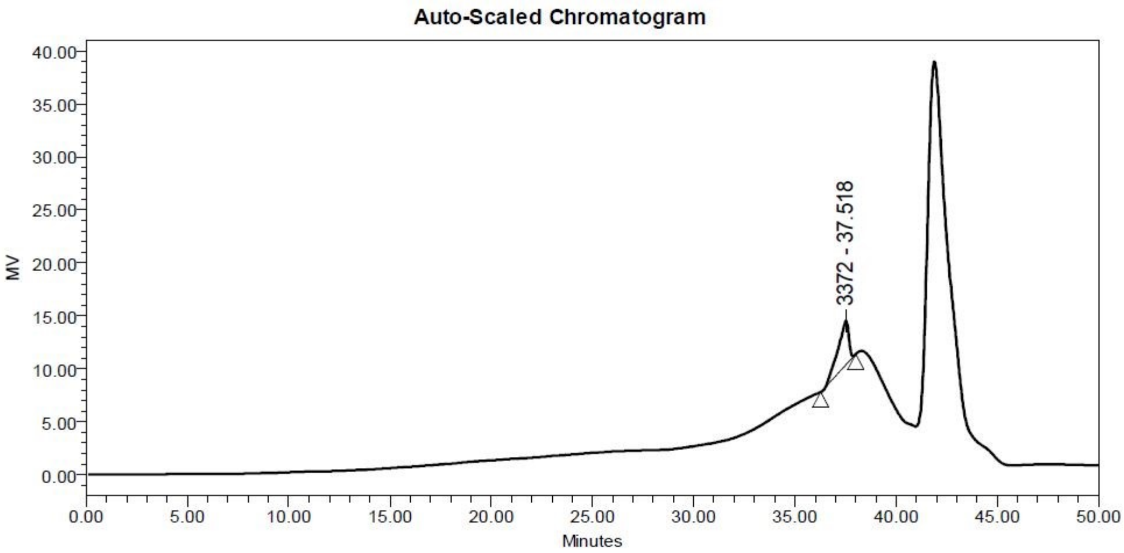

GPC Results

	Dist Name	Mn	Mw	MP	Mz	Mz+1	Mv	Polydispersity	MW Marker 1	MW Marker 2
1		3687	3755	3372	3828	3907		1.018429		

Fig. S60. GPC trace of polyester from CHO/MA using **2c** and TPPCl in toluene (Table 3, Entry 6).

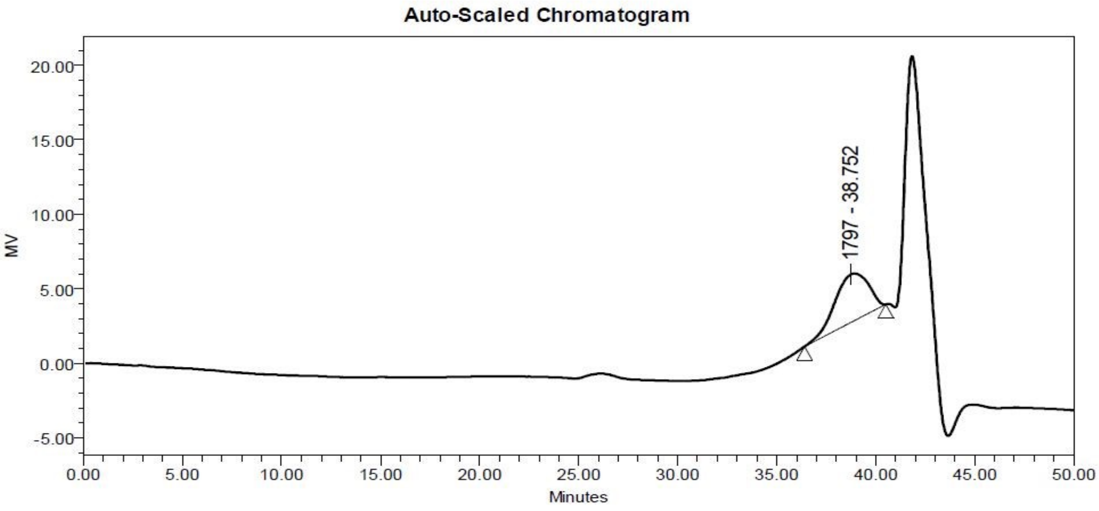

GPC Results

	Dist Name	Mn	Mw	MP	Mz	Mz+1	Mv	Polydispersity	MW Marker 1	MW Marker 2
1		1688	1936	1797	2227	2548		1.147023		

Fig. S61. GPC trace of polyester from CHO/MA using **2d** and TPPCl in toluene (Table 3, Entry 7).

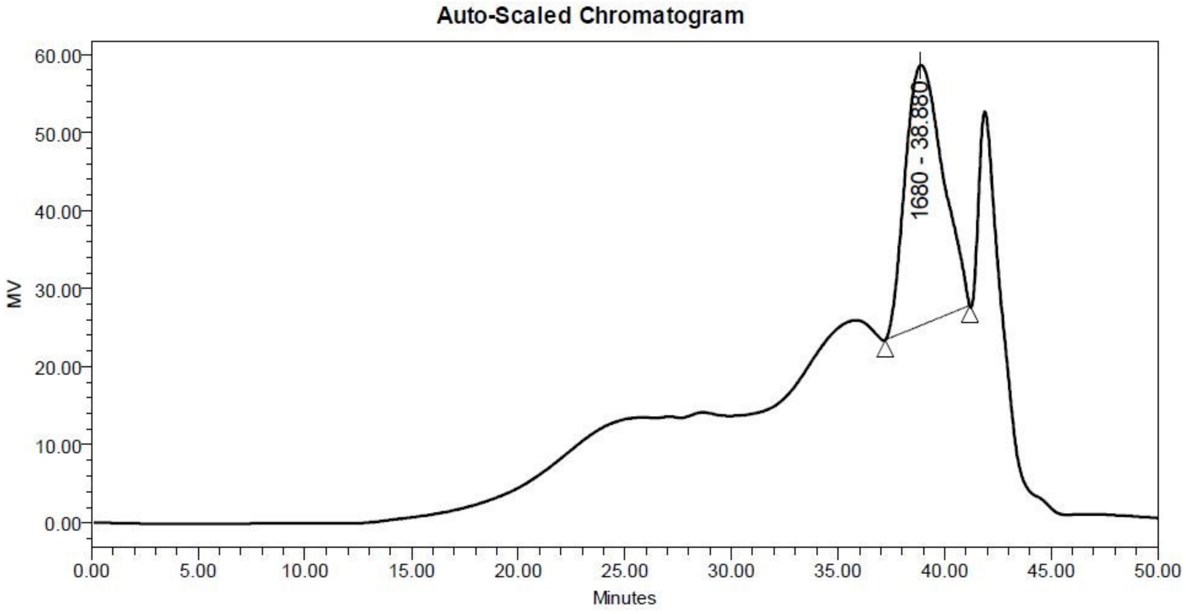

GPC Results

	Dist Name	Mn	Mw	MP	Mz	Mz+1	Mv	Polydispersity	MW Marker 1	MW Marker 2
1		1341	1586	1680	1827	2045		1.182254		

Fig. S62. GPC trace of polyester from CHO/MA using **2a** and TPPCl (Table 3, Entry 1).

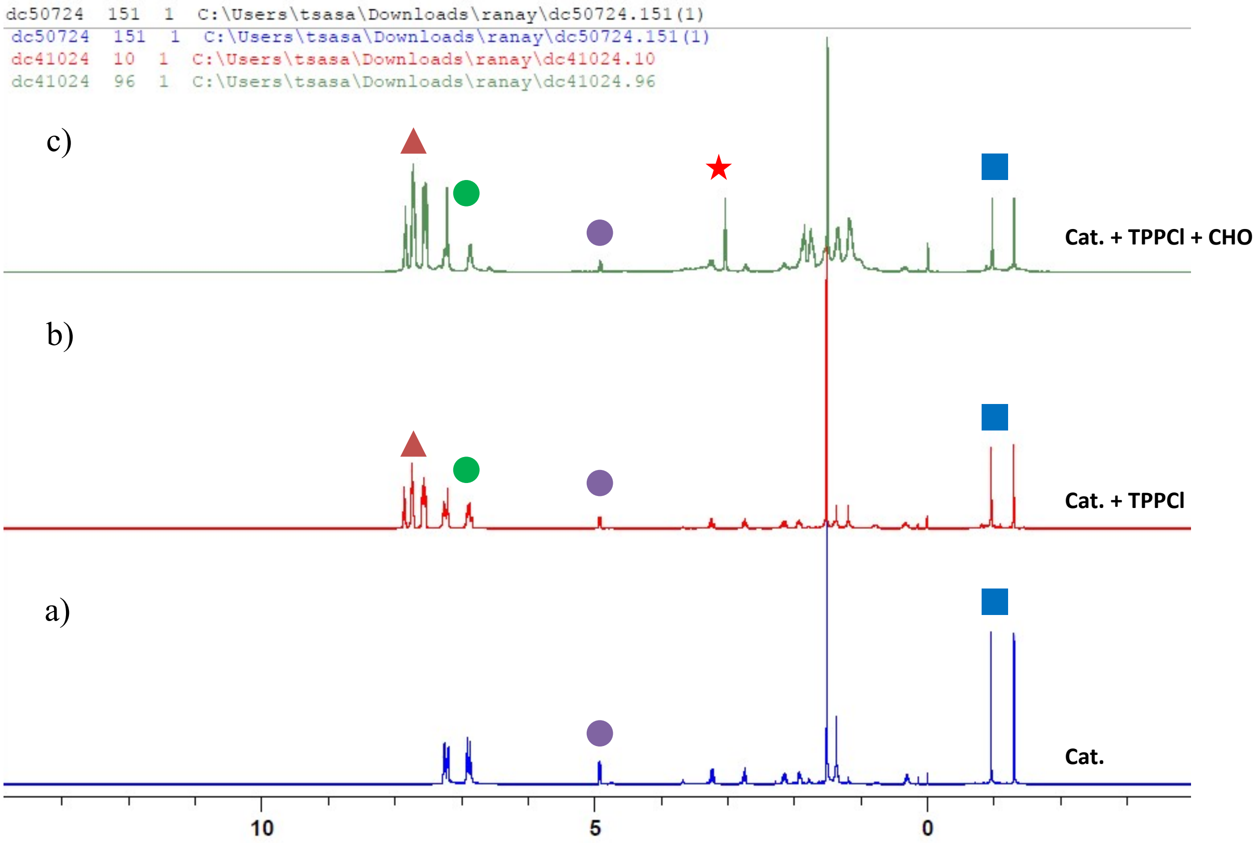

Fig. S63. Stacked ^{1}H NMR spectrum ($CDCl_3$, 400 MHz) a) Cat. **2a;** b) Cat. **2a** + TPPCl (1:1 mixture); c) Cat. **2a** + TPPCl + CHO (1:1:2 mixture). Purple circle: NC**H** proton signal; Green circle: catalytic pair signai; Brown triangle: phosphonium ion signal; Blue circle: methyl protons signal; Red star: CHO and homopolymerized product signal.

Signal	Cat.	Cat. + TPPCl	Cat. + TPPCl + CHO
N-C**H**	4.99	4.98	4.96
H_3C−Al	-0.94, -1.28	-0.93, -1.26	-0.92, -1.25

Compound Details

Cpd. 1: C24 H32 Al Cl N O3

Name	Formula	Mass m/z
	C24 H32 Al Cl N O3	444.1900

Species	m/z
(M+H)+	445.2010
(M+NH4)+	462.2330
(M+Na)+	467.1781

Compound Spectra (overlaid)

Spectrum Peaks

m/z	Z	Diff (ppm)	Ion Species	Formula
445.2010	1	11.59	(M+H)+	C24H32AlClNO3
462.2330	1	22.80	(M+NH4)+	C24H32AlClNO3
467.1781	1	0.66	(M+Na)+	C24H32AlClNO3
468.1743	1	-14.65	(M+Na)+	C24H32AlClNO3
469.1807	1	10.28	(M+Na)+	C24H32AlClNO3

Compound ID Table

Cpd Key	Formula	Mass	Cal. Mass	Species	Diff (mDa)
947	C24 H32 Al Cl N O3	444.1900	444.1886	(M+H)+ (M+NH4)+ (M+Na)+	1.4

Compound Spectra

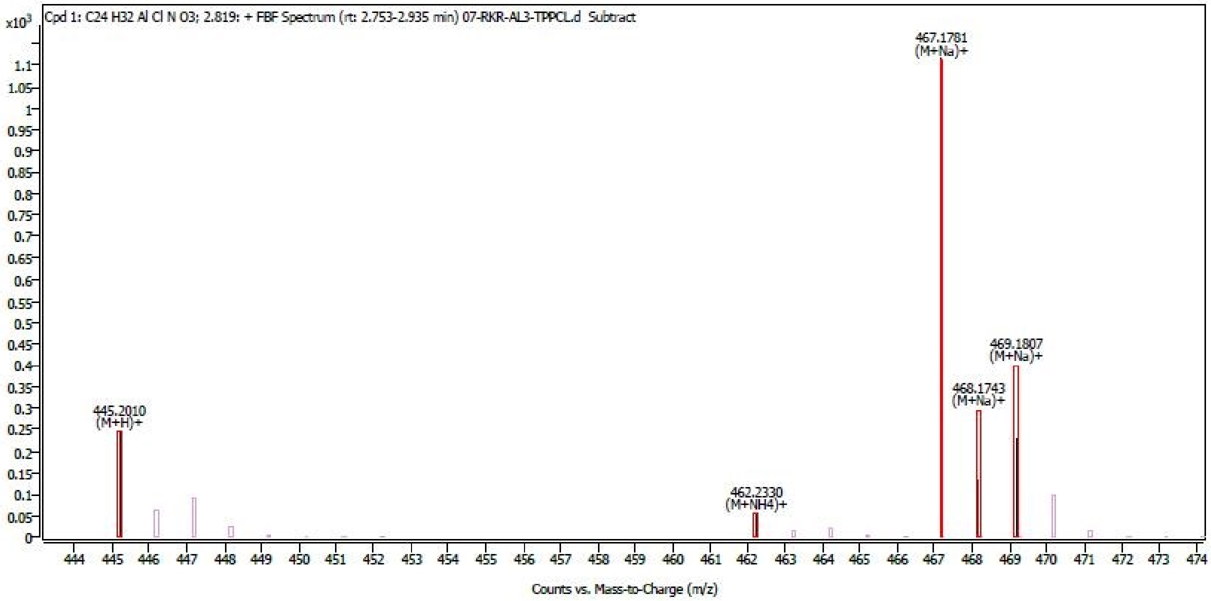

Fig. S64. HRMS spectrum of **A**.

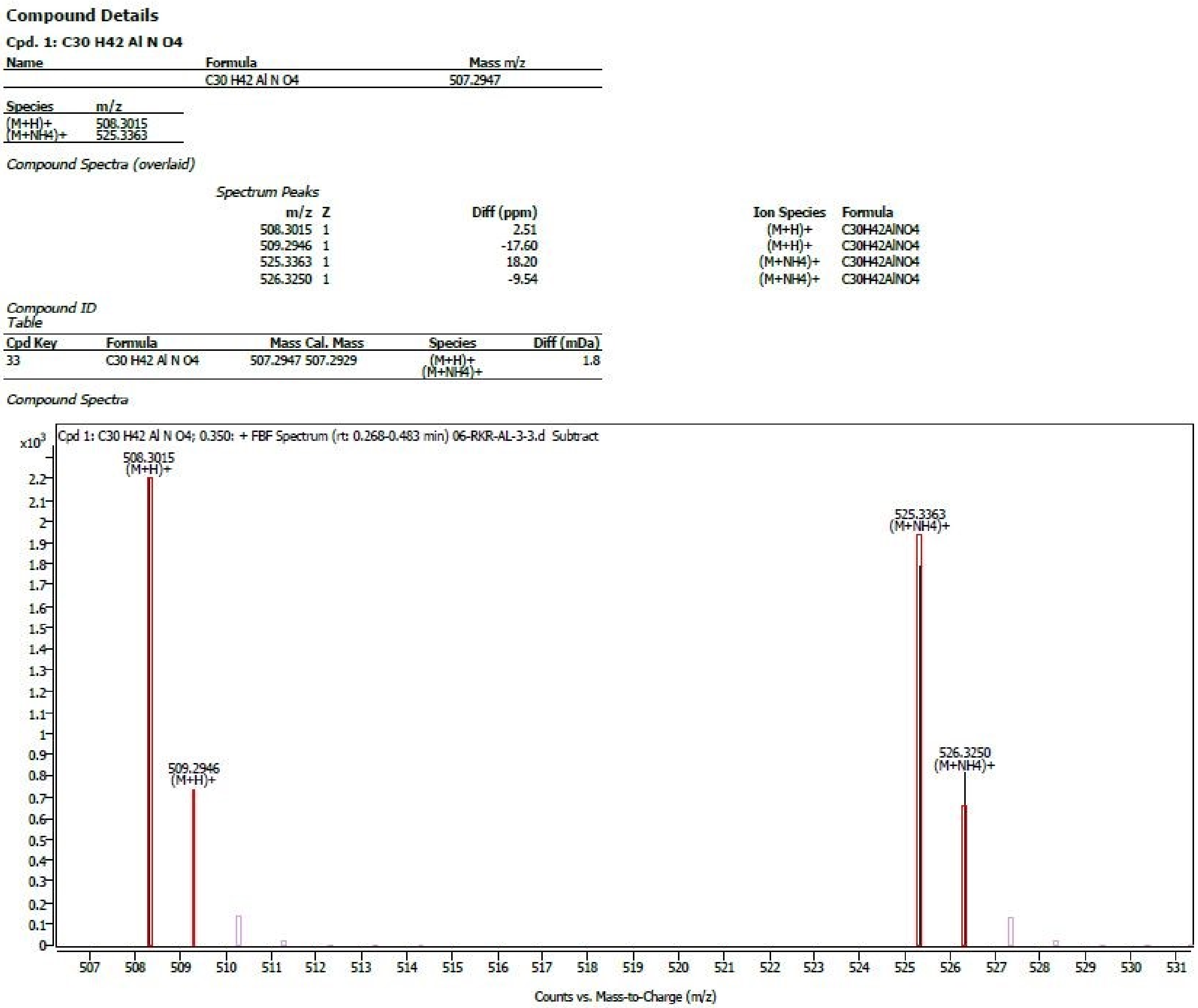

Compound Details

Cpd. 1: C30 H42 Al N O4

Name	Formula	Mass m/z
	C30 H42 Al N O4	507.2947

Species	m/z
(M+H)+	508.3015
(M+NH4)+	525.3363

Compound Spectra (overlaid)

Spectrum Peaks

m/z	Z	Diff (ppm)	Ion Species	Formula
508.3015	1	2.51	(M+H)+	C30H42AlNO4
509.2946	1	-17.60	(M+H)+	C30H42AlNO4
525.3363	1	18.20	(M+NH4)+	C30H42AlNO4
526.3250	1	-9.54	(M+NH4)+	C30H42AlNO4

Compound ID Table

Cpd Key	Formula	Mass	Cal. Mass	Species	Diff (mDa)
33	C30 H42 Al N O4	507.2947	507.2929	(M+H)+ (M+NH4)+	1.8

Compound Spectra

Cpd 1: C30 H42 Al N O4; 0.350: + FBF Spectrum (rt: 0.268-0.483 min) 06-RKR-AL-3-3.d Subtract

Fig. S65. HRMS spectrum of **B**.

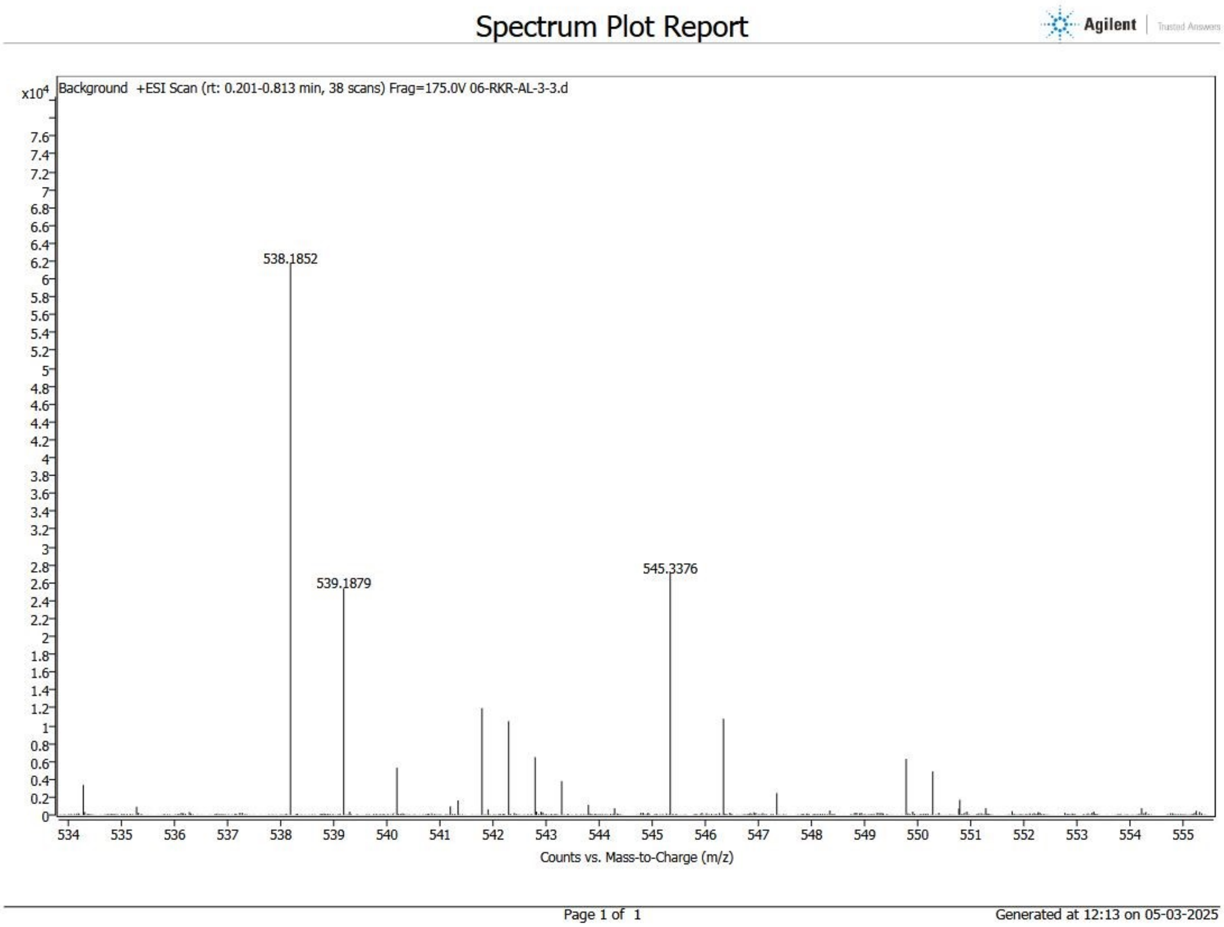

Spectrum Plot Report

Page 1 of 1

Generated at 12:13 on 05-03-2025

Fig. S66. ESI mass spectrum of **C**.

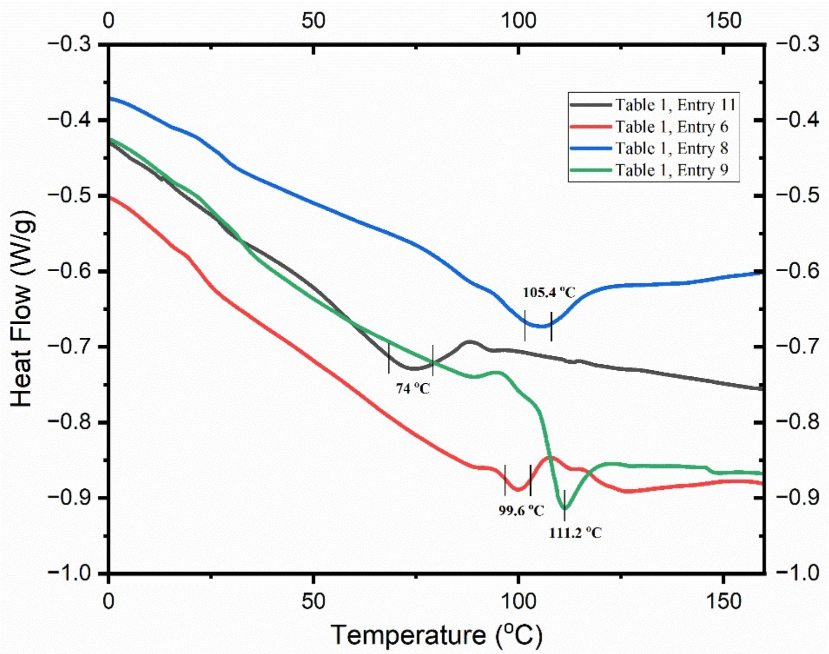

Fig. S67. DSC trace of poly(PA-*alt*-CHO) synthesized by **2a**, **2b**, **2c** and **2d**.

Catalyst	$M_{n,obs}$ of poly(PA-*alt*-CHO) (g/mol)	T_g (°C)
2d	5049	74
2c	6803	99.6
2a	7550	105.4
2b	9602	112

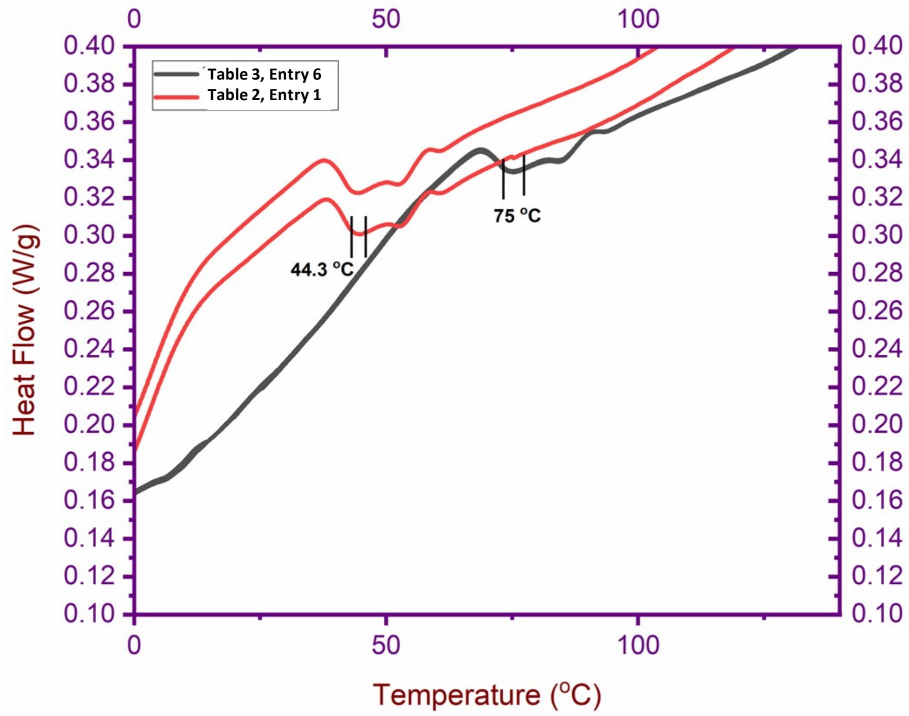

Fig. S68. DSC trace of polyester synthesized from CHO/SA/**2a**/TPPCl and CHO/MA/**2c**/TPPCl. Red curve: poly(SA-*alt*-CHO) and black curve: poly(MA-*alt*-CHO).

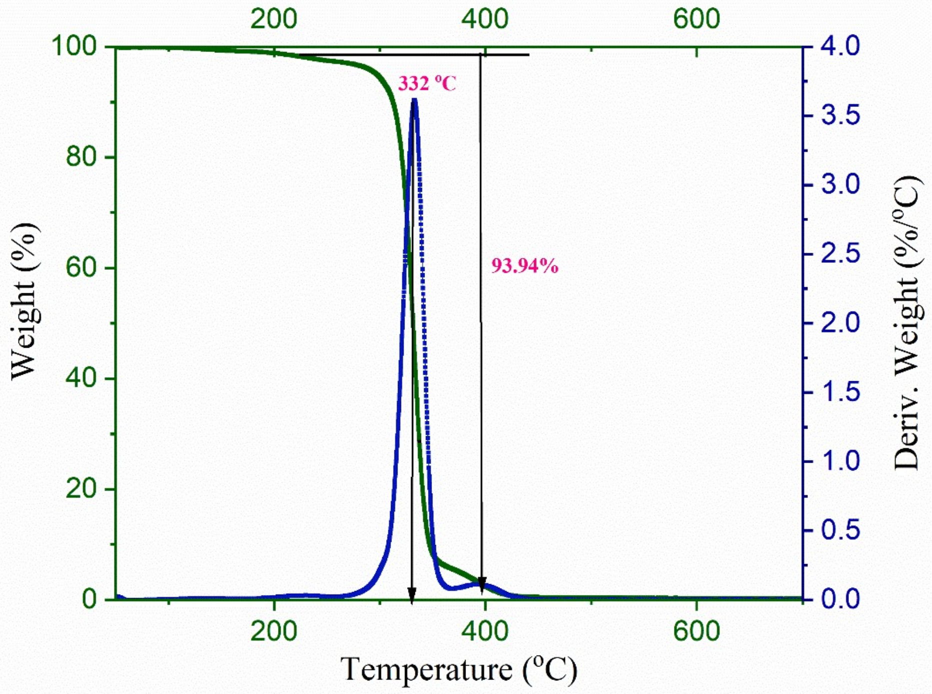

Fig. S69. TGA data of polyester synthesized from CHO/PA/**2a**/TPPCl.

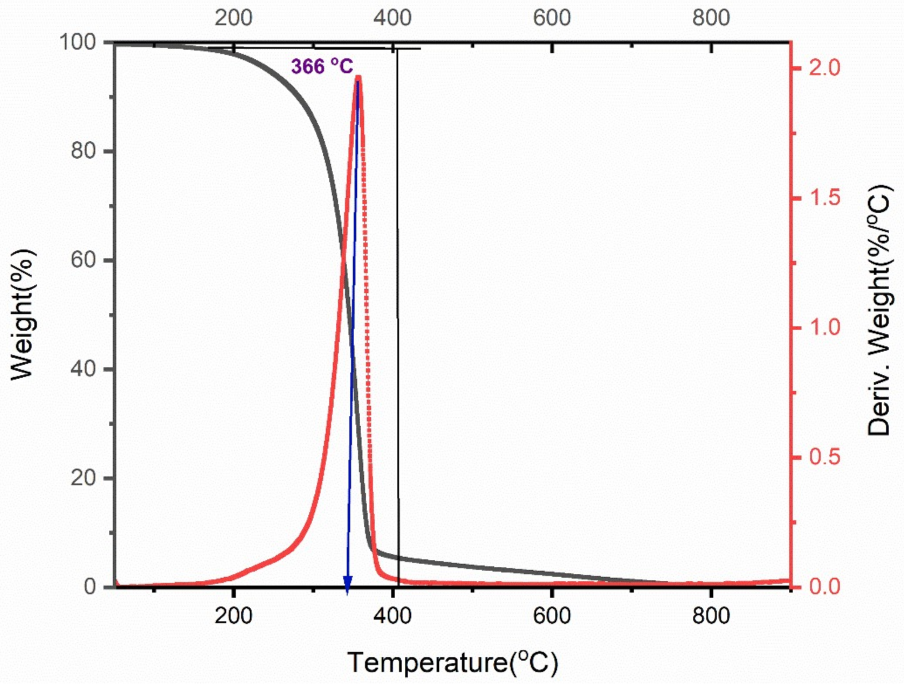

Fig. S70. TGA data of polyester synthesized from CHO/SA/**2a**/TPPCl.

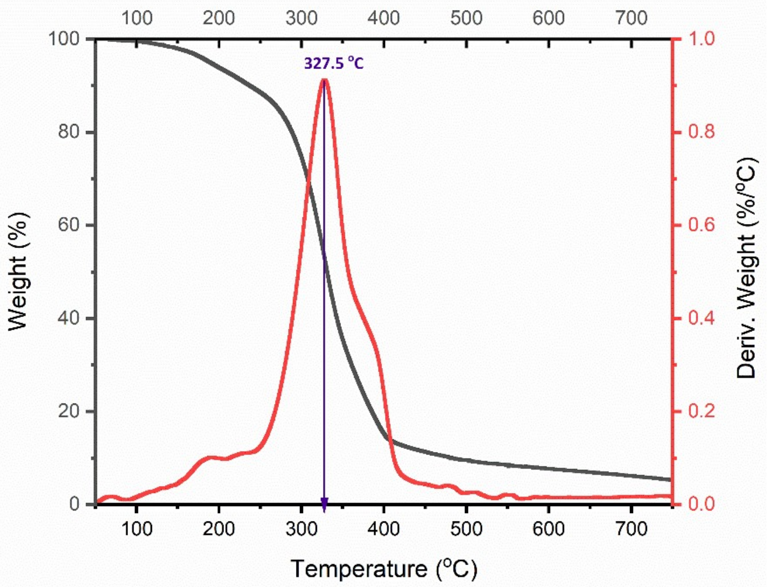

Fig. S71. TGA data of polyester synthesized from CHO/MA/**2a**/TPPCl.

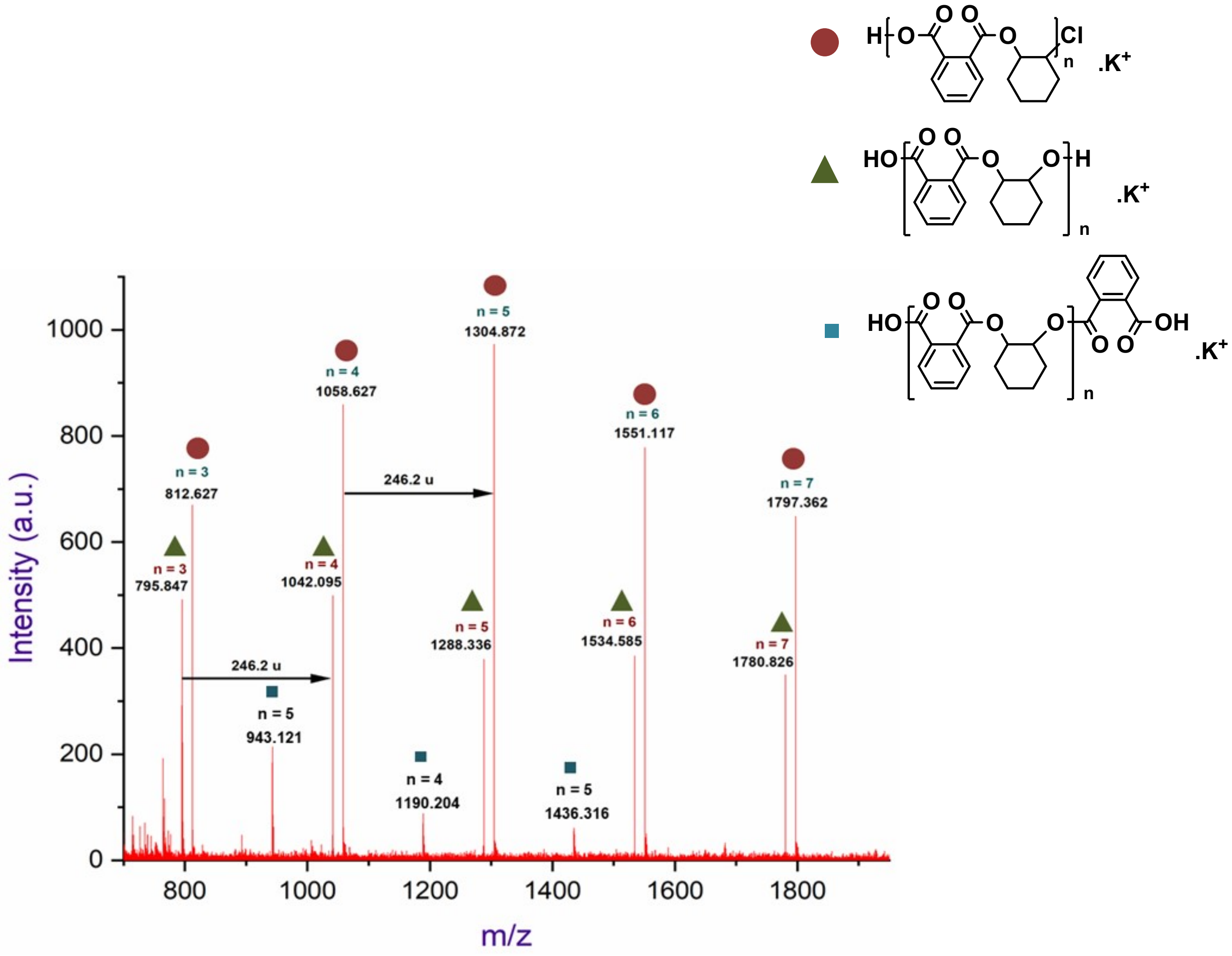

Fig. S72. MALDI-TOF spectrum of oligomer prepared from ROCOP of PA and CHO using **2a.**

Table S3. Experimental data for the plots to determine the order of ROCOP of CHO and PA with respect to catalyst and cocatalyst TPPCl

Entry	[Catalyst] (M)	Initial rate [a] (M/min) (Compound **2a**)	Initial rate [a] (M/min) (Compound **2d**)
1	0.01235	0.03747	0.0355
2	0.02471	0.04071	0.03613
3	0.03706	0.04232	0.03684
4	0.04942	0.04404	0.03764

Entry	[TPPCl] (M)	Initial rate [a] (M/min) (Compound **2a**)
1	0.01235	0.04023
2	0.02471	0.04053
3	0.03706	0.04105
4	0.04942	0.04185

[a] the rate of polyester formation (CHO/PA) was determined from the slope of the linear range of conversion of PA with time. The data was obtained by taking aliquots at specific reaction times and analyzing them for individual composition by ^{1}H NMR.

Table S4. Experimental data for the plots to determine the order of ROCOP of CHO and SA with respect to **2a** and **2d**.

Entry	[Catalyst] (M)	Initial rate [a] (M/h) (Compound **2a**)	Initial rate [a] (M/h) (Compound **2d**)
1	0.04492	3.13064	3.6654
2	0.08984	3.23252	3.72003
3	0.13477	3.35392	3.76191
4	0.17969	3.47100	3.80958

[a] the rate of polyester formation (CHO/SA) was determined from the slope of the linear range of conversion of SA with time. The data was obtained by taking aliquots at specific reaction times and analyzing them for individual composition by ^{1}H NMR.

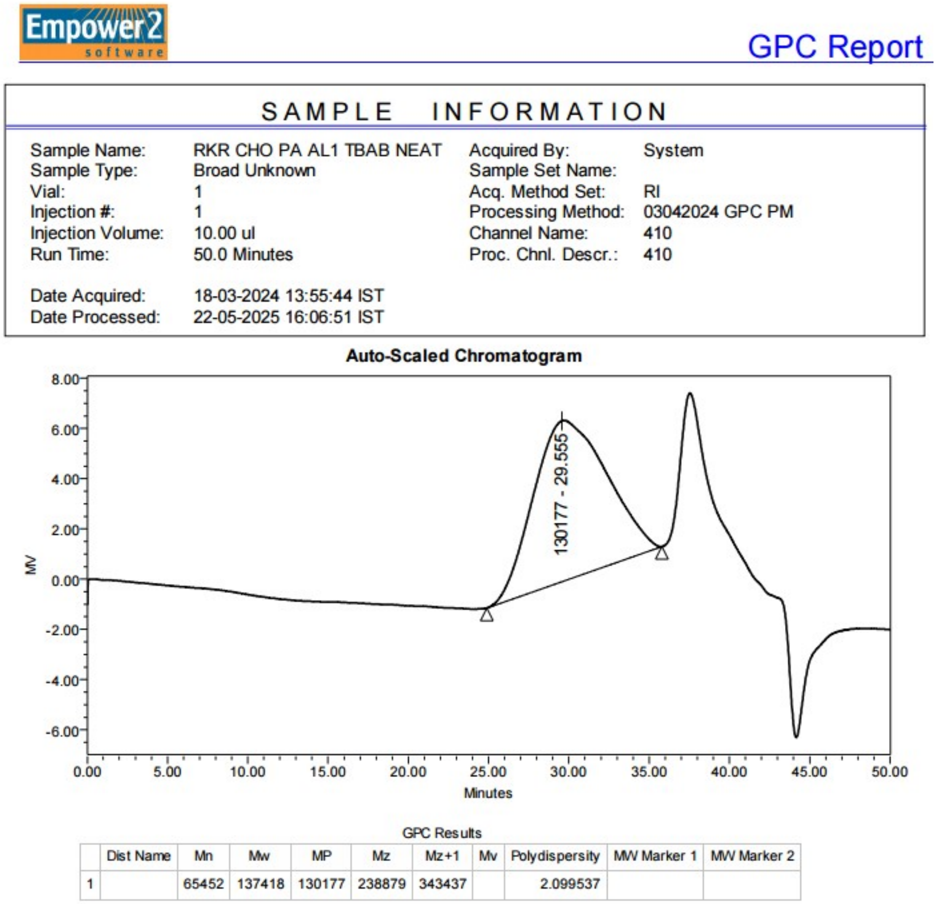

GPC Report

SAMPLE INFORMATION

Sample Name:	RKR CHO PA AL1 TBAB NEAT	Acquired By:	System
Sample Type:	Broad Unknown	Sample Set Name:	
Vial:	1	Acq. Method Set:	RI
Injection #:	1	Processing Method:	03042024 GPC PM
Injection Volume:	10.00 ul	Channel Name:	410
Run Time:	50.0 Minutes	Proc. Chnl. Descr.:	410
Date Acquired:	18-03-2024 13:55:44 IST		
Date Processed:	22-05-2025 16:06:51 IST		

GPC Results

	Dist Name	Mn	Mw	MP	Mz	Mz+1	Mv	Polydispersity	MW Marker 1	MW Marker 2
1		65452	137418	130177	238879	343437		2.099537		

Fig. S73. GPC trace of polyester from PA/CHO using **2a** and TBAB in neat condition (Table 1, Entry 3).

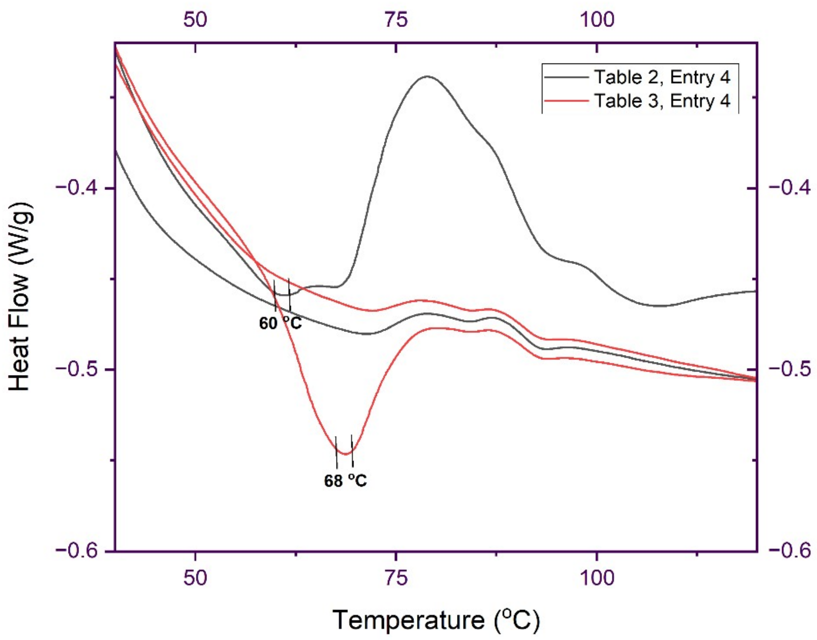

Fig. S74. DSC trace of polyester synthesized from CHO/SA/**2d**/TPPCl and CHO/MA/**2d**/TPPCl. Red curve: poly(MA-alt-CHO) and black curve: poly(SA-alt-CHO).

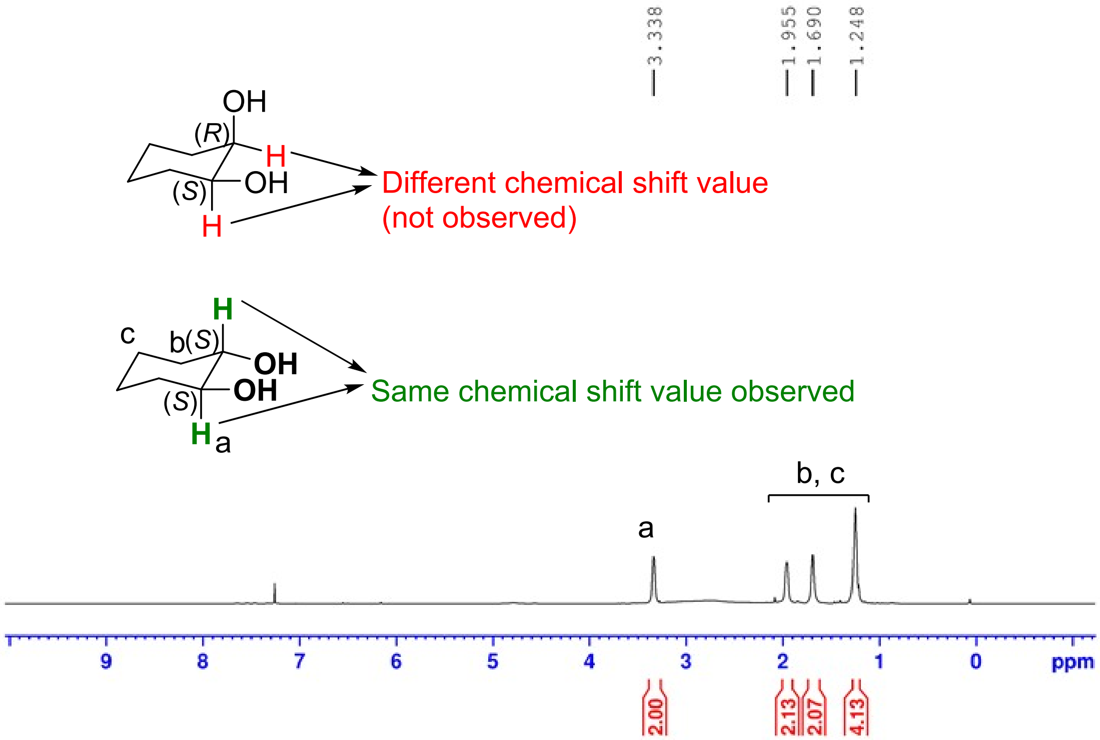

Fig. S75. ^{1}H NMR ($CDCl_3$, 500 MHz) spectrum of the hydrolyzed polyester

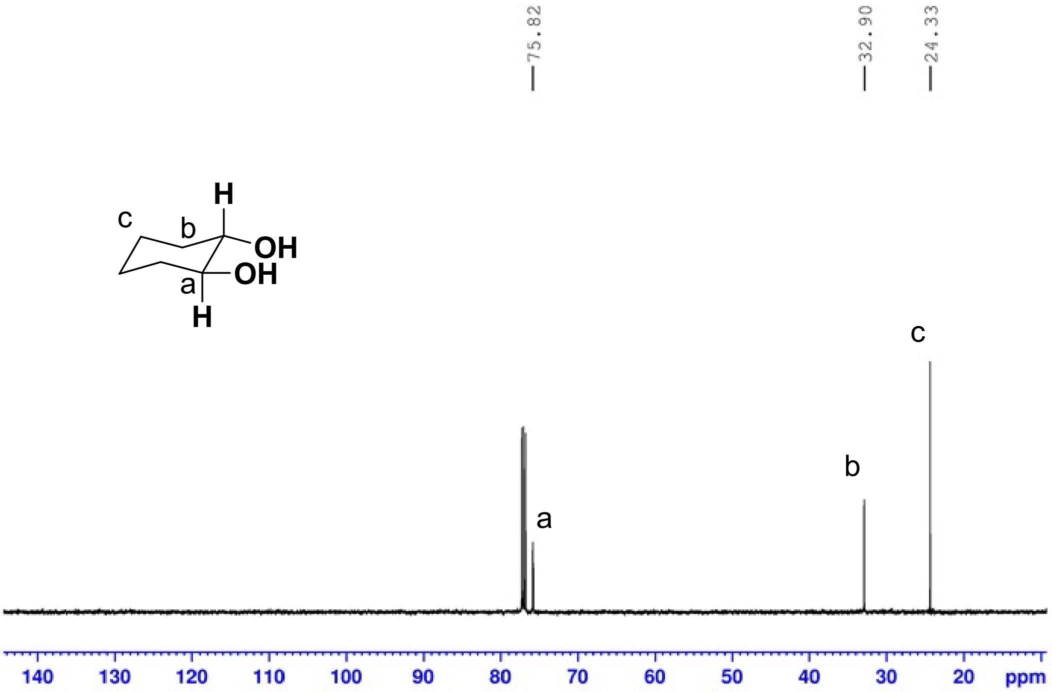

Fig. S76. ^{13}C NMR ($CDCl_3$, 500 MHz) spectrum of the hydrolyzed polyester

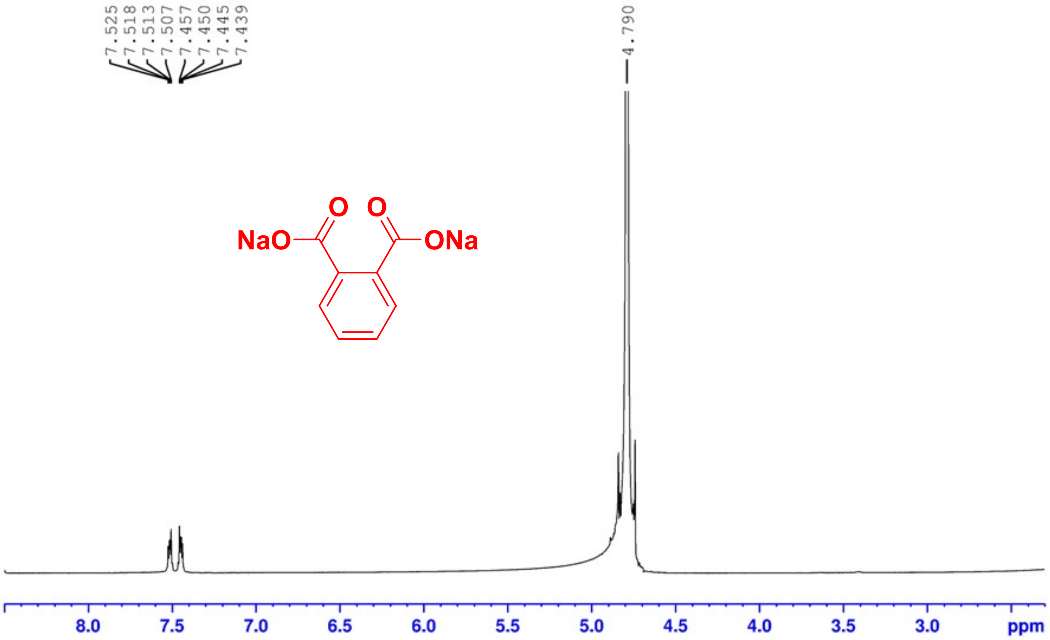

Fig. S77. ^1H NMR (D_2O, 500 MHz) spectrum of the aqueous fraction of the hydrolyzed polyester

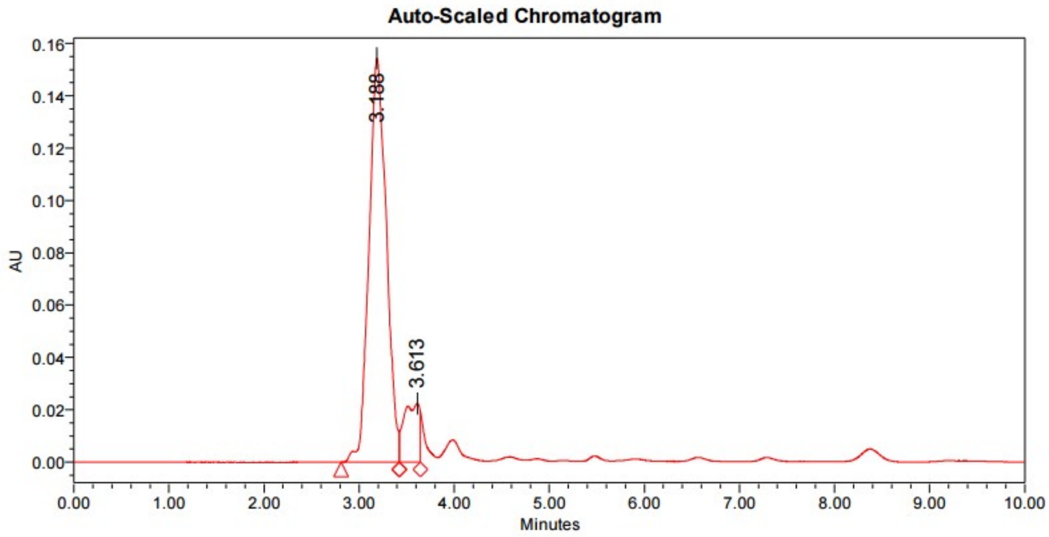

Peak Results

	RT	Area	Height	% Area	SampleName
1	3.188	1961780	154263	88.51	DC-AK-267
2	3.613	254650	22386	11.49	DC-AK-267

Fig. S78. HPLC chromatogram of polyester upon hydrolysis prepared from catalyst **2a (Table S5**, **Entry 1)**.

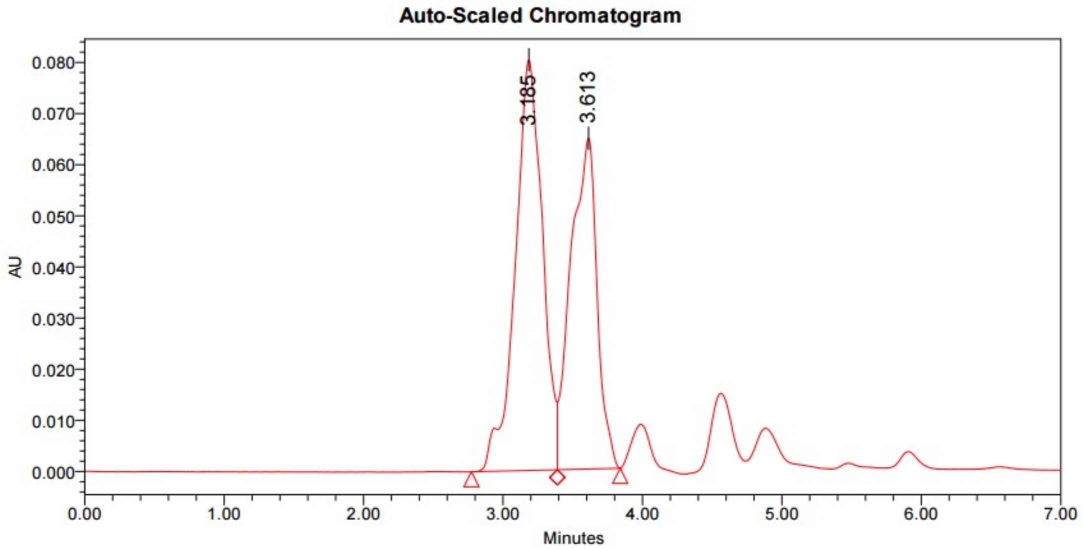

Peak Results

	RT	% Area	% Height	Area (µV*sec)	Height (µV)
1	3.185	56.30	55.39	1092832	80298
2	3.613	43.70	44.61	848389	64676

Fig. S79. HPLC chromatogram of polyester upon hydrolysis prepared from catalyst **2d (Table S5**, **Entry 2)**.

Table S5. Enantiomeric excess of 1,2-cyclohexanediol obtained upon hydrolysis of polyester.

Entry	Catalyst	(*R, R*) diol	(*S, S*) diol	%ee = {[(R-S)/(R+S)]x100}
1	**2a**	88.51	11.49	[(88.51-11.49)/(88.51+11.49)]x100 = 77.02
2	**2d**	56.30	43.70	[(56.30-43.70)/(56.30+43.70)]x100 = 12.6

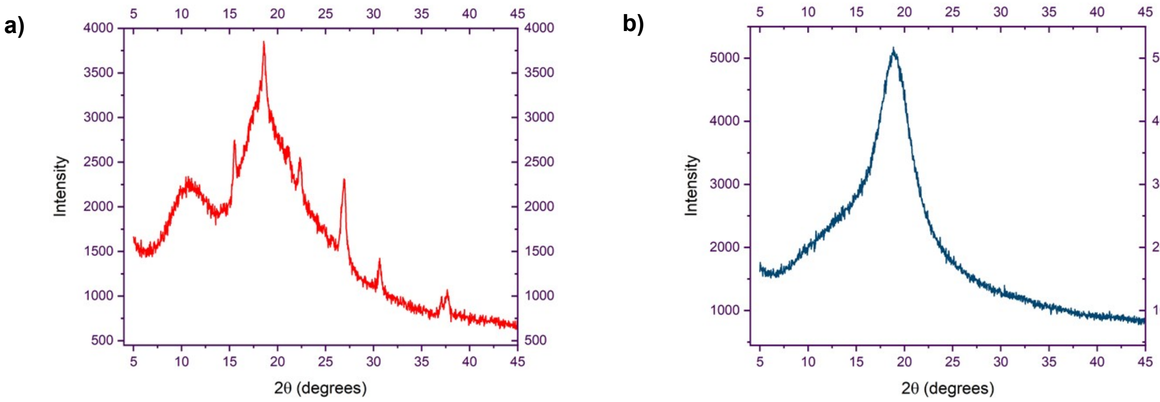

Fig. S80. WAXD profiles of a) Semicrystalline CHO/PA polyester produced by **2a** and b) amorphous CHO/PA polyester produced by **2d**.

References

1. Bruker (2021)– APEX4-SAINT Bruker AXS Inc., Madison, Wisconsin, USA.
2. SADABS-2016/2 - Bruker AXS area detector scaling and absorption Correction, Krause, L., Herbst-Irmer, R., Sheldrick G.M. & Stalke D., *J. Appl. Cryst.*, 2015, **48**, 3-10.
3. G. M. Sheldrick, "SHELXT - Integrated space-group and crystal-structure determination", *Acta Cryst.*, 2015, A71, 3-8.
4. G. M. Sheldrick, Crystal structure refinement with SHELXL", *Acta Cryst.*, 2015, C71, 3-8.
5. L. J. Farrugia, WinGX for Windows, *J. Appl. Crystallogr.* 2012, **45**, 849-854.

6. S. Sarkar, S. S. Roy, S. Krishnaswamy and D. Chakraborty, *Eur. Polym. J.*, 2024, **216**, 113281.
7. L. Zhao, B. Han, Z. Huang, M. Miller, H. Huang, D. S. Malashock, Z. Zhu, A. Milan, D. E. Robertson, D. P. Weiner and M. J. Burk, *J. Am. Chem. Soc.* 2004, **126**, 11156–11157.